National Defence
Research and Development Branch

Défense nationale
Bureau de recherche et développement

TECHNICAL MEMORANDUM 98/227
October 1998

HIGH FREQUENCY RESPONSE OF A STIFFENED BOX STRUCTURE

Layton E. Gilroy — Malcolm J. Smith

Defence Research Establishment Atlantic

Centre de Recherches pour la Défense Atlantique

Canada

DEFENCE RESEARCH ESTABLISHMENT ATLANTIC

9 GROVE STREET
P.O. BOX 1012
DARTMOUTH, N.S.
CANADA B2Y 3Z7

TELEPHONE: (902) 426-3100
FACSIMILE: (902) 426-9654

CENTRE DE RECHERCHES POUR LA DÉFENSE ATLANTIQUE

9 GROVE STREET
C.P. BOX 1012
DARTMOUTH, N.É.
CANADA B2Y 3Z7

National Defence
Research and Development Branch

Défense nationale
Bureau de recherche et développement

HIGH FREQUENCY RESPONSE OF A STIFFENED BOX STRUCTURE

L.E. Gilroy — M.J. Smith†

October 1998

Approved by: J.L. Kennedy
Head / Warship Signatures and Safety Section

TECHNICAL MEMORANDUM 98/227

Defence Research Establishment Atlantic

Centre de Recherches pour la Défense Atlantique

†Martec Limited

Canada

Abstract

Power Flow Finite Element Analysis (PFFEA) has been under development at Defence Research Establishment Atlantic (DREA) in support of the Ship Noise Project. PFFEA is an analysis method for predicting high frequency structural acoustic and vibration response. The method is based on a vibrational conductivity approach in which the flow of vibrational energy is modelled in a similar fashion to heat conduction with convective losses. This report discusses experiments performed with DREA's ship tank test model to assist in the validation of the PFFEA software for high frequency structural vibrations. The experiments involved excitation of the steel box structure at relatively high frequencies using an electromagnetic shaker driving either the centre plate of the test model or one of three typical plate intersections (a symmetric and unsymmetric T-plate junction and an L-plate junction) making up the structure. Both the input mobility to and the response of the test model were measured under broadband excitation using an accelerometer. The input mobilities predicted by the PFFEA code compared extremely well with the experimental measurements. While the power flow method is unable to accurately predict modal response (in this case frequencies up to about 3 kHz), the model accurately predicted the average behaviour for all four cases. When looking at the response of the ship tank panels, in general, the PFFEA program was able to predict the amplitude of the transfer mobility with some degree of accuracy. However, there were significant variations in amplitude with frequency in the measured data which were not modelled with the PFFEA code. As a result, the PFFEA program should primarily be used when predictions are required over a band of frequencies rather than in support of a harmonic analysis.

Résumé

Le Centre de recherches pour la défense (Atlantique) - CRDA - mène présentement des travaux sur l'analyse de la chaîne cinématique par la méthode des éléments finis (ACCEF) dans le cadre du projet sur la signature sonore des navires. L'ACCEF sert à prévoir la réponse vibratoire et acoustique haute fréquence des structures. Cette méthode s'articule sur le concept de la conductivité vibratoire; la chaîne cinématique de l'énergie vibratoire est modélisée de façon similaire à la conduction thermique avec pertes par convection. Le rapport traite des expériences réalisées avec le modèle d'essai en bassin du CRDA dans le but de valider le logiciel ACCEF pour les vibrations structurales haute fréquence. On a soumis une structure à caisson d'acier à des vibrations relativement élevées à l'aide d'un vibrateur électromagntique raccordé soit à la plaque centrale de la structure, soit à l'une des trois intersections de plaques types de celle-ci (joints en T symétriques et asymétriques et joints en L). La mobilité d'entrée et la réponse de la structure ont été mesurées sur toute la plage des fréquences d'excitation à l'aide d'un accéléromètre. Les mobilités d'entrée établies avec le code ACCEF se sont très bien comparées aux mesures prises sur la structure. Même si la méthode de l'analyse par la chaîne cinématique ne peut révéler avec précision la réponse modale (dans le cas présent, les fréquences allant jusqu'à environ 3 kHz), il a été possible de prévoir avec précision le comportement moyen dans les quatre situations expérimentales. Pour ce qui est de la réponse des parois de réservoir des navires, on constate que l'ACCEF permet, en général, de prévoir l'amplitude de la mobilité de transfert avec un certain degré de précision. Cependant, on a relevé des écarts importants d'amplitude des fréquences dans les données mesurées qui n'avaient pas été modélisés avec le code ACCEF. En conclusion, le logiciel ACCEF est avantageux lorsque les prévisions demandées doivent couvrir une vaste plage de fréquences, mais l'est moins pour supporter une analyse des harmoniques.

DREA TM/98/227

High Frequency Response of a Stiffened Box Structure

by

L. E. Gilroy and M.J. Smith

Executive Summary

Introduction

Power Flow Finite Element Analysis (PFFEA) has been under development in the Structural Acoustics and Strength group of the Defence Research Establishment Atlantic (DREA) in support of the Ship Noise Project in which the objective is to provide DND with the expertise and tools necessary to solve current noise problems on CF vessels and to permit future reductions in their underwater acoustic signatures. PFFEA (also known as the Power Flow Finite Element Method, PFFEM) is an analysis method for predicting high frequency structural acoustic and vibration response. The method is based on a vibrational conductivity approach in which the flow of vibrational energy is modelled in a similar fashion to heat conduction with convective losses.

The PFFEM is not a mature technology and the bulk of the work at DREA has been focussed on the development of the methodology with initial work being directed towards the prediction of vibrational energy flow in beam and plate networks. As the method is developmental, relatively little work has been done to date to validate the computer codes against actual structural experiments. In light of this, DREA decided to perform a series of experiments involving test structures used previously in low frequency structurally radiated noise experiments. This technical memorandum discusses experiments performed with DREA's ship tank test model to assist in the validation of the PFFEA software for high frequency structural vibrations.

Principal Results

Four sets of trials were performed with the electromagnetic shaker in one of four positions. These included the centre of the thin plate at the bottom of the centre tank, the intersection of one of the internal walls with the centre plate at the midpoint in the transverse direction (an unsymmetric T-plate junction), the intersection of three plates of the same thickness (a symmetric T-plate junction), and the outside edge of the test model at the midpoint in the transverse direction (an L-plate junction). The shaker was excited over the frequency range from 0 to 8 kHz.

Input mobility measurements were taken for each drive point and, for each shaker location, the transfer mobility for each of the 37 panels in the model was recorded over the 8 kHz frequency band. The input mobilities predicted by the PFFEA code compared extremely well (in a frequency-averaged sense) with the experimental measurements. While the power flow method is unable to accurately predict the response in frequency regions of low modal density (in this case frequencies up to about 3 kHz), the model accurately predicted the average behaviour

for all four cases. When looking at the response of the ship tank panels, in general, the PFFEA program was able to predict the amplitude of the transfer mobility with some degree of accuracy. However, there were significant variations in amplitude with frequency in the measured data which were not modelled with the PFFEA code. As a result, the PFFEA program should primarily be used when predictions are required over a band of frequencies rather than in support of a harmonic analysis.

Significance of Results

The PFFEA program was able to accurately predict the average input mobility to the system for a structure that is a good approximation of structures commonly encountered on naval platforms. Using the predicted inputs, the program was able to give a reasonably accurate description of the amplitude of the response throughout the structure over relatively wide frequency bands.

Future Plans

Future validations for the code would benefit from measuring the response over a particular band rather than the narrow band measurements used here. Further investigations should also be performed into validating the performance of accelerometers and force transducers and the various mounting techniques to widen the frequency band which could be considered. To date, the PFFEA code has only been validated against laboratory scale measurements and has not been used to predict either in-air or underwater radiated noise. Further tests of the DREA ring-stiffened cylinder (with an internal deck added) are planned to examine in-air radiated noise (and possibly underwater radiated noise) and the DREA Acoustic Calibration Barge will be used as a test bed to validate the program for fluid-loaded plates.

Contents

1 Introduction

Power Flow Finite Element Analysis (PFFEA) has been under development in the Structural Acoustics and Strength group of the Defence Research Establishment Atlantic (DREA) in support of the Ship Noise Project in which the objective is to provide DND with the expertise and tools necessary to solve current noise problems on CF vessels and to permit future reductions in their underwater acoustic signatures. PFFEA (also known as the Power Flow Finite Element Method, PFFEM) is an analysis method for predicting high frequency structural acoustic and vibration response. The method is based on a vibrational conductivity approach in which the flow of vibrational energy is modelled in a similar fashion to heat conduction with convective losses.

The PFFEM is not a mature technology and the bulk of the work at DREA has been focussed on the development of the methodology with initial work being directed towards the prediction of vibrational energy flow in beam and plate networks [1, 2, 3, 4, 5, 6]. Recent work includes the development of methods for predicting the vibratory response in fluid-loaded structures and the resulting radiated noise. As the method is developmental, relatively little work has been done to date to validate the computer codes produced against actual structural experiments, although a pilot study involving the examination of a simulated semi-infinite beam [7] and experimental measurements using a ring-stiffened cylinder [8] have been carried out. In light of this, DREA decided to perform a series of experiments involving test structures used previously in low frequency radiated noise experiments. These include DREA's 3m ring-stiffened cylinder [9, 10] mentioned above, the ship tank test model, and the Acoustic Calibration Barge [11].

This technical memorandum discusses experiments performed with the ship tank test model to assist in the validation of the PFFEA software for high frequency structural vibrations. The memorandum will discuss briefly the background to the PFFEA method and then describe the experimental procedure and equipment used. Comparisons will be made between the measured response of the test model and the predicted response based on the PFFEM.

2 Background

Power flow finite element analysis (PFFEA) is a new and potentially powerful method for vibroacoustic analysis of structures. It uses a vibrational conductivity modelling of structural components in which the flow of vibratory energy is treated in a way analogous to the steady state flow of thermal energy. This comes about by applying time-averaged and local space-averaged expressions for energy density and power flow for a unit volume of a structural component. This results in a second-order conductivity equation governing the distribution of vibrational energy. The basic equations for PFFEA are obtained by spatial discretization of the differential equation. Energy in each vibration type (e.g. flexural, torsional, etc.) can be modelled separately with PFFEA, with coupling occurring at junctions of components.

The real advantage to PFFEA comes from the time and space averaging, which ensures that the predicted vibration energy distributions will be smoothly varying across a structural com-

ponent. This makes the method highly suitable for random or broadband excitation, in which local variations in the vibratory response tend to be smeared out. Such response profiles cannot be computed with coarse FE meshes (or meshes fine enough to give good stress distributions), making PFFEA much more efficient than FE analysis for higher frequency vibrations. A further advantage comes from its capability as a design tool. PFFEA not only predicts the vibrational energy distribution, but also maps out the flow of vibrational energy in the structure. With conductivity modelling, only the irreversible (i.e. non-reactive) power flow is mapped, enabling the visualization of dominant transmission paths. This may be a valuable aid in the design of a structural system, and may also lend insight to an appropriate vibration control strategy.

PFFEA is in a sense an interdisciplinary method. It utilizes many of the physical concepts already accepted in the realm of structural acoustics, while applying the equation solving power of the finite element method. PFFEA also enjoys some important advantages over the standard method in vibroacoustics: statistical energy analysis (SEA). This method treats entire structural components much like an element of volume in PFFEA. Only a single response value for each energy type can be computed for a component, as opposed to the spatial variation and inclusion of all wave types generated by PFFEA. Moreover, SEA modelling can be very cumbersome in complex systems, as individual coupling elements must be supplied at every interface. Because PFFEA is FE based, the vibroacoustic model can be based directly on the geometry of an existing FE model. Also, the PFFEA equations are in the same form as for linear static FE analysis and can therefore be solved with standard analysis routines. Unlike SEA, PFFEA has the capability for modelling nonuniform distributions of damping material. This is important in modelling layers of viscoelastic material applied to structural members, a common technique for passive vibration control.

The development of PFFEA has progressed to a stage at which relatively complex structural models can now be evaluated. The PFFEA system consists of a PFFEA translator program which converts an FE model to a PFFE model and the field equation solver VASTF [12] which performs the PFFEA analysis. The system has been tested on a variety of structural models including frames, stiffened and unstiffened plates, and cylinders. Recent efforts have been directed toward the modelling of input power to arbitrary junctions of components. PFFEA can now be applied to most structural configurations involving nearly all types of one- and two-dimensional elements.

3 Experimental Procedures

3.1 Equipment

The ship tank test model is 1.83m long, 1.22m wide, and 0.61m deep. It comprises an outer box with an internal tank-like structure equal in depth to the main box. All vertical surfaces are stiffened horizontally with 6.4mm x 50.8mm flat bar stiffeners at their top edges and midheight. The box is constructed entirely of 6.4mm mild steel with the exception of the bottom of the centre tank which is a 3.2mm mild steel plate. The test model is of welded construction and has

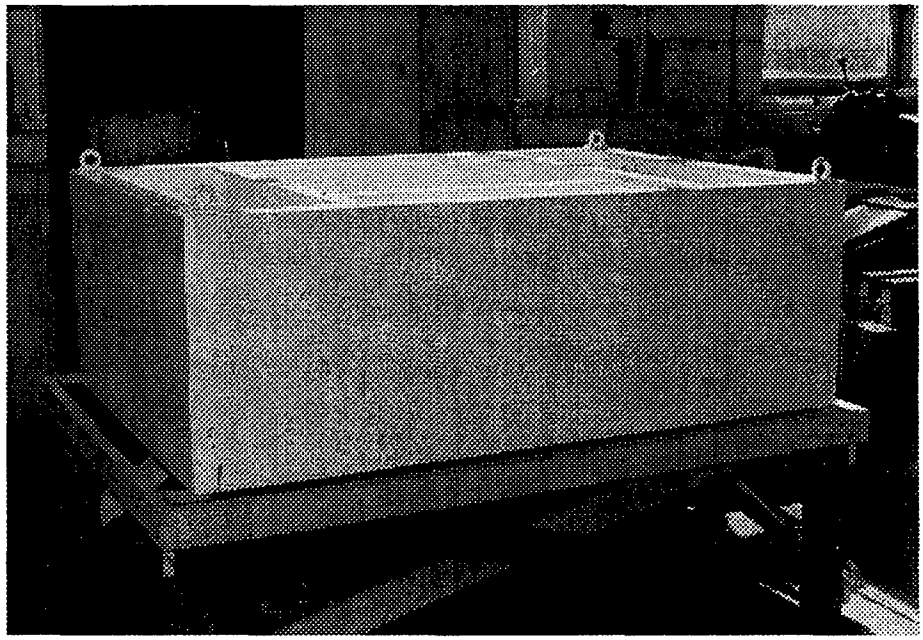

Figure 1: Ship Tank Test Model

been heat-treated in an attempt to remove any residual stresses. A photograph of the ship tank model on its test frame is shown in Figure 1. The frame was constructed to minimize contact with the test model and thus, minimize opportunities for vibration to be conducted via multiple paths. The frame is constructed of lumber and the test model is very close to point-supported at each of the four corners. Using welded studs, multiple 19mm x 19mm mounting blocks were attached to the test model at various locations to facilitate the mounting of accelerometers and force tranducers.

A B&K Model 4809 electromechanical shaker was used to provide the loading on the test model. Four sets of trials were performed with the shaker in one of four positions. A schematic of the test setup with the shaker in the first position is shown in Figure 2. The four shaker positions are shown in Figure 3 as seen from above. The shaker was always placed so that it was driving the test model from below in the vertical direction. The first location was at the centre of the thin plate at the bottom of the centre tank. The second location was at the intersection of one of the internal walls with the centre plate at the midpoint in the transverse direction. This formed an unsymmetric T-plate junction as the centre plate is thinner than the others. The third location was at an intersection of three plates of the same thickness forming a symmetric T-plate junction. The final location was at the outside edge of the test model at the midpoint in the transverse direction forming an L-plate junction.

A stinger was connected from the shaker to a Kistler Model 9712A500 force transducer mounted on a block on the test model. The test model response was measured using B&K Model 4333 accelerometers attached to B&K Model 2635 charge amplifiers. The response was viewed using an HP35670A Signal Analyzer which was also used to provide the excitation voltage to the shaker. A 50% burst chirp signal (broad frequency content) was used with a uniform window and RMS averaging (50 averages). The frequency response of the accelerometer signal (measuring velocity) with respect to the input force was recorded using appropriate calibration units (resulting in units of dB re 1 m/sN).

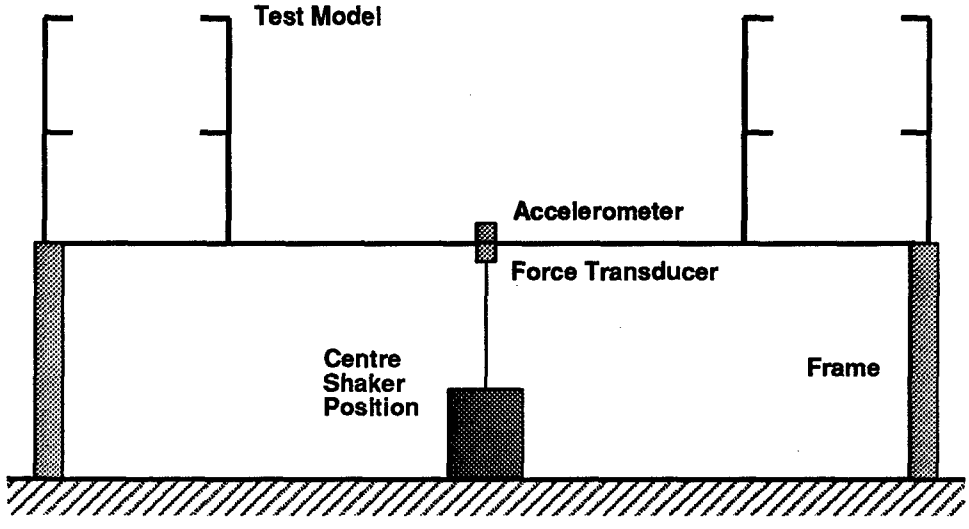

Figure 2: Schematic of Test Setup (section along long axis of box)

3.2 Measurements

The test model was placed on the wooden frame in the Heavy Engine Lab at DREA. The shaker was installed so that it rested on a 25mm layer of viscoelastic damping material on the floor of the lab and the stinger was attached to the force transducer located on the mounting block attached to the test model. The shaker was excited with the burst chirp signal covering frequencies from 0 Hz to 8 kHz. Narrow band input mobility measurements were taken for each drive point. Interim testing determined that a single point measurement gave a reasonable approximation to the transfer mobility of a whole panel over this frequency range (where a panel was defined as a section of plate bounded by the flat bar stiffeners). This approximation would not be valid if the frequency band of interest was dominated by only modal response. For each shaker location, the narrow band transfer mobility for each panel in the model (there are 37 in total) was recorded over the 8 kHz frequency band. The numbering used to identify

the panels is shown in Figure 4.

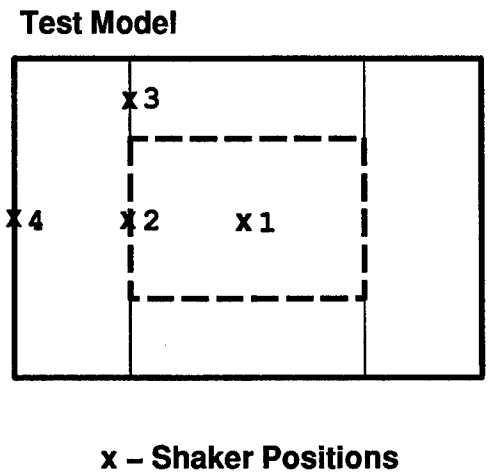

Figure 3: Shaker Locations (viewed from above)

Initial measurements of both the input and transfer mobilities showed large deviations from predicted levels at frequencies approaching 12 kHz. Upon further examination using very light PCB Model 353B18 accelerometers, it became apparent that the combination of the heavier B&K accelerometer and mounting block was producing a very broad peak in the measured accelerations centred around 12 kHz which was not being produced by the ship tank test model. As it was not feasible to use the smaller accelerometers to measure the transfer mobility (it would have been far too time-consuming to move them from point-to-point as it would have been necessary to have had them glued on), it was decided to limit the measurements to the indicated frequency range of 0 Hz to 8 kHz.

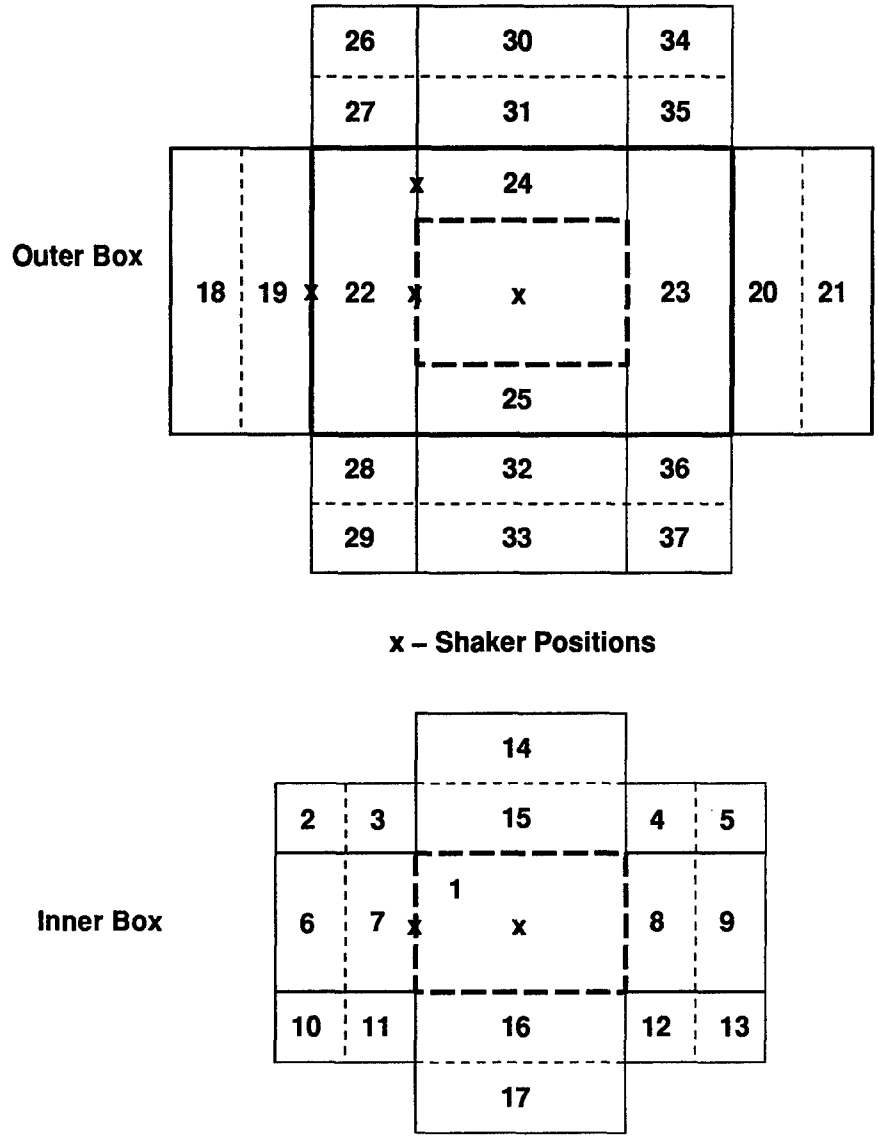

Figure 4: Ship Tank Test Model Plate Numbering

4 Numerical Model

4.1 Input Mobility

The numerical model used to obtain the theoretical input mobility involved idealizing the ship tank test model as either an infinite flat plate, in the case of excitation of the centre plate, or as a semi-infinite plate junction, in the case of excitation at the second through fourth locations. Modelling a finite system by its infinite equivalent is discussed in [13]. The idea is that when the driving point frequency response is plotted on a log scale, it is possible to plot a curve through the response that is equidistant from the resonant peaks and antiresonant troughs. In the limit of high frequency, the resonances and antiresonances converge toward this mean curve. This high frequency limit is conceptually the same as the moving the boundaries out to infinity while keeping the frequency constant. Therefore, the mean curve is just the driving point response of the equivalent infinite system. This holds regardless of the type of structure, provided one is looking at the driving point response. It does not hold for transfer mobilities, which is why it is necessary to use PFFEA to get the response at locations other than the driving point.

It was also necessary to include the masses of the mounting blocks (55 grams each) and the measurement accelerometer (15 grams) in the impedance calculations for the input mobility for the centre plate. These masses were also included for the remaining input mobility calculations, but were not found to have a significant effect.

4.2 Response

The numerical model used in the PFFEM analysis is shown in Figure 5 (due to limitations in the imaging software, the stiffeners are not shown). For this analysis, this model consists of 53 components (37 plates and 16 beams) and 56 junctions (16 L-plate, 24 T-plate, and 16 beam-plate junctions). The material properties used are those of mild steel (Young's modulus of 200 GPa, Poisson's ratio of 0.3, density of 7600 kg/m^3, and a loss factor of 0.005).

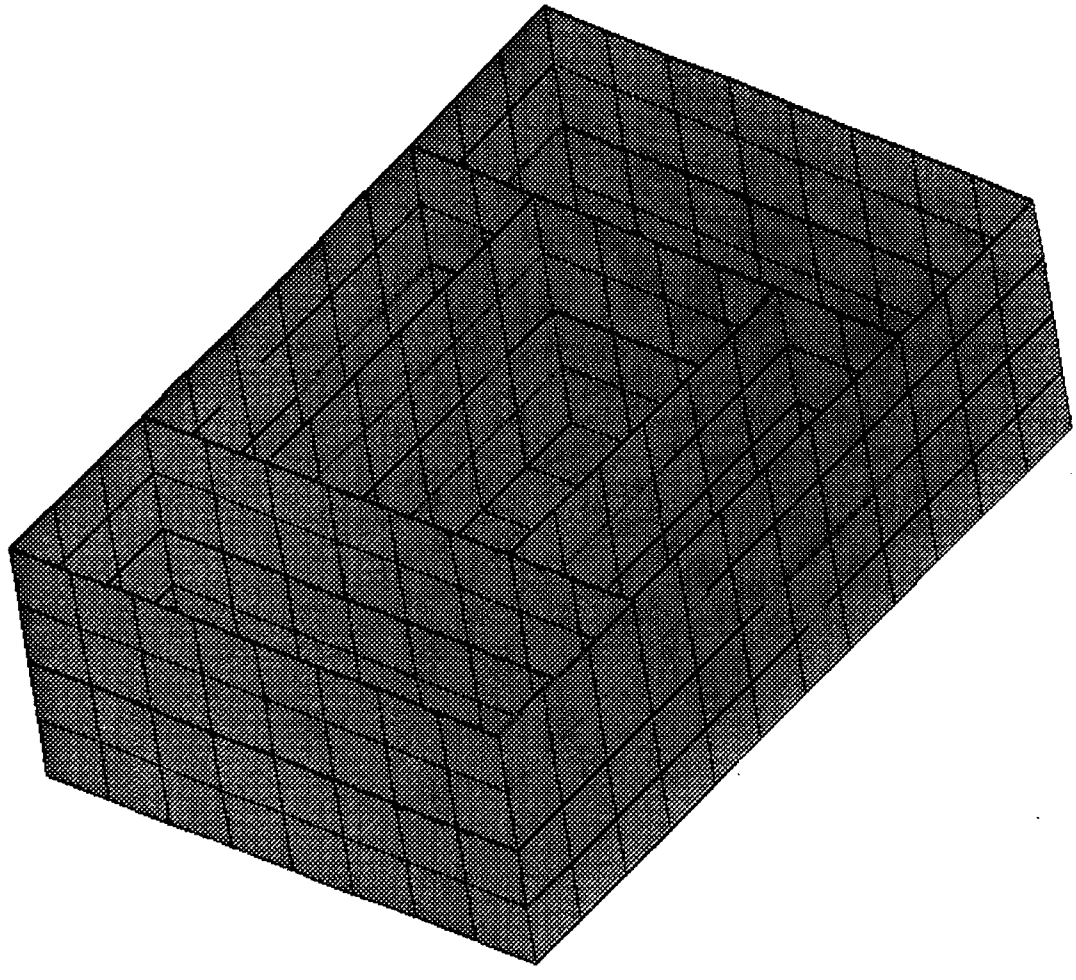

Figure 5: PFFEA Model of Ship Tank Test Model (beam stiffeners not shown)

5 Results

Measurements were made of both the input mobility and the transfer mobilities for all panels for each of the four test cases. The measured curves were stored to disk on the HP signal analyzer and transferred to a spreadsheet for further analysis and comparison to predicted results.

5.1 Input Mobility

The measured and predicted input mobility for the four test cases are shown in Figures 6 through 9. As can be seen, the predicted mobility compared very well to the measured values over the entire frequency range considered. The three cases involving intersections all show an input mobility increasing with frequency while that for the centre plate input decreases with frequency. The power flow method is unable to accurately predict modal response but, even over the predominantly modal region (up to about 3 kHz in the centre plate case), the model accurately predicted the average behaviour. The other three cases appear to show some modal behaviour over the entire frequency range which may be a result of much increased stiffness of the junctions. Of the four cases shown, the least accurate appears to be the symmetric T-plate intersection. In this case, the T-section is quite short in length, so approximating it as an infinite intersection is not as good an assumption as for the other three cases. The high amplitude very low frequency spike seen in Figures 7 through 9 is most likely an artifact of the analyzer and not indicative of a poor match between the predicted and measured values.

While the agreement between the predicted and measured mobilities appears to be good, for the more complicated junctions, there is a fair amount of variability with frequency on the narrow band plots. The measured data can be on the order of 10 dB above or below the theoretical prediction and this indicates the theoretical result gives an average or 'best fit' response and should not be used to make predictions at single frequencies.

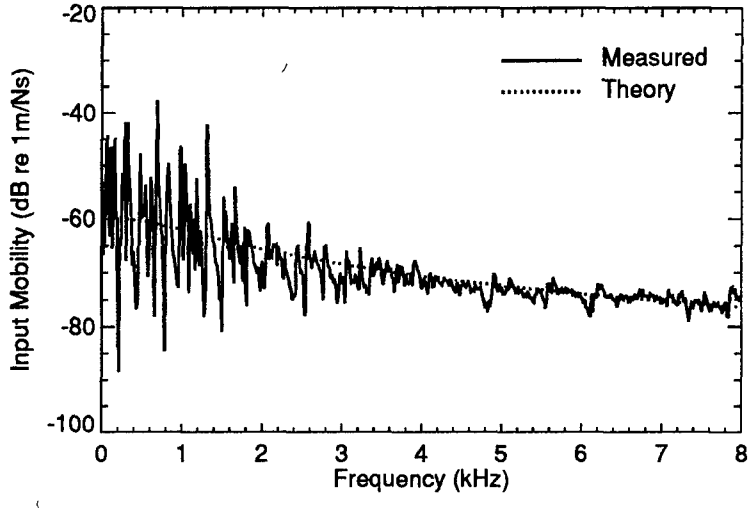

Figure 6: Centre Plate Input Mobility

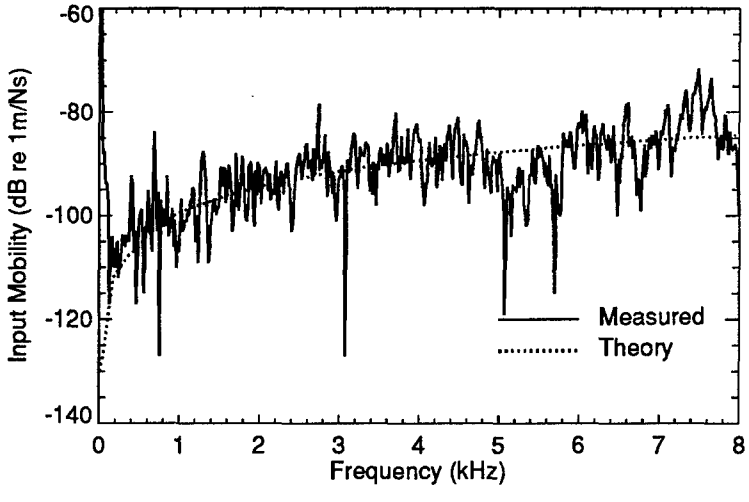

Figure 7: Unsymmetric T-Plate Intersection Input Mobility

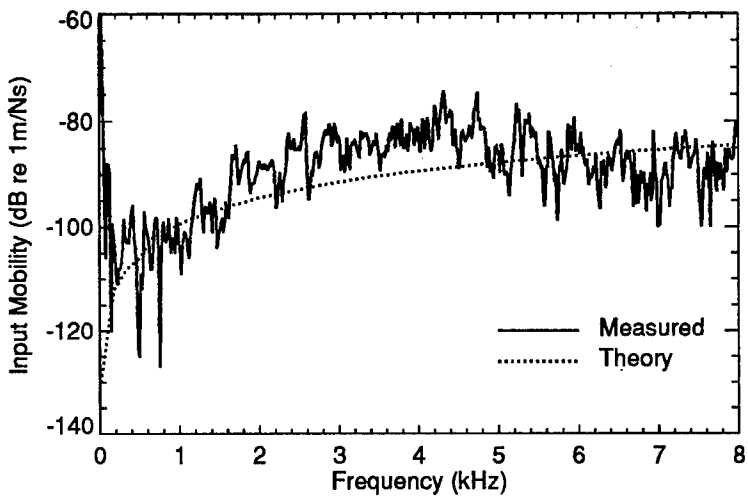

Figure 8: Symmetric T-Plate Intersection Input Mobility

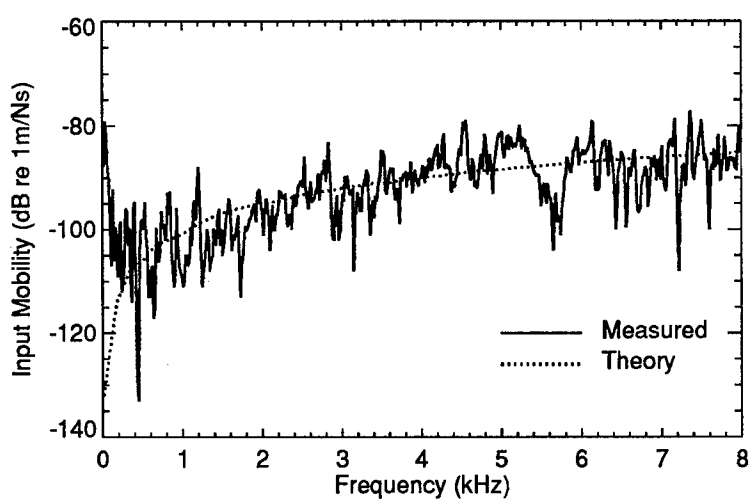

Figure 9: L-Plate Intersection Input Mobility

5.2 Transfer Mobility

The following plots show both the measured and the predicted response for a representative set of the panels. The complete set of experimental and predicted tranfer mobility plots is located in Appendix A. The input mobility used for the numerical model is the theoretical mobility calculated in the previous section. Figures 10 to 15 show the panel responses for the centre plate location of the shaker, Figures 16 to 21 show the responses for the unsymmetric T-plate intersection location, Figures 22 to 27 show the responses for the symmetric T-plate intersection location, and Figures 28 to 33 show the responses for the L-plate intersection location. The transfer mobility for panel 1 for the centre plate case is the mobility measured at any point away from the input point.

In general, the plots show that the PFFEA code predicts the transfer mobility of the ship tank model panels with reasonable accuracy. As with the input mobility, there is a significant decrease in the predicted transfer mobility with frequency for the centre plate case. Unlike the input mobility, for the plate junction cases, there is very little variation with frequency for the predicted transfer mobilities. For these cases, in general, the response varies by little more than 5 dB over all panels and frequencies and, for both T-plate junctions, the predicted response increases with frequency for some panels and decreases for others. For all cases but the L-plate junction, the response of the centre plate (panel 1) is 5 to 10 dB higher than the other panels due to the decreased thickness of this plate (3.2mm versus 6.4mm).

The measured mobilities show significant variations in amplitude with frequency which are not predicted by the numerical model; however, the numerical model does provide a reasonably close match to the average response (with respect to frequency). Although some plate responses were predicted better than others, there is no obvious pattern which would indicate which plate responses will be well predicted. As was indicated in the discussion of the input mobility, the average level appears to be reasonable, but the code should not be used for making predictions at particular frequencies. In all cases, predictions should be limited to a band of frequencies, such as a 1/3-octave band.

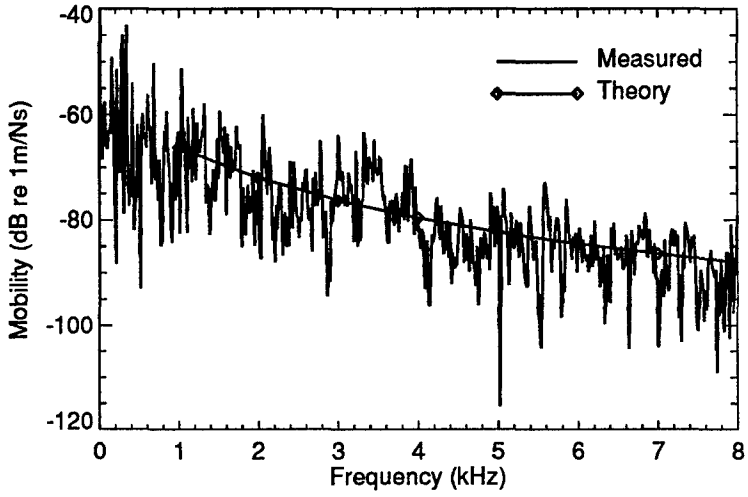

Figure 10: Transfer Mobility, Centre Plate Input, Plate 1

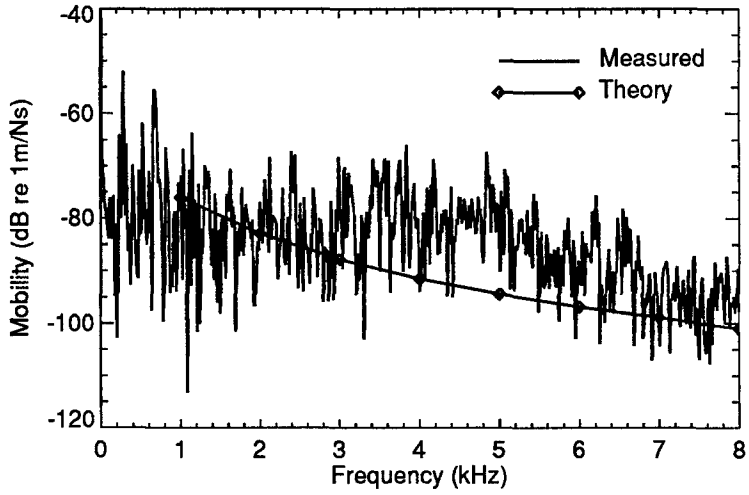

Figure 11: Transfer Mobility, Centre Plate Input, Plate 6

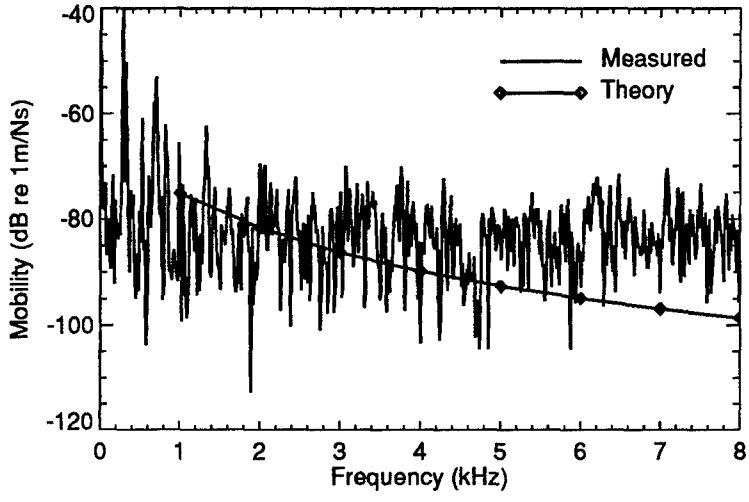

Figure 12: Transfer Mobility, Centre Plate Input, Plate 7

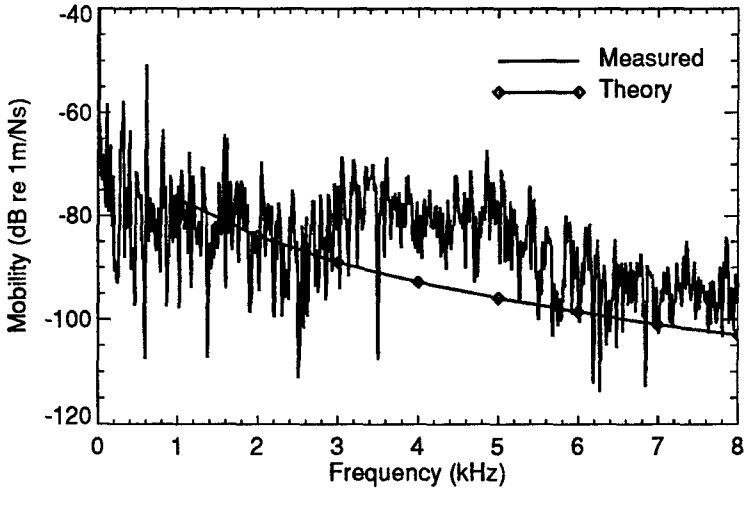

Figure 13: Transfer Mobility, Centre Plate Input, Plate 18

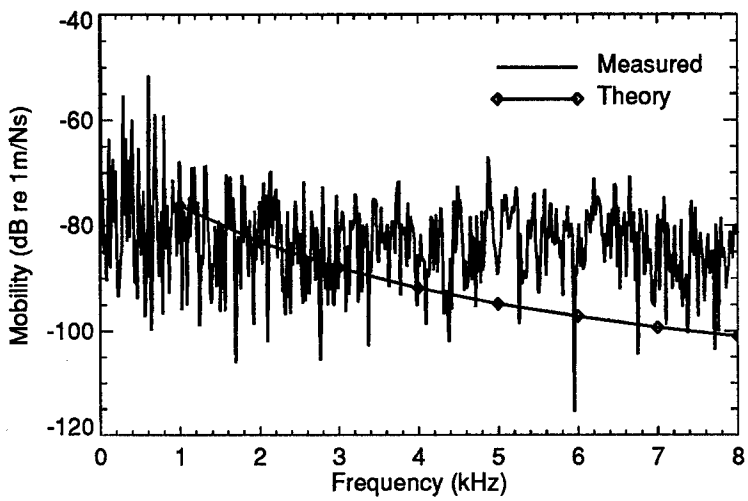

Figure 14: Transfer Mobility, Centre Plate Input, Plate 19

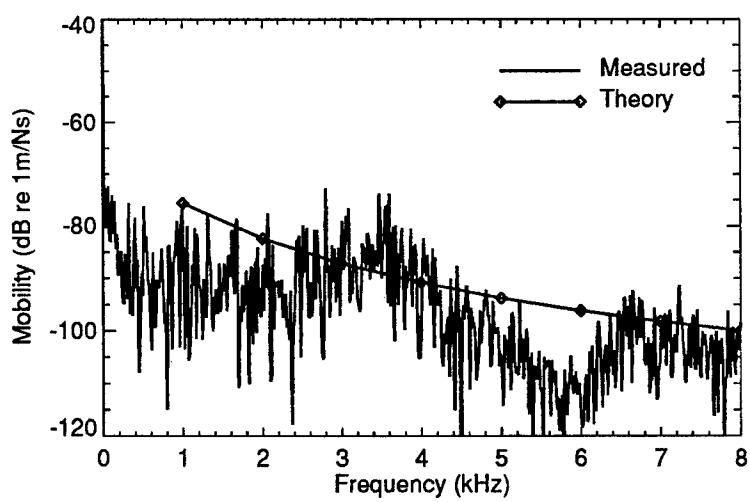

Figure 15: Transfer Mobility, Centre Plate Input, Plate 22

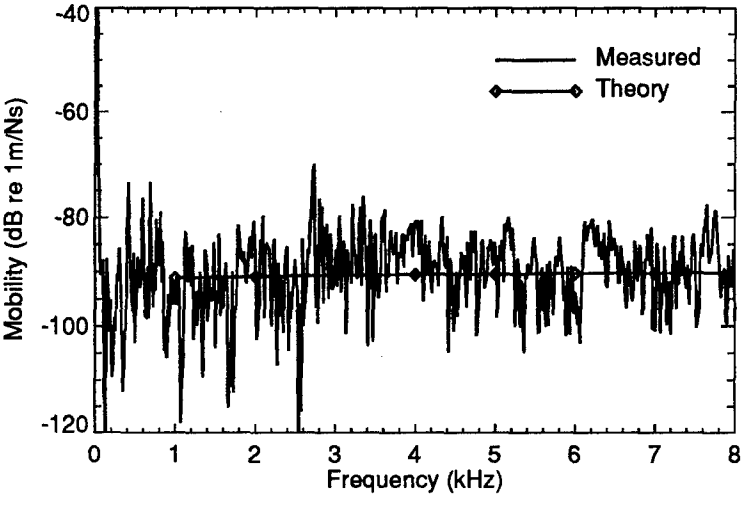

Figure 16: Transfer Mobility, Unsymmetric T-Plate Intersection Input, Plate 1

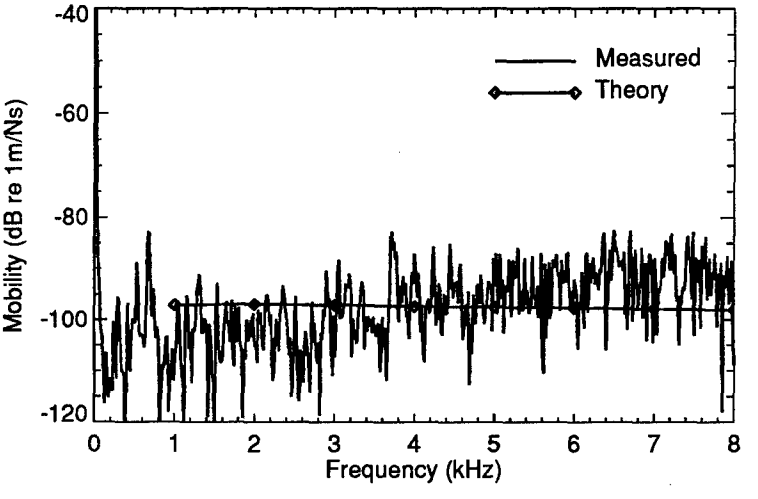

Figure 17: Transfer Mobility, Unsymmetric T-Plate Intersection Input, Plate 6

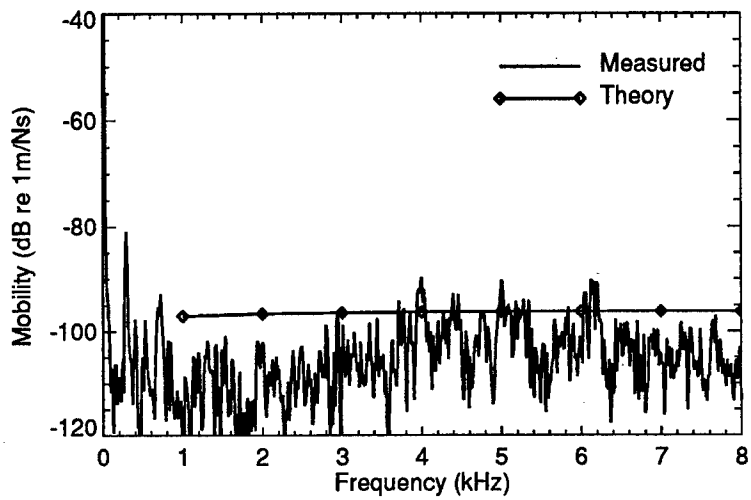

Figure 18: Transfer Mobility, Unsymmetric T-Plate Intersection Input, Plate 7

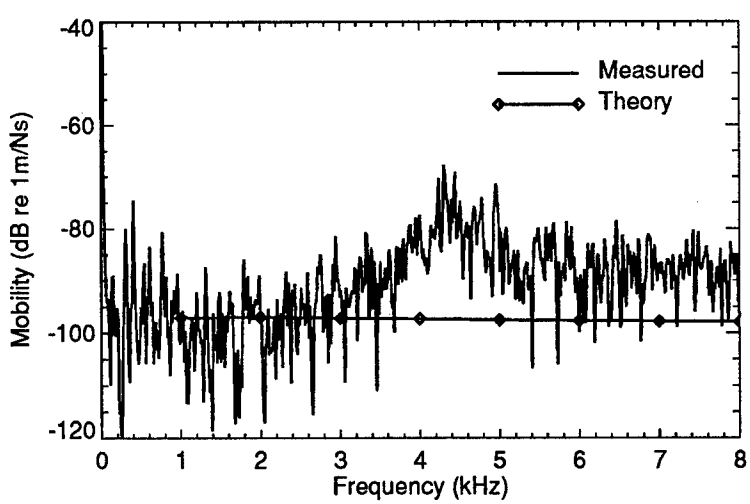

Figure 19: Transfer Mobility, Unsymmetric T-Plate Intersection Input, Plate 18

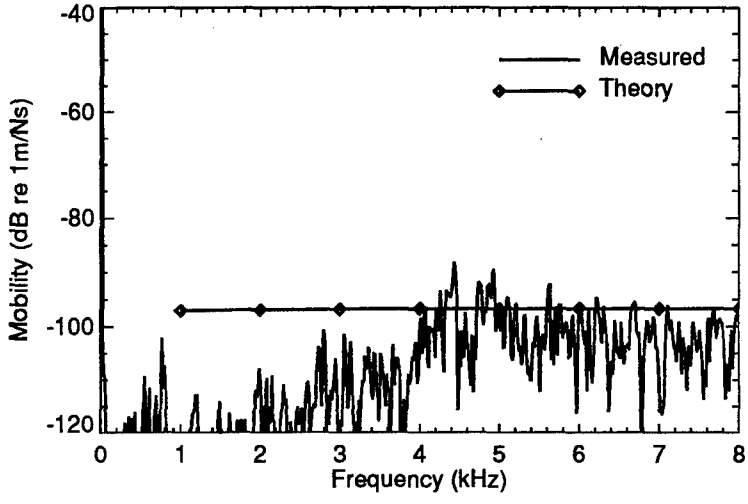

Figure 20: Transfer Mobility, Unsymmetric T-Plate Intersection Input, Plate 19

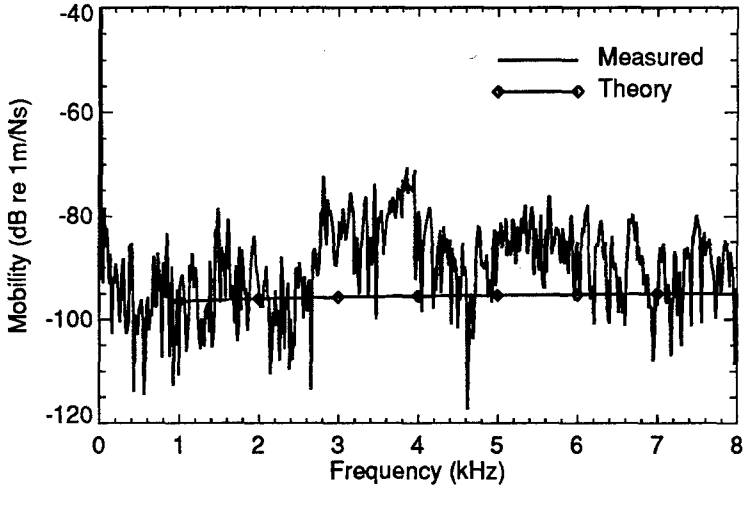

Figure 21: Transfer Mobility, Unsymmetric T-Plate Intersection Input, Plate 22

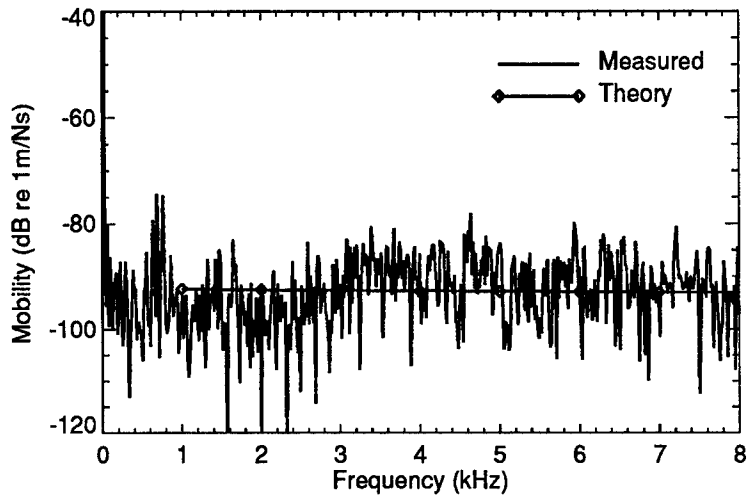

Figure 22: Transfer Mobility, Symmetric T-Plate Intersection Input, Plate 1

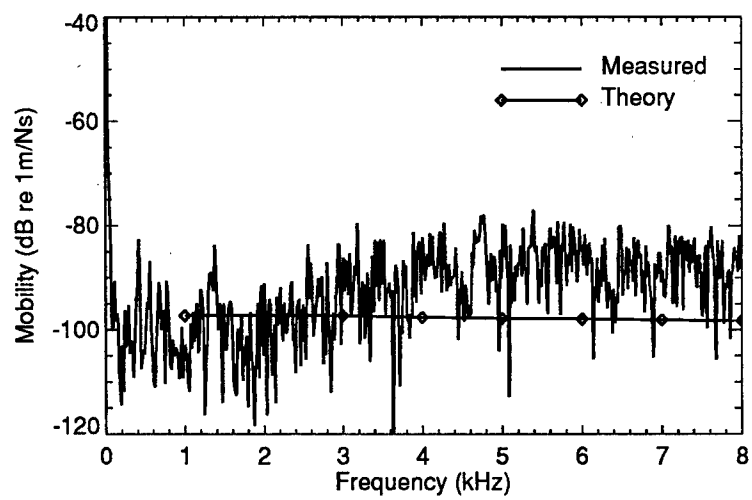

Figure 23: Transfer Mobility, Symmetric T-Plate Intersection Input, Plate 6

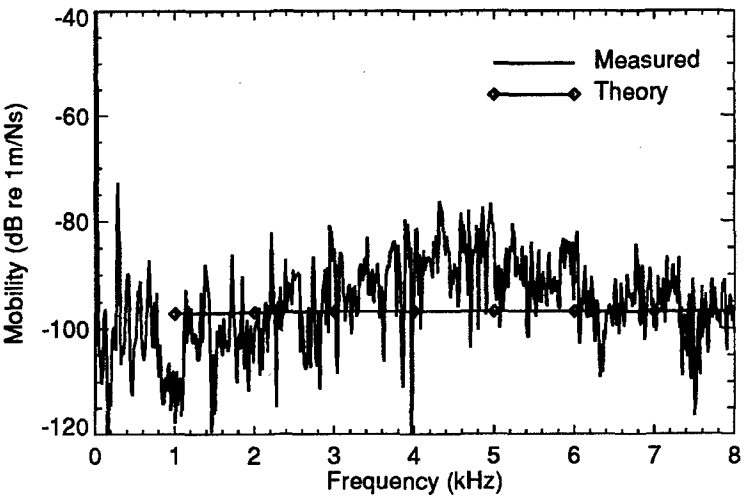

Figure 24: Transfer Mobility, Symmetric T-Plate Intersection Input, Plate 7

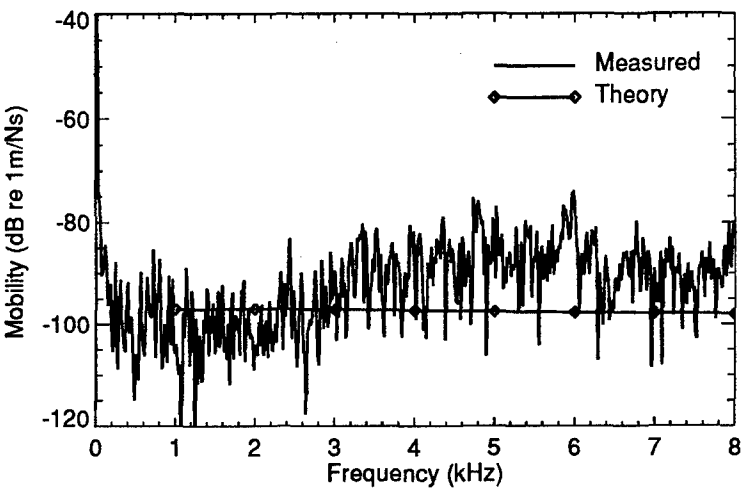

Figure 25: Transfer Mobility, Symmetric T-Plate Intersection Input, Plate 18

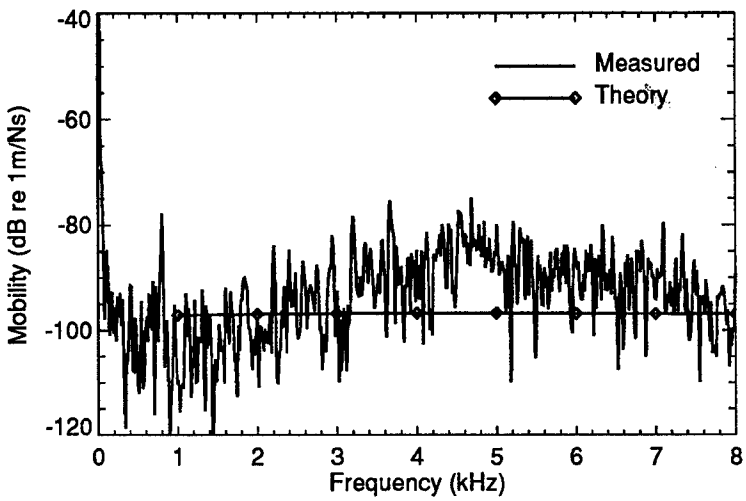

Figure 26: Transfer Mobility, Symmetric T-Plate Intersection Input, Plate 19

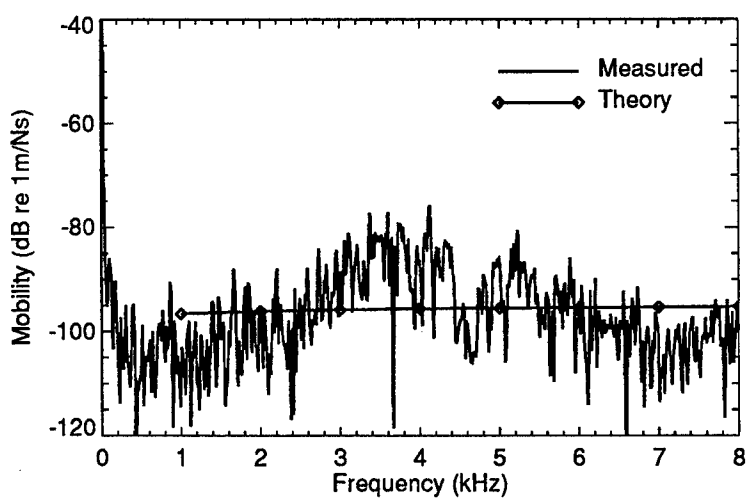

Figure 27: Transfer Mobility, Symmetric T-Plate Intersection Input, Plate 22

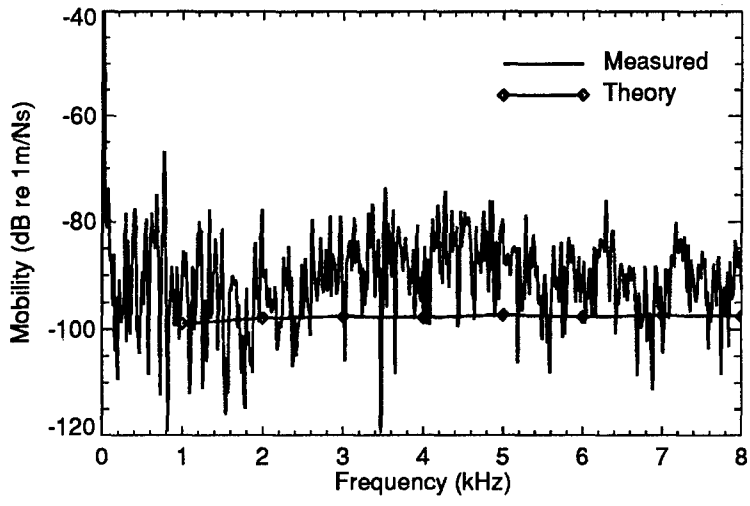

Figure 28: Transfer Mobility, L-Plate Intersection Input, Plate 1

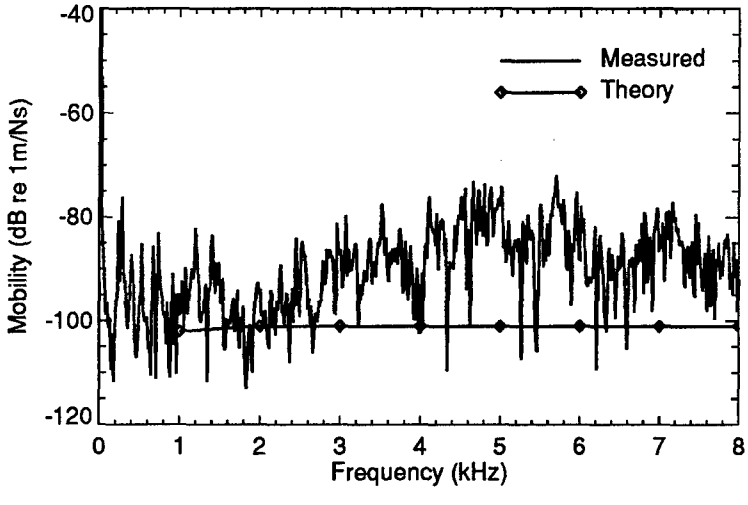

Figure 29: Transfer Mobility, L-Plate Intersection Input, Plate 6

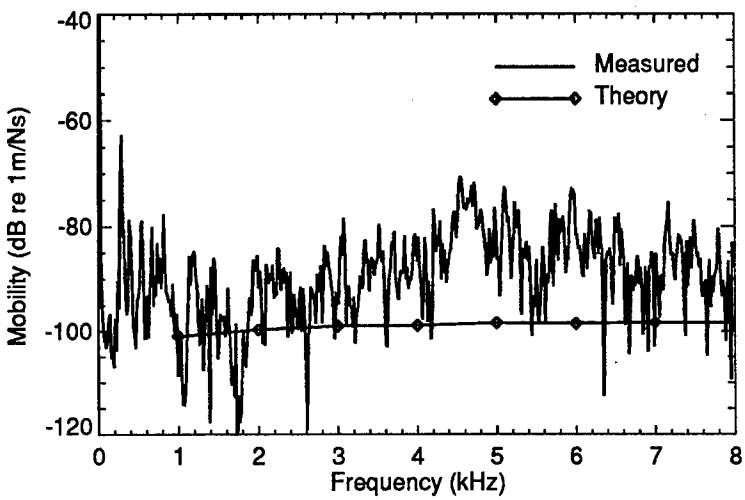

Figure 30: Transfer Mobility, L-Plate Intersection Input, Plate 7

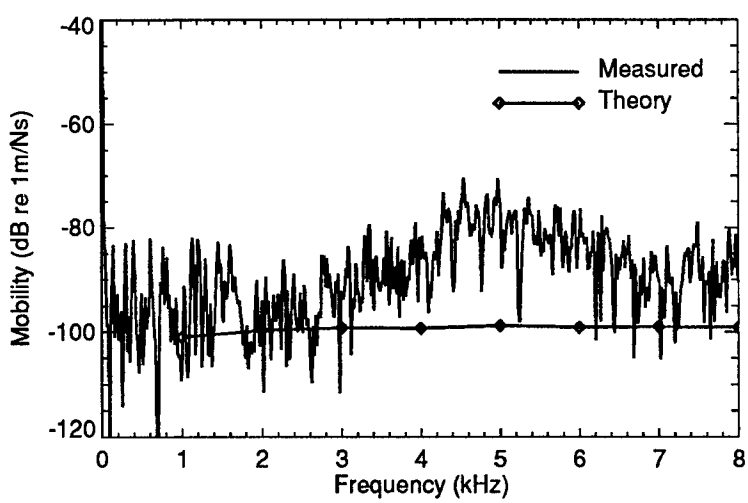

Figure 31: Transfer Mobility, L-Plate Intersection Input, Plate 18

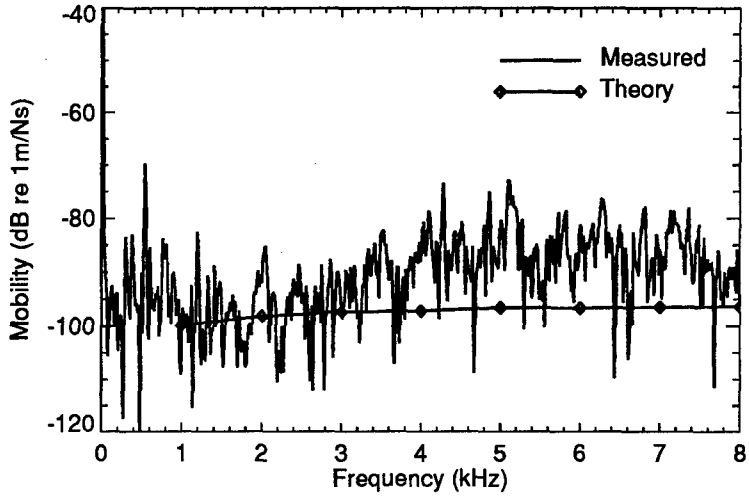

Figure 32: Transfer Mobility, L-Plate Intersection Input, Plate 19

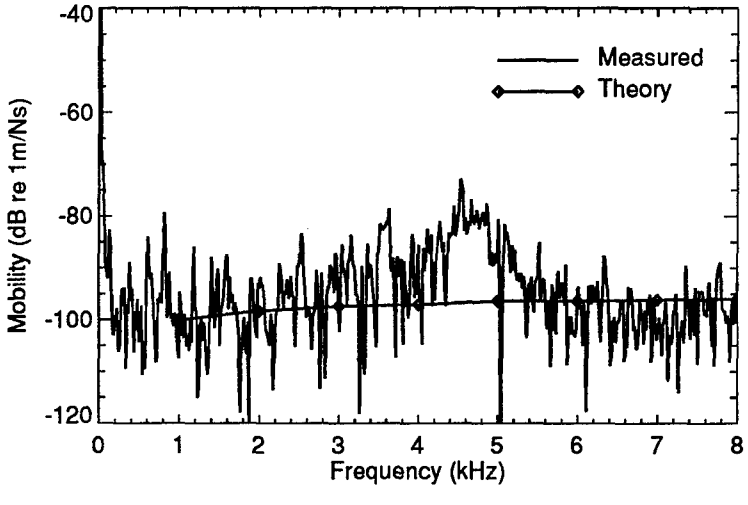

Figure 33: Transfer Mobility, L-Plate Intersection Input, Plate 22

6 Conclusions

Experiments were performed with DREA's ship tank test model to assist in the validation of the PFFEA software for high frequency structural vibrations. The test model was placed on a wooden frame in the Heavy Engine Lab at DREA and an electromagnetic shaker was installed so that it rested on a layer of viscoelastic damping material on the floor of the lab and the stinger was attached to a force transducer located on a mounting block attached to the test model. The shaker was excited with the burst chirp signal covering frequencies from 0 Hz to 8 kHz. Four sets of trials were performed with the shaker in one of four positions. These included the centre of the thin plate at the bottom of the centre tank, the intersection of one of the internal walls with the centre plate at the midpoint in the transverse direction (an unsymmetric T-plate junction), the intersection of three plates of the same thickness (a symmetric T-plate junction), and the outside edge of the test model at the midpoint in the transverse direction (an L-plate junction).

Input mobility measurements were taken for each drive point and, for each shaker location, the transfer mobility for each of the 37 panels in the model was recorded over the 8 kHz frequency band. The input mobilities predicted by the PFFEA code compared extremely well (in a frequency-averaged sense) with the experimental measurements. While the power flow method is unable to accurately predict the response in frequency regions of low modal density (in this case frequencies up to about 3 kHz), the model accurately predicted the average behaviour for all four cases. When looking at the response of the ship tank panels, in general, the PFFEA program was able to predict the level of the transfer mobility with some degree of accuracy. However, there were significant variations with frequency in the measured data which were not modelled with the PFFEA code. As a result, the PFFEA program should primarily be used when predictions are required over a band of frequencies rather than in support of a harmonic analysis.

The PFFEA program was able to accurately predict the average input mobility to the system for a structure that is a good approximation to structures commonly encountered on naval platforms. Using the predicted inputs, the program was able to give a reasonably accurate description of the level of the response throughout the structure over a relatively wide frequency band. Future validations for the code would benefit from measuring the response over a particular band rather than the narrow band measurements used here. This could be accomplished by analyzing the existing results and converting the narrow band results to 1/3-octave bands. Further investigations should also be performed into validating the performance of accelerometers and force transducers and the various mounting techniques to widen the frequency band which could be considered. To date, the PFFEA code has only been validated against laboratory scale measurements and has not been used to predict either in-air or underwater radiated noise. Further tests of the DREA ring-stiffened cylinder (with an internal deck added) are planned to examine in-air radiated noise (and possibly underwater radiated noise) and the DREA Acoustic Calibration Barge will be used as a test bed to validate the program for fluid-loaded plates.

A Transfer Mobility

The following plots show the complete set of measured transfer mobilities for all four sets of tests. Figures 34 to 70 show the panel responses for the centre plate location of the shaker, Figures 71 to 107 show the responses for the unsymmetric plate intersection, Figures 108 to 144 show the responses for the symmetric plate intersection, and Figures 145 to 181 show the responses for the L-plate intersection.

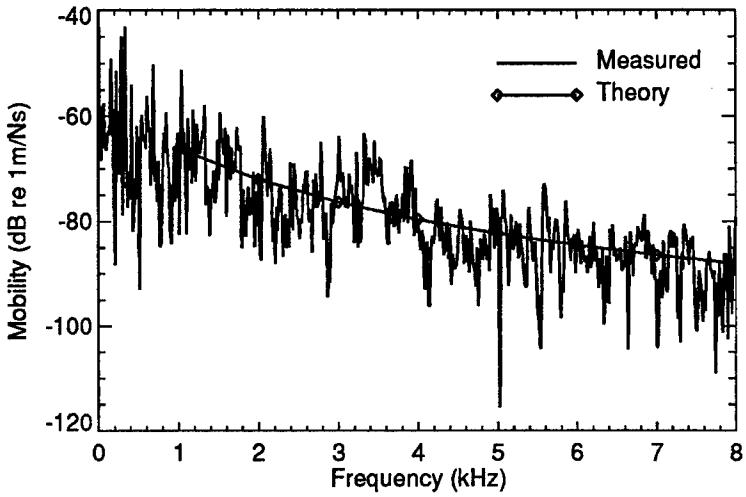

Figure 34: Transfer Mobility, Centre Plate Input, Plate 1

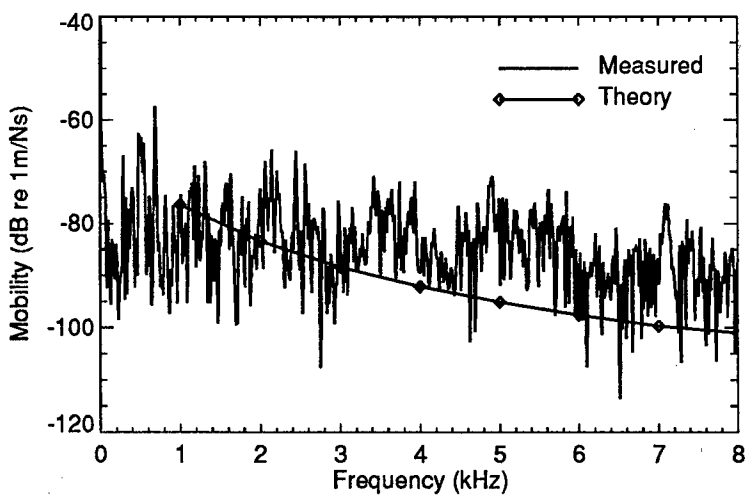

Figure 35: Transfer Mobility, Centre Plate Input, Plate 2

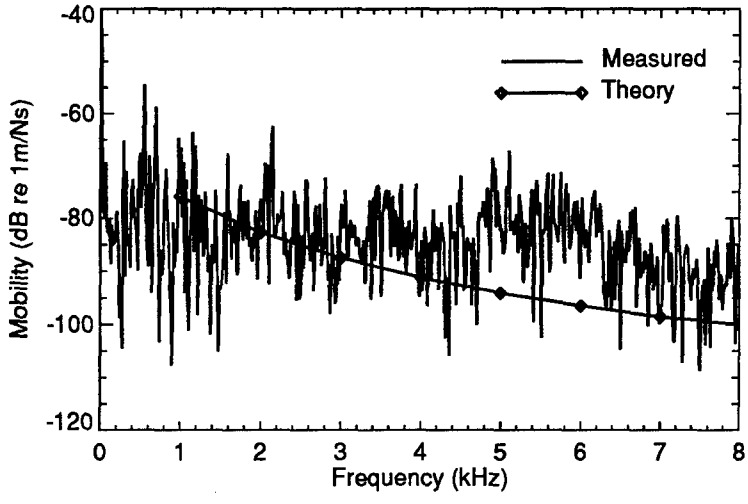

Figure 36: Transfer Mobility, Centre Plate Input, Plate 3

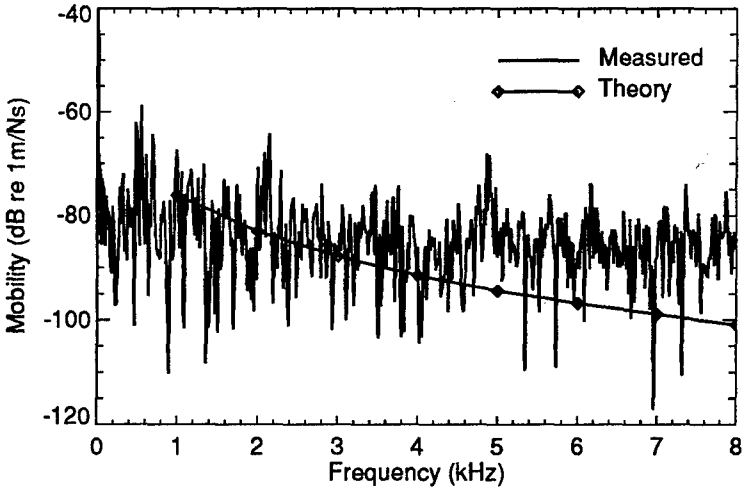

Figure 37: Transfer Mobility, Centre Plate Input, Plate 4

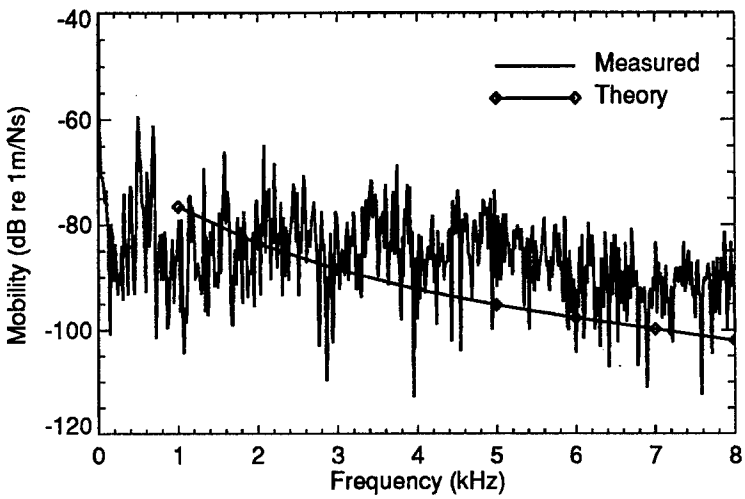

Figure 38: Transfer Mobility, Centre Plate Input, Plate 5

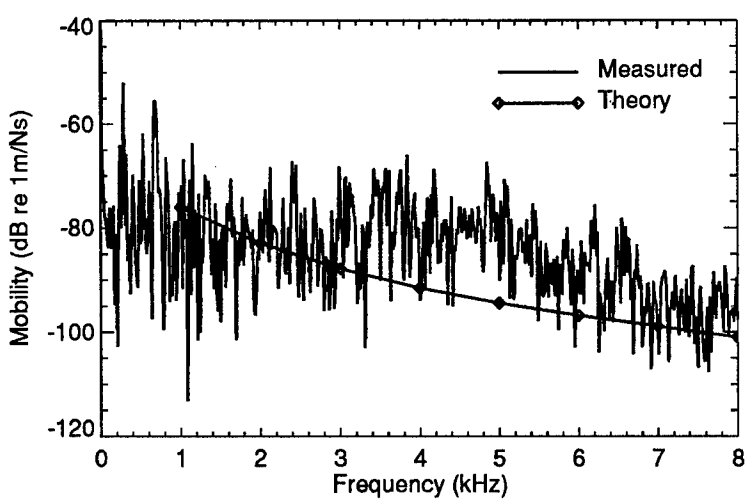

Figure 39: Transfer Mobility, Centre Plate Input, Plate 6

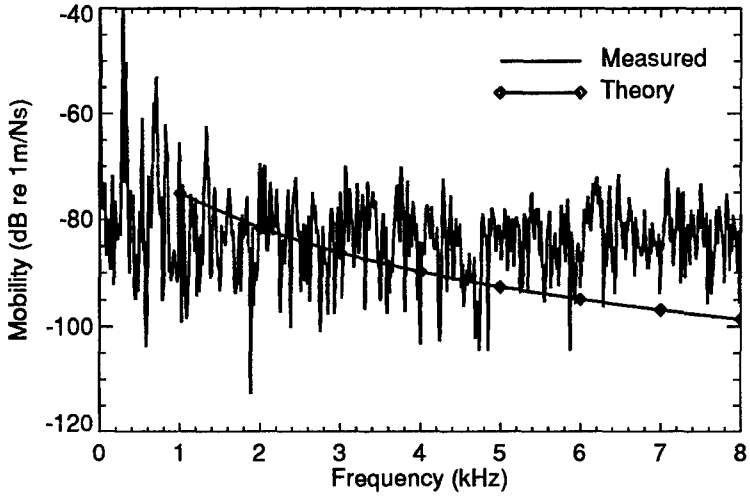

Figure 40: Transfer Mobility, Centre Plate Input, Plate 7

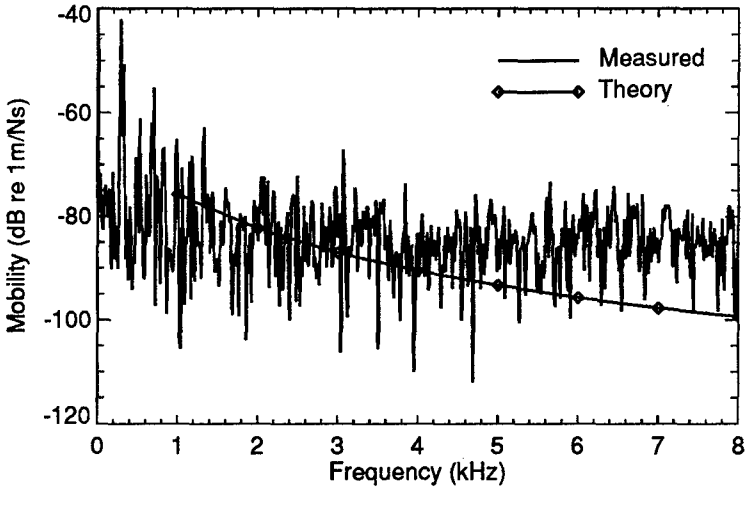

Figure 41: Transfer Mobility, Centre Plate Input, Plate 8

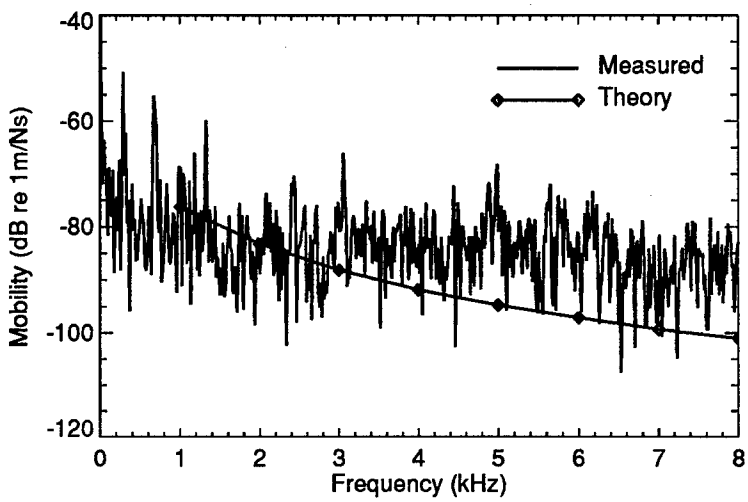

Figure 42: Transfer Mobility, Centre Plate Input, Plate 9

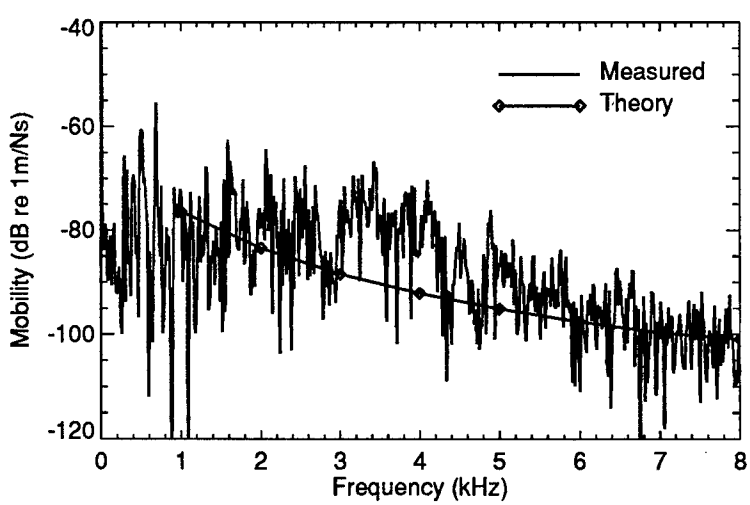

Figure 43: Transfer Mobility, Centre Plate Input, Plate 10

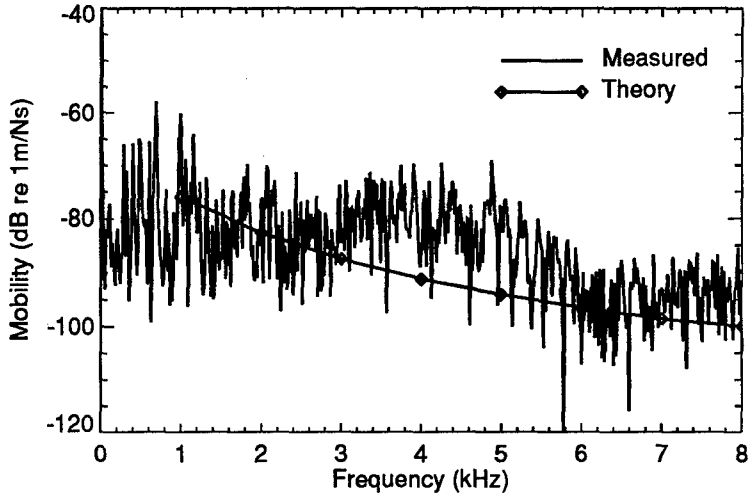

Figure 44: Transfer Mobility, Centre Plate Input, Plate 11

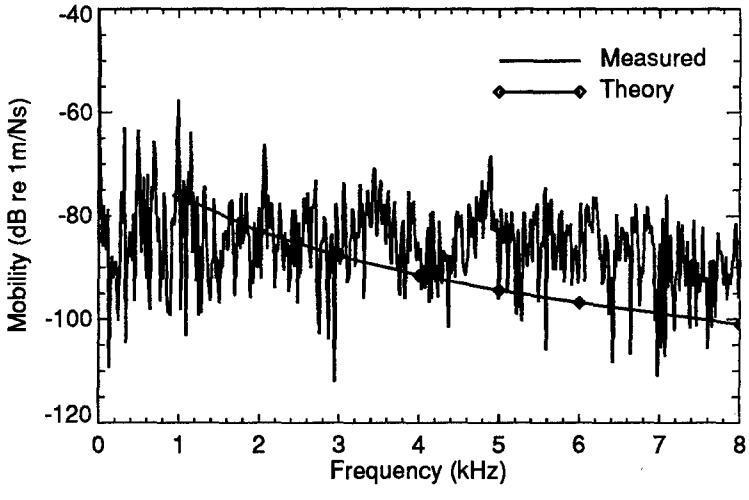

Figure 45: Transfer Mobility, Centre Plate Input, Plate 12

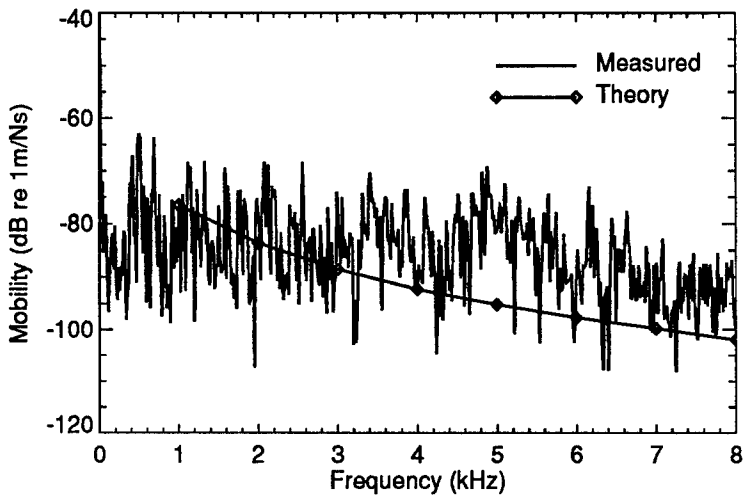

Figure 46: Transfer Mobility, Centre Plate Input, Plate 13

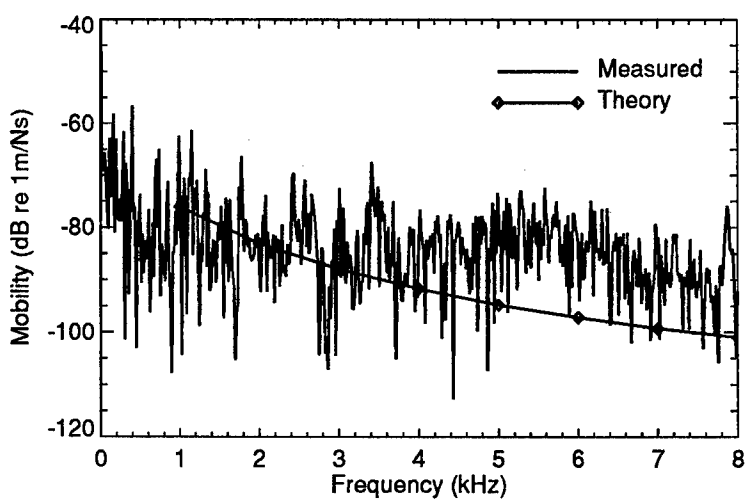

Figure 47: Transfer Mobility, Centre Plate Input, Plate 14

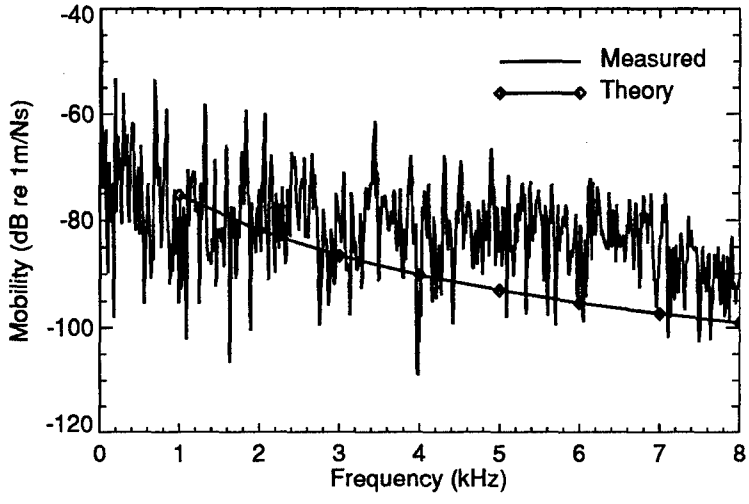

Figure 48: Transfer Mobility, Centre Plate Input, Plate 15

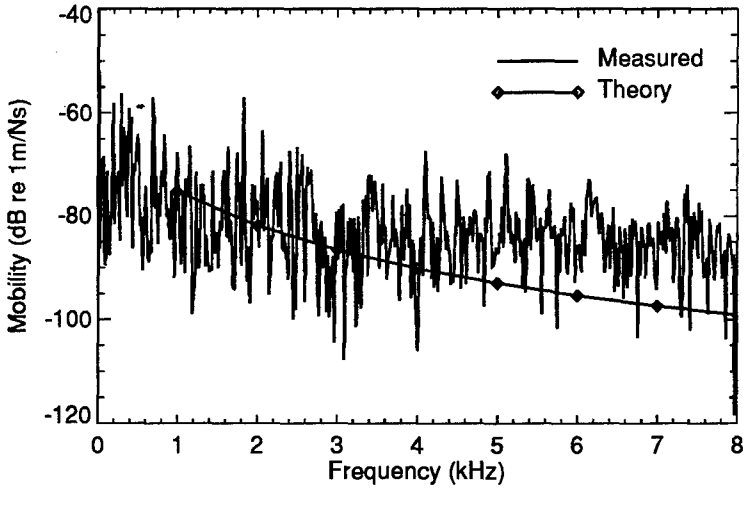

Figure 49: Transfer Mobility, Centre Plate Input, Plate 16

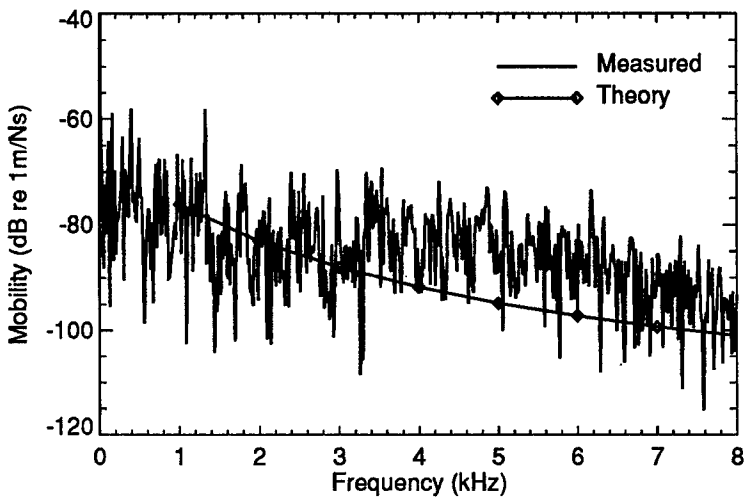

Figure 50: Transfer Mobility, Centre Plate Input, Plate 17

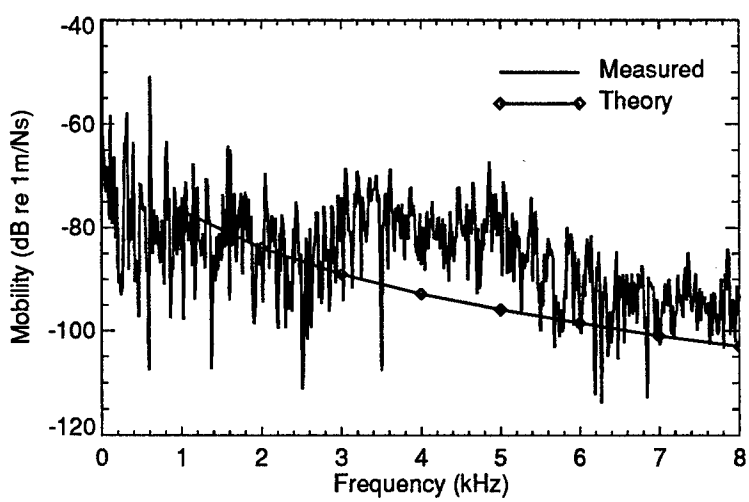

Figure 51: Transfer Mobility, Centre Plate Input, Plate 18

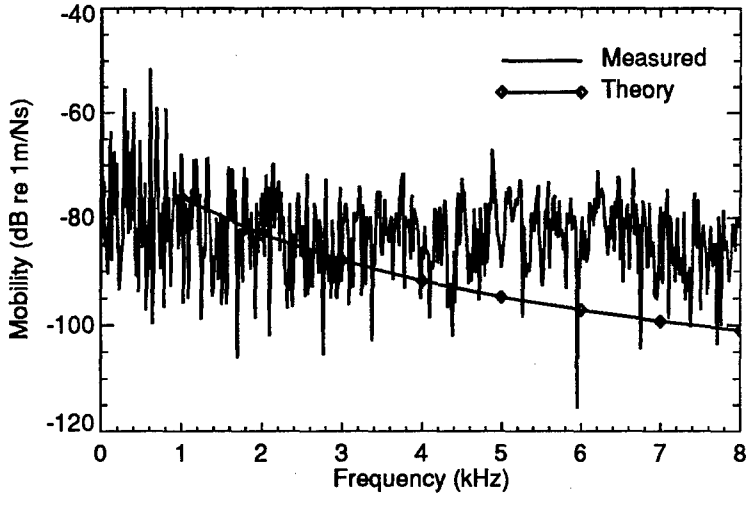

Figure 52: Transfer Mobility, Centre Plate Input, Plate 19

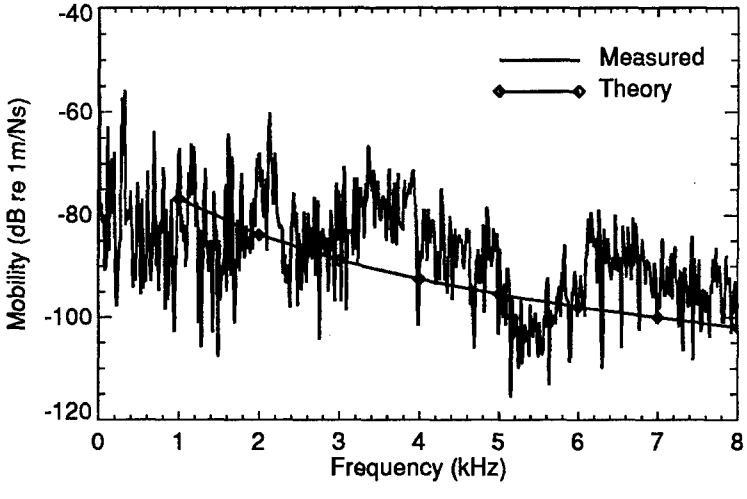

Figure 53: Transfer Mobility, Centre Plate Input, Plate 20

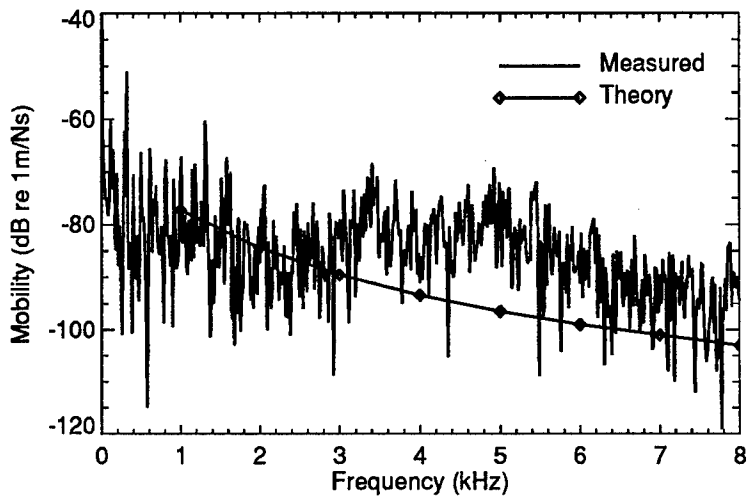

Figure 54: Transfer Mobility, Centre Plate Input, Plate 21

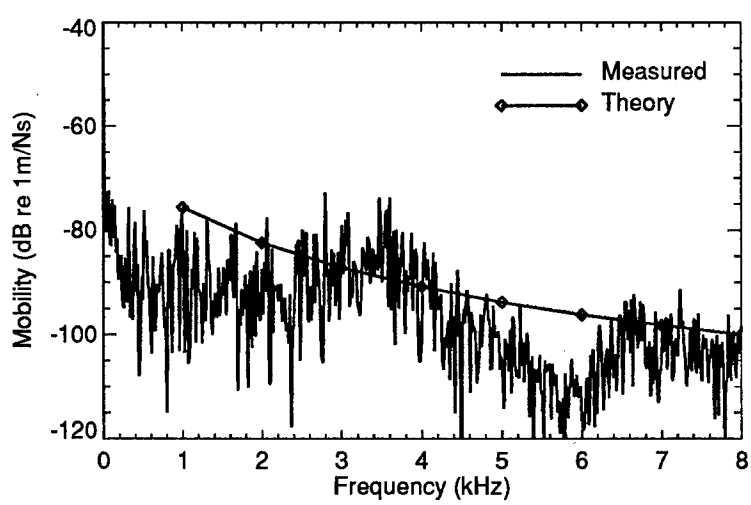

Figure 55: Transfer Mobility, Centre Plate Input, Plate 22

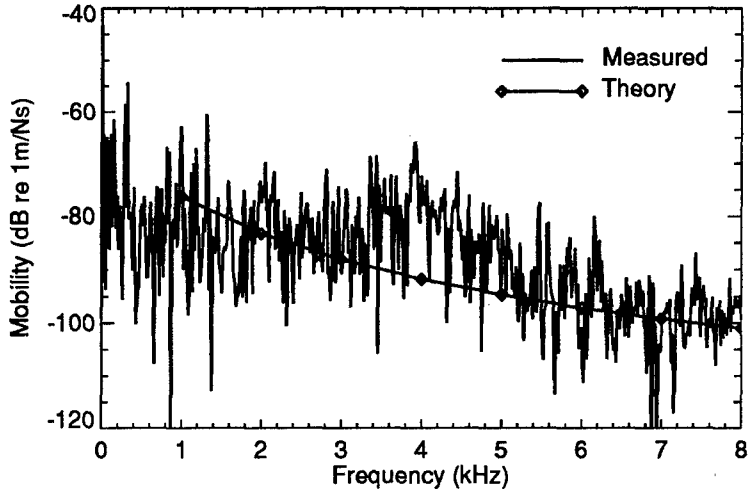

Figure 56: Transfer Mobility, Centre Plate Input, Plate 23

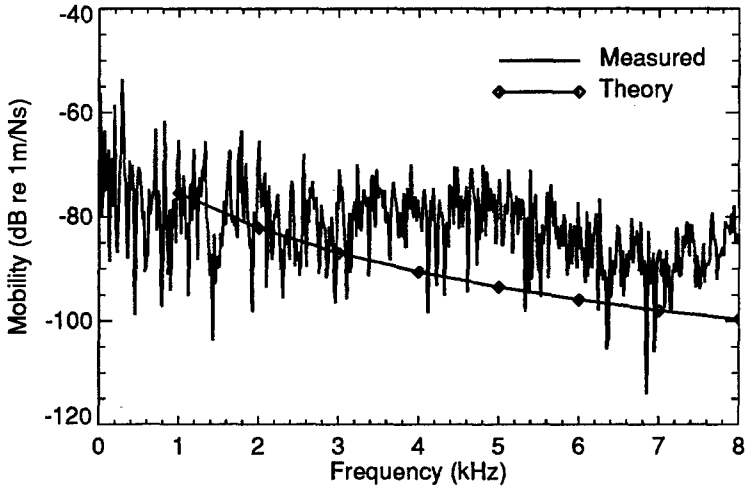

Figure 57: Transfer Mobility, Centre Plate Input, Plate 24

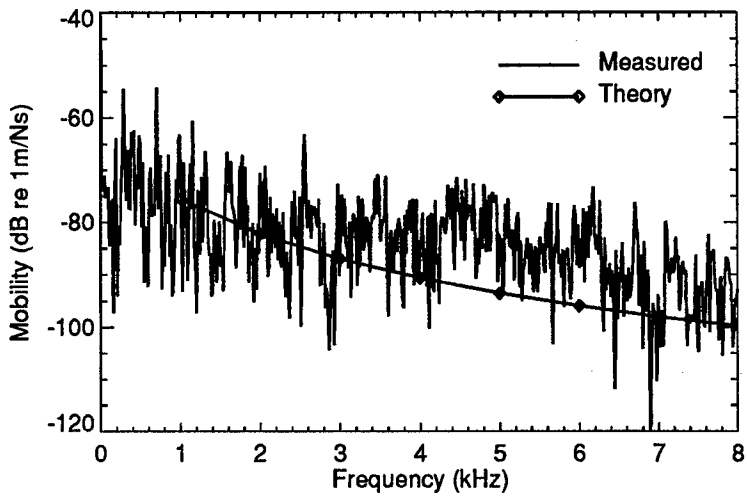

Figure 58: Transfer Mobility, Centre Plate Input, Plate 25

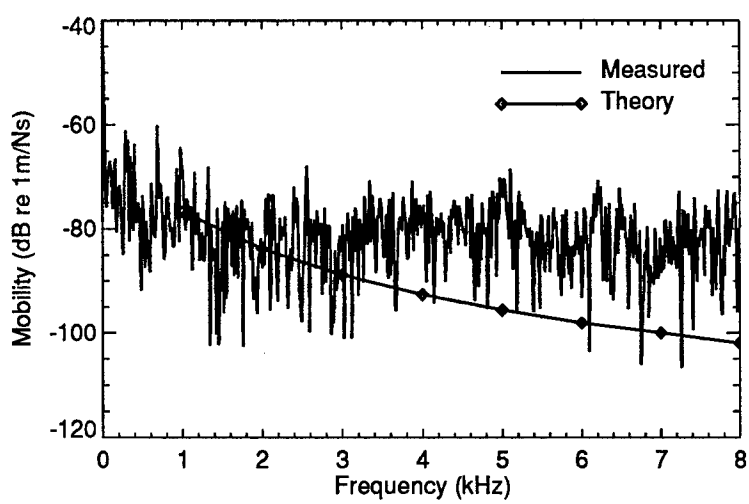

Figure 59: Transfer Mobility, Centre Plate Input, Plate 26

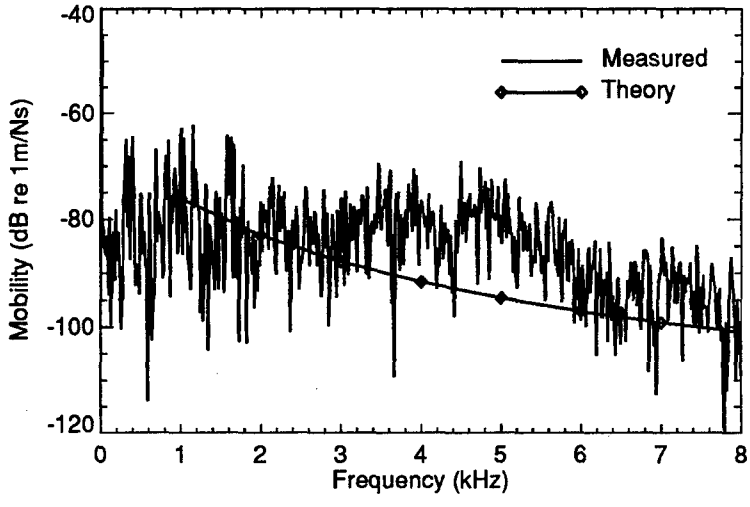

Figure 60: Transfer Mobility, Centre Plate Input, Plate 27

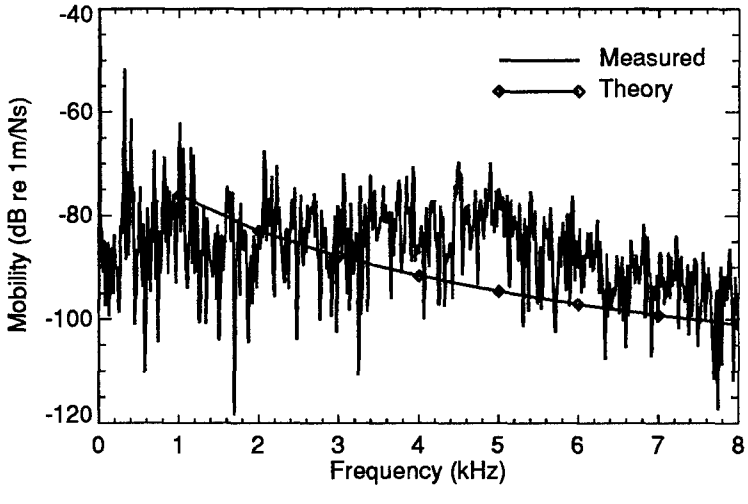

Figure 61: Transfer Mobility, Centre Plate Input, Plate 28

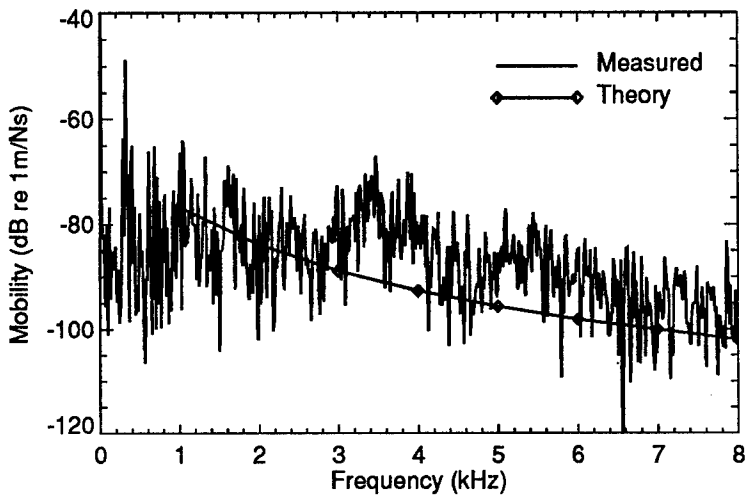

Figure 62: Transfer Mobility, Centre Plate Input, Plate 29

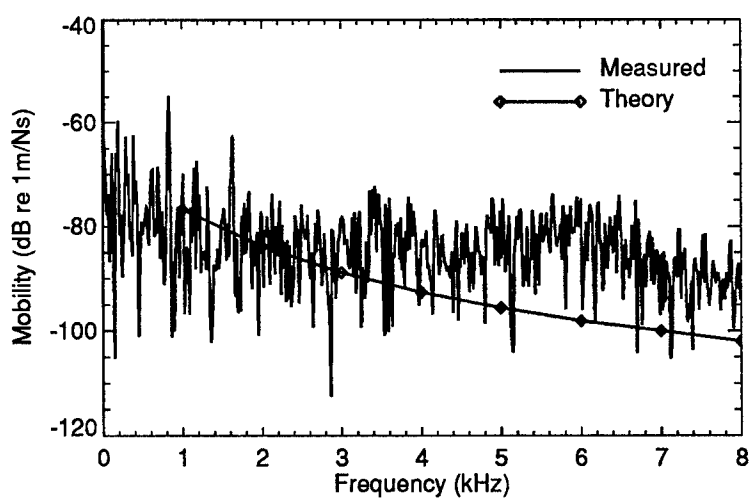

Figure 63: Transfer Mobility, Centre Plate Input, Plate 30

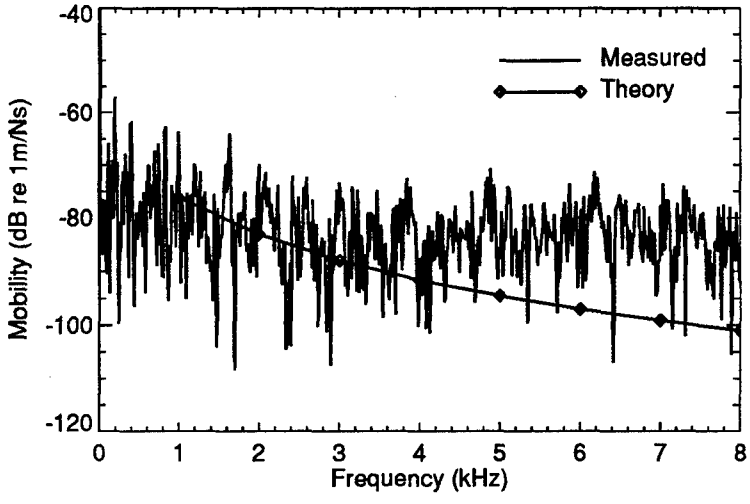

Figure 64: Transfer Mobility, Centre Plate Input, Plate 31

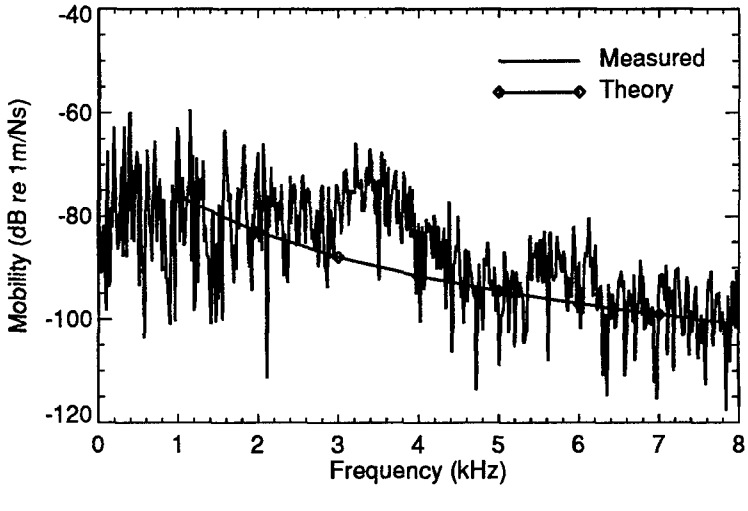

Figure 65: Transfer Mobility, Centre Plate Input, Plate 32

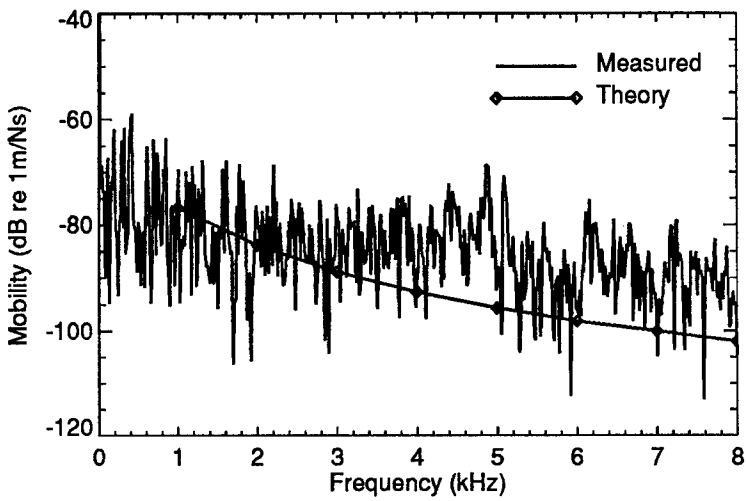

Figure 66: Transfer Mobility, Centre Plate Input, Plate 33

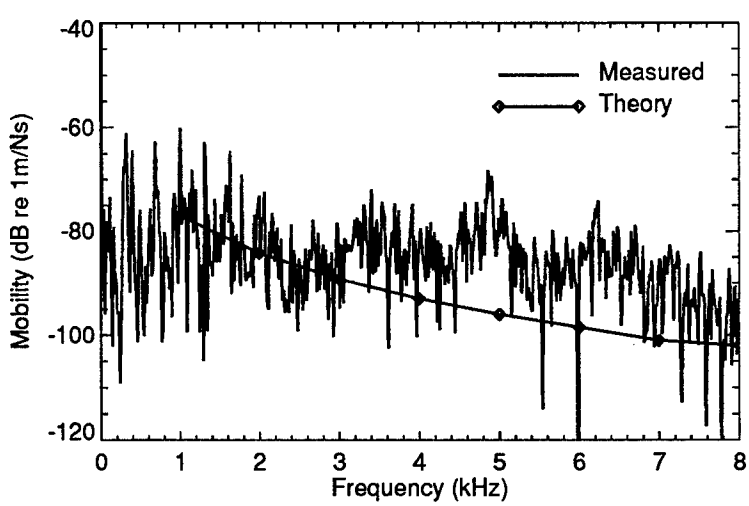

Figure 67: Transfer Mobility, Centre Plate Input, Plate 34

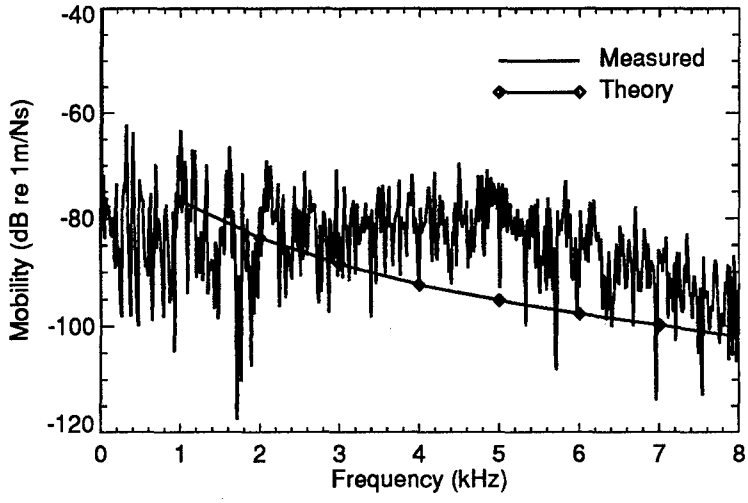

Figure 68: Transfer Mobility, Centre Plate Input, Plate 35

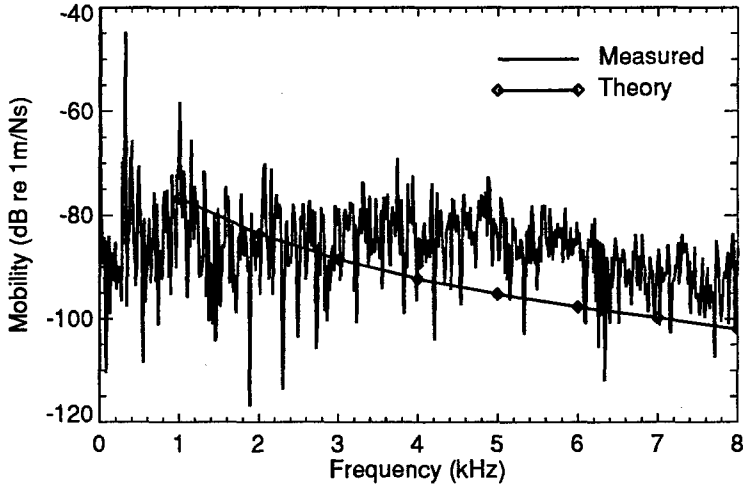

Figure 69: Transfer Mobility, Centre Plate Input, Plate 36

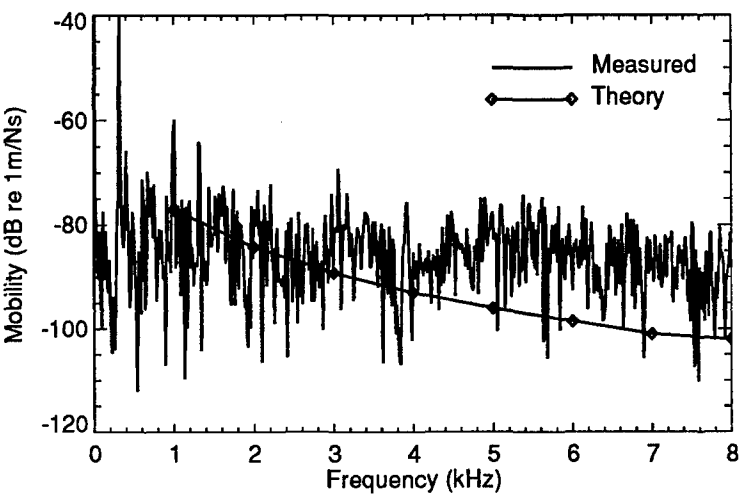

Figure 70: Transfer Mobility, Centre Plate Input, Plate 37

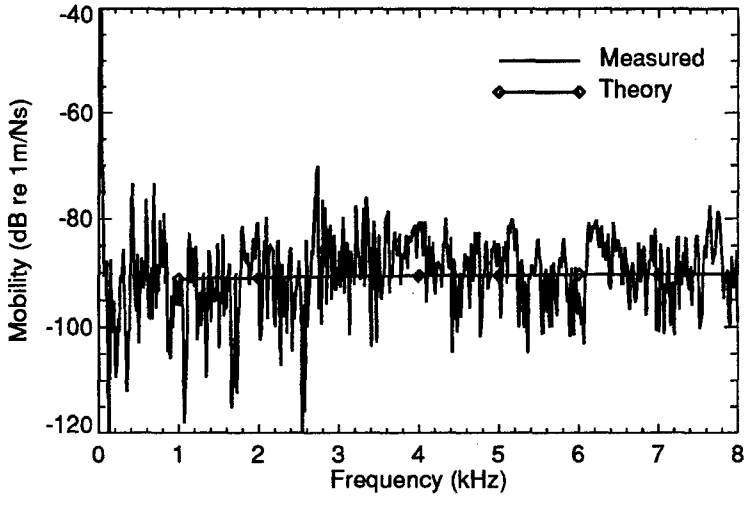

Figure 71: Transfer Mobility, Unsymmetric T-Plate Intersection Input, Plate 1

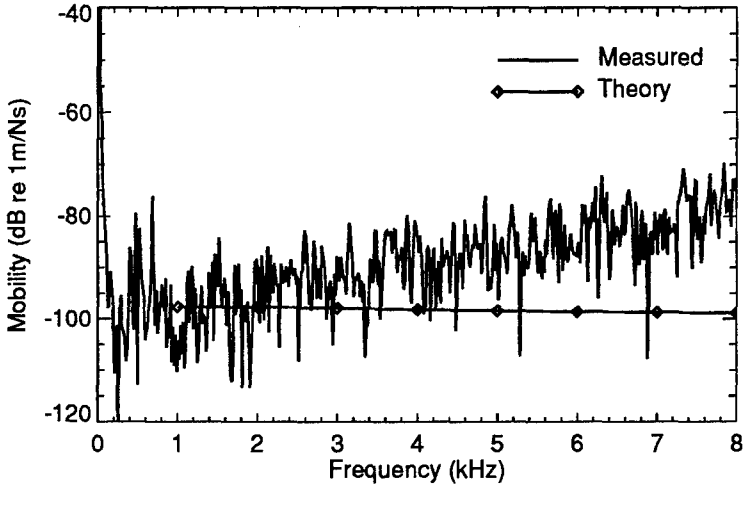

Figure 72: Transfer Mobility, Unsymmetric T-Plate Intersection Input, Plate 2

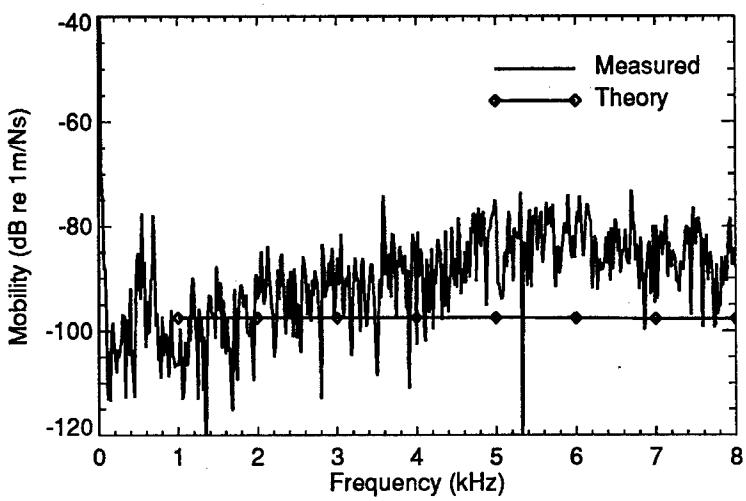

Figure 73: Transfer Mobility, Unsymmetric T-Plate Intersection Input, Plate 3

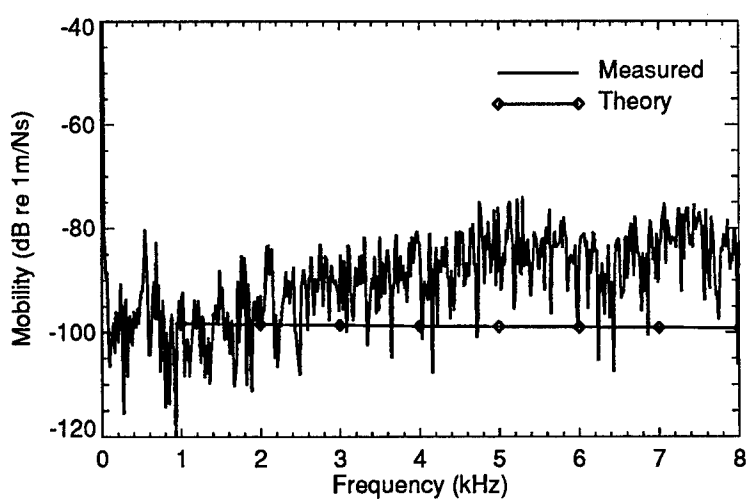

Figure 74: Transfer Mobility, Unsymmetric T-Plate Intersection Input, Plate 4

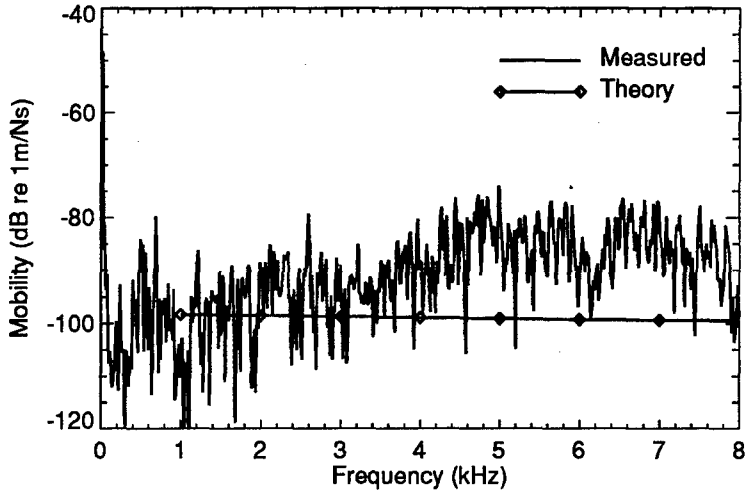

Figure 75: Transfer Mobility, Unsymmetric T-Plate Intersection Input, Plate 5

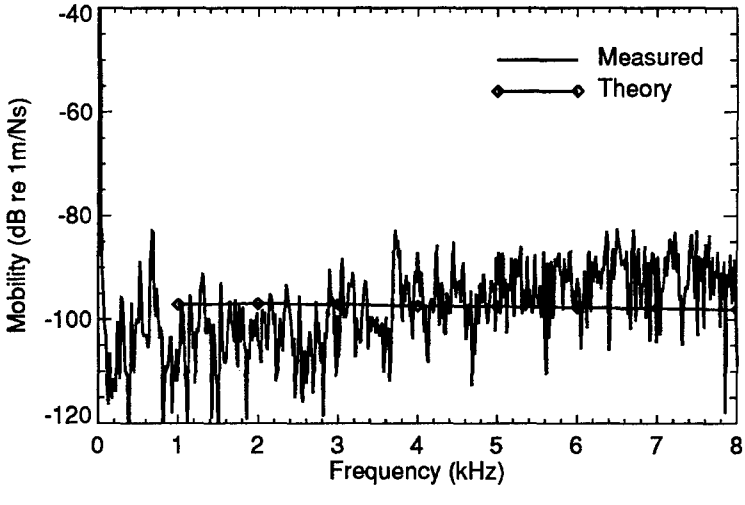

Figure 76: Transfer Mobility, Unsymmetric T-Plate Intersection Input, Plate 6

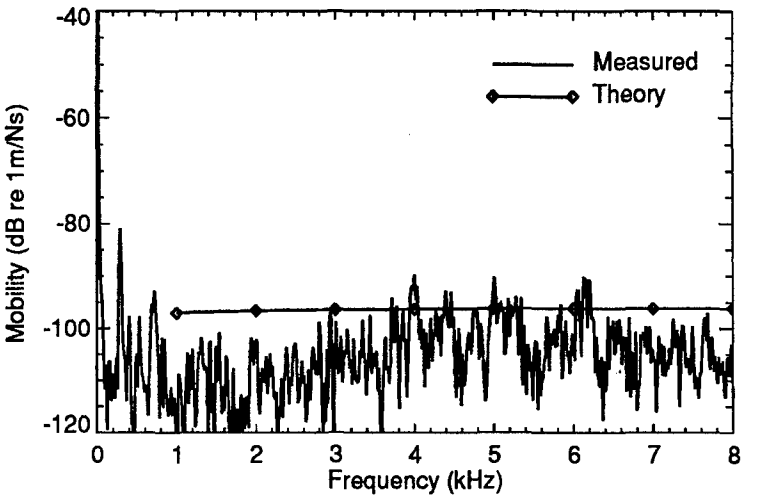

Figure 77: Transfer Mobility, Unsymmetric T-Plate Intersection Input, Plate 7

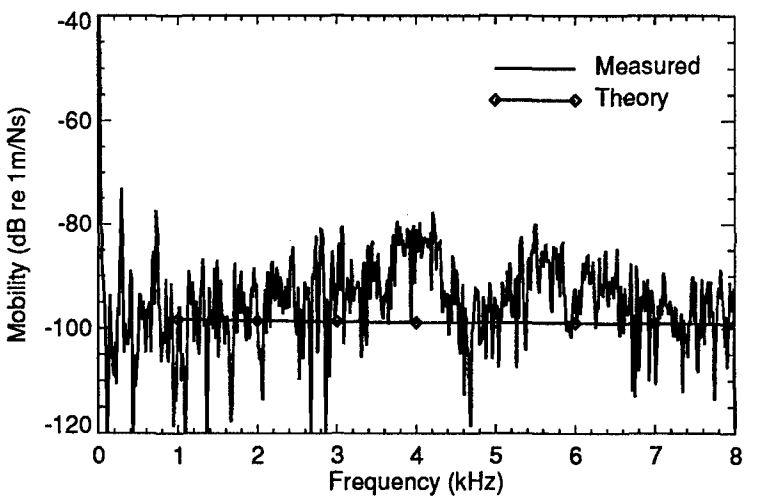

Figure 78: Transfer Mobility, Unsymmetric T-Plate Intersection Input, Plate 8

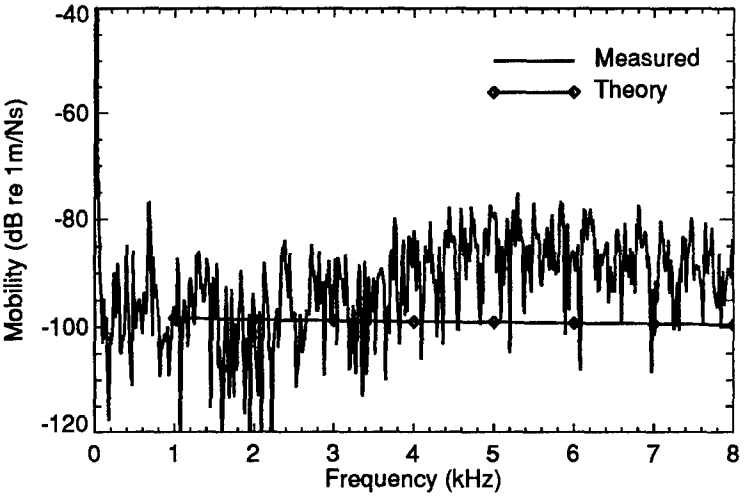

Figure 79: Transfer Mobility, Unsymmetric T-Plate Intersection Input, Plate 9

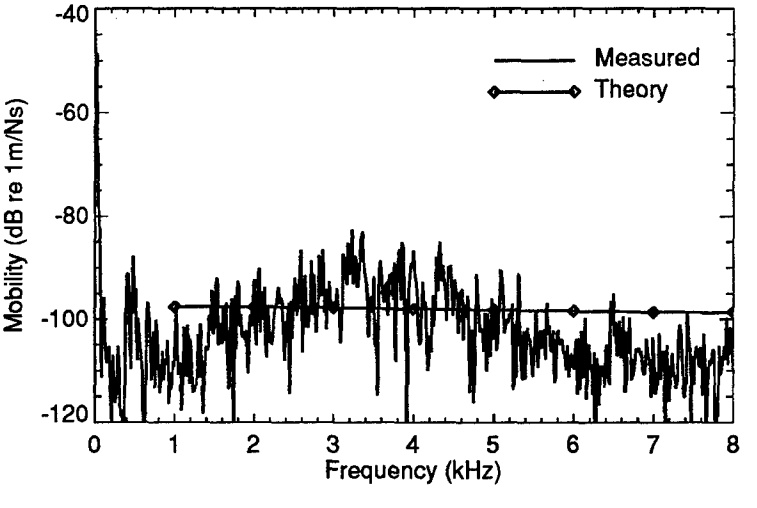

Figure 80: Transfer Mobility, Unsymmetric T-Plate Intersection Input, Plate 10

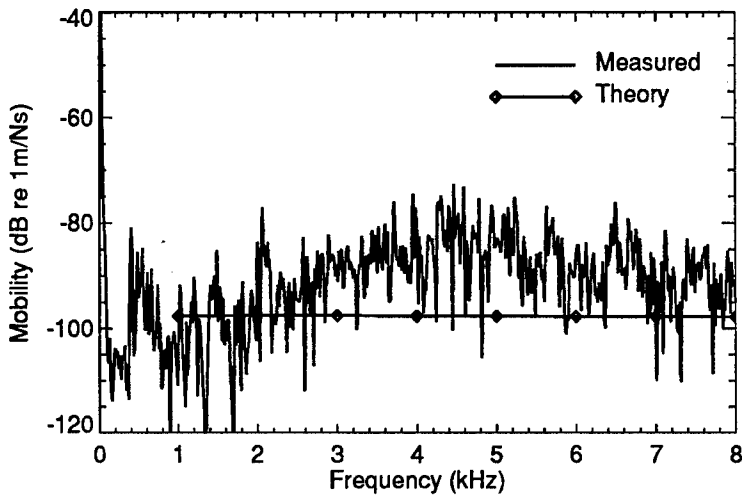

Figure 81: Transfer Mobility, Unsymmetric T-Plate Intersection Input, Plate 11

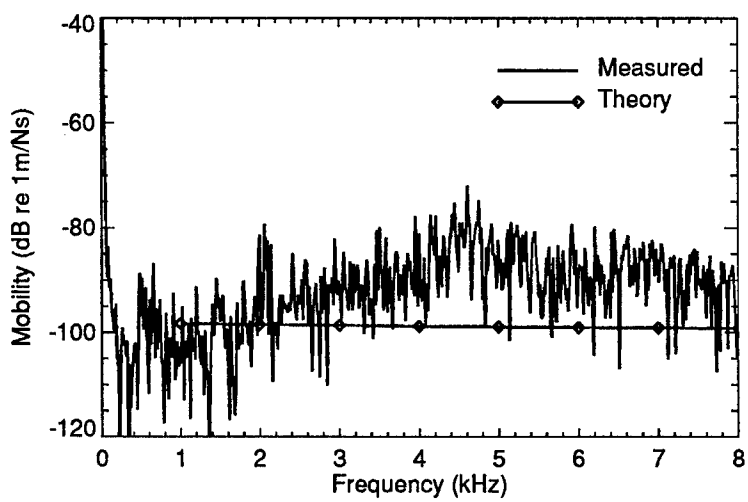

Figure 82: Transfer Mobility, Unsymmetric T-Plate Intersection Input, Plate 12

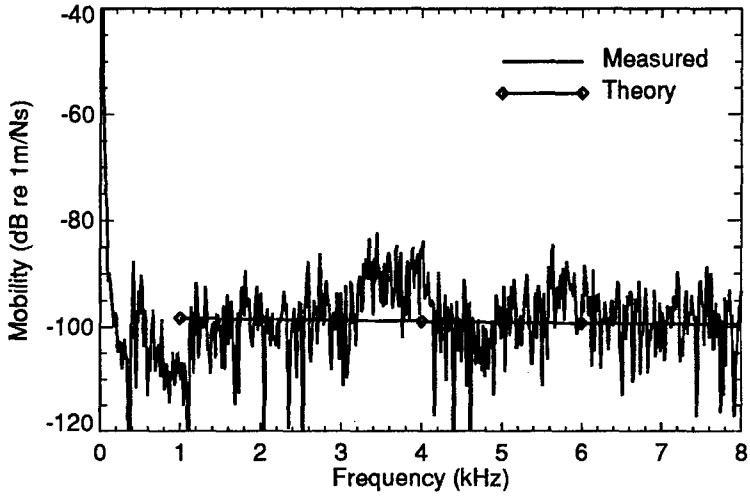

Figure 83: Transfer Mobility, Unsymmetric T-Plate Intersection Input, Plate 13

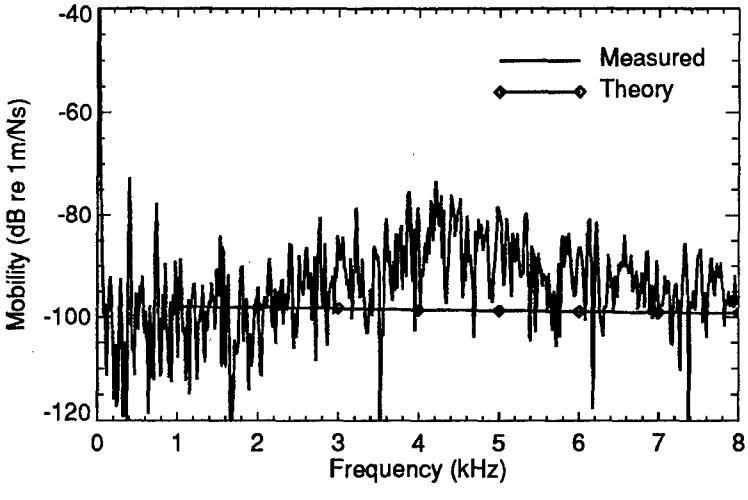

Figure 84: Transfer Mobility, Unsymmetric T-Plate Intersection Input, Plate 14

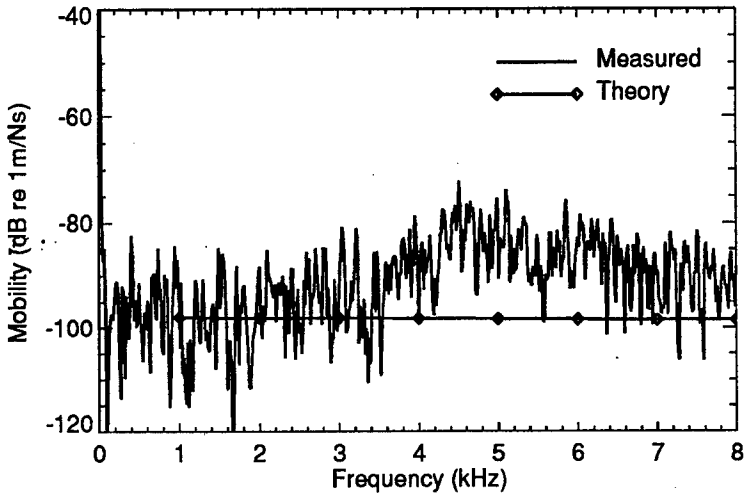

Figure 85: Transfer Mobility, Unsymmetric T-Plate Intersection Input, Plate 15

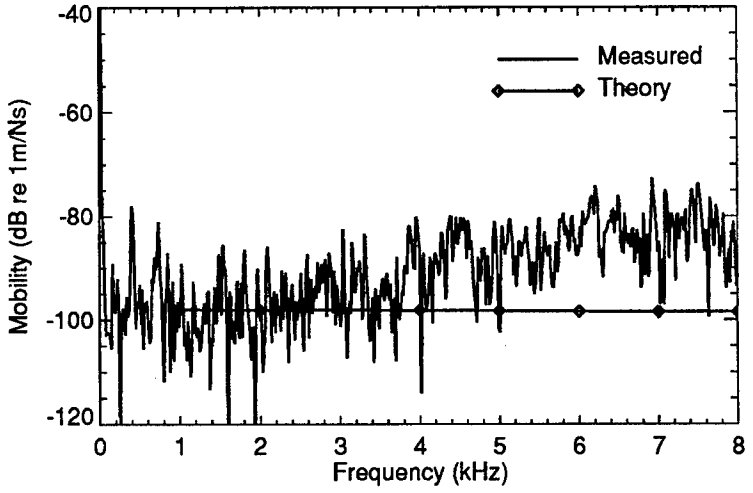

Figure 86: Transfer Mobility, Unsymmetric T-Plate Intersection Input, Plate 16

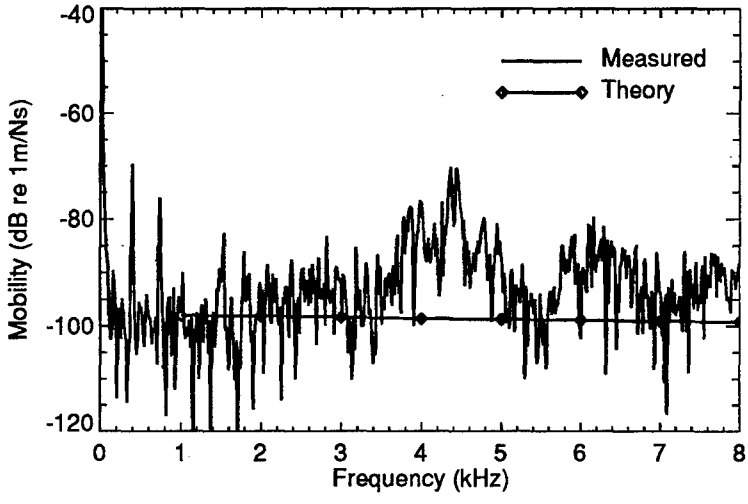

Figure 87: Transfer Mobility, Unsymmetric T-Plate Intersection Input, Plate 17

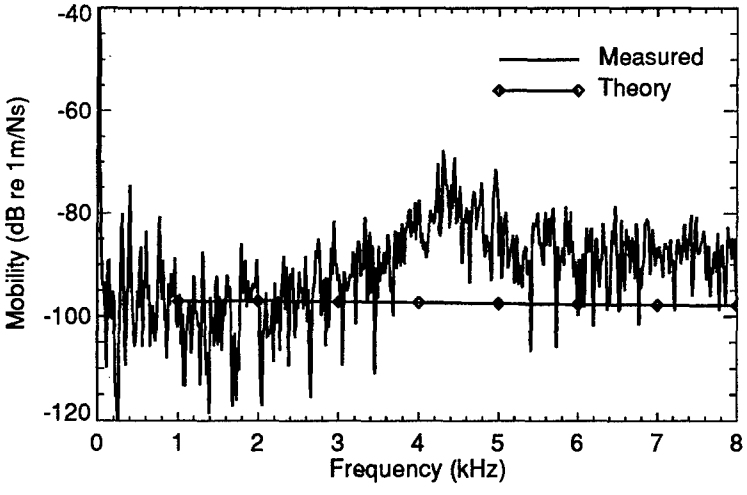

Figure 88: Transfer Mobility, Unsymmetric T-Plate Intersection Input, Plate 18

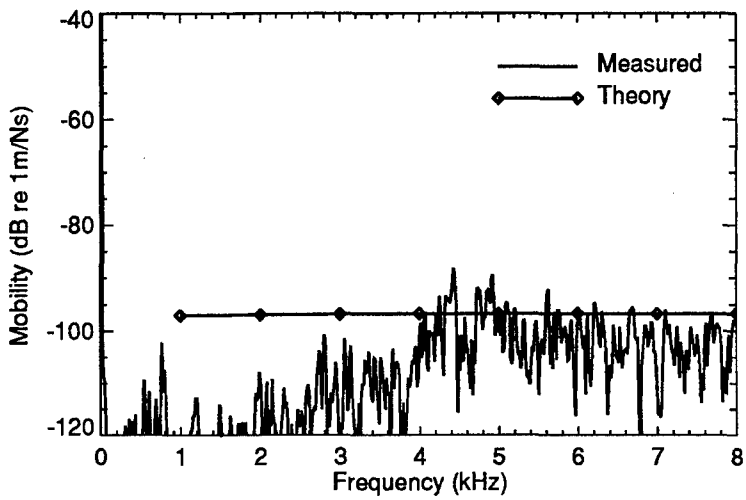

Figure 89: Transfer Mobility, Unsymmetric T-Plate Intersection Input, Plate 19

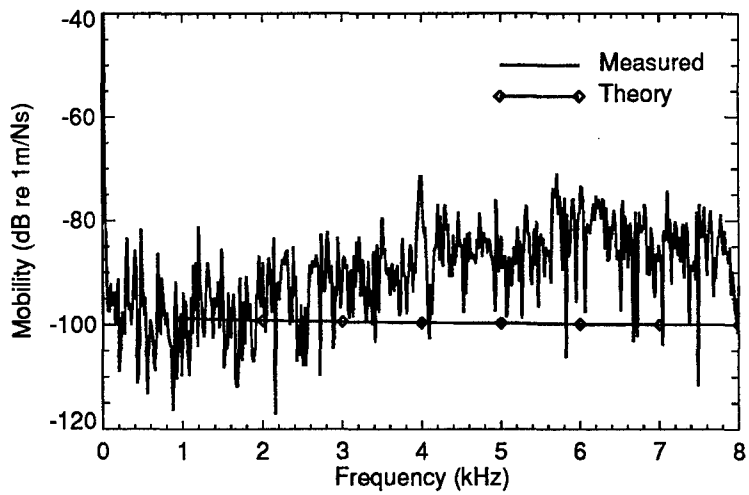

Figure 90: Transfer Mobility, Unsymmetric T-Plate Intersection Input, Plate 20

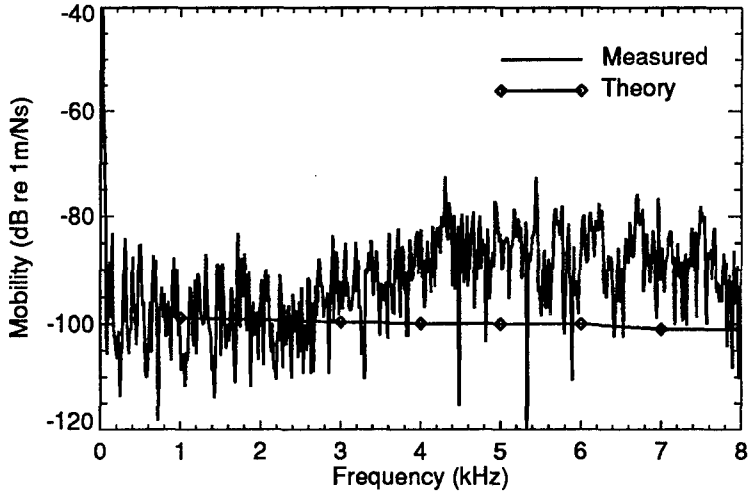

Figure 91: Transfer Mobility, Unsymmetric T-Plate Intersection Input, Plate 21

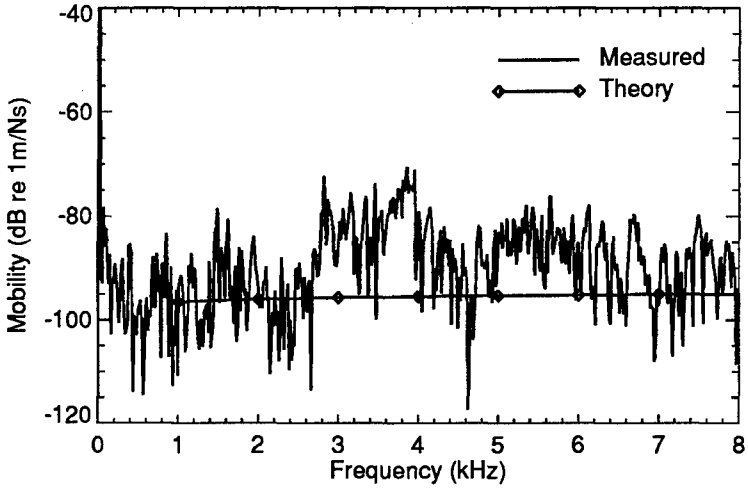

Figure 92: Transfer Mobility, Unsymmetric T-Plate Intersection Input, Plate 22

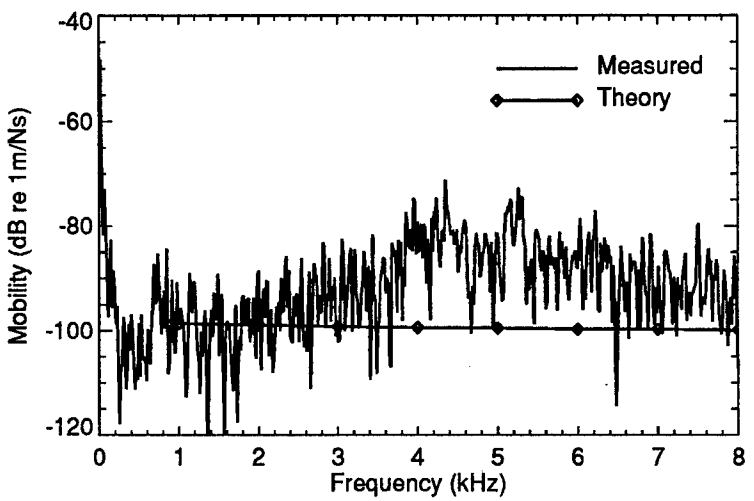

Figure 93: Transfer Mobility, Unsymmetric T-Plate Intersection Input, Plate 23

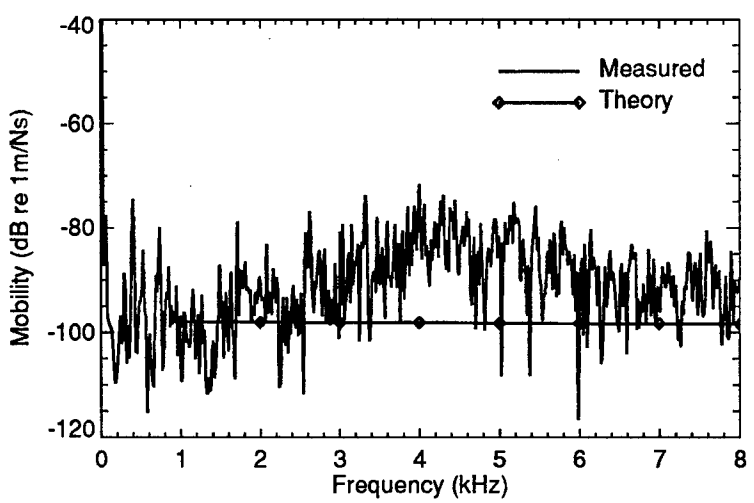

Figure 94: Transfer Mobility, Unsymmetric T-Plate Intersection Input, Plate 24

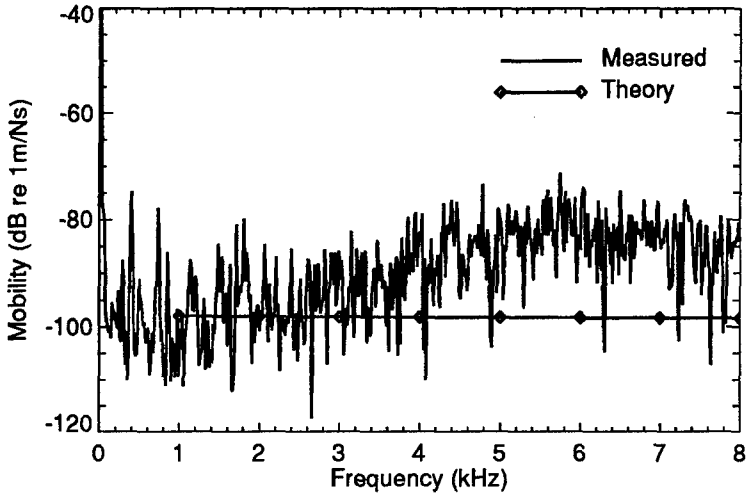

Figure 95: Transfer Mobility, Unsymmetric T-Plate Intersection Input, Plate 25

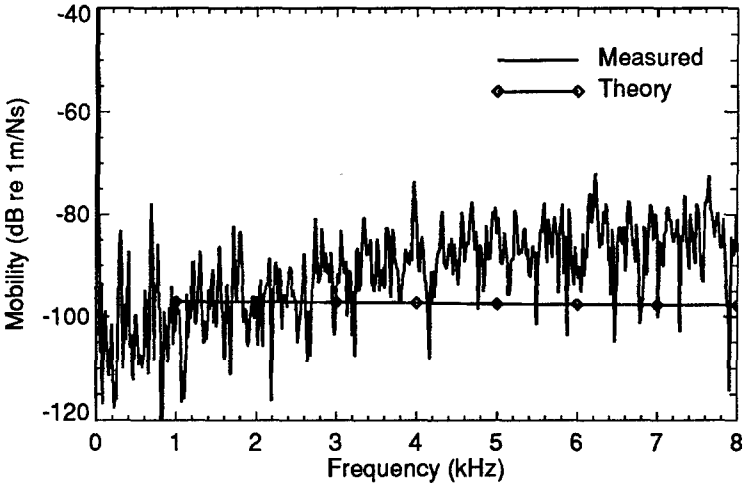

Figure 96: Transfer Mobility, Unsymmetric T-Plate Intersection Input, Plate 26

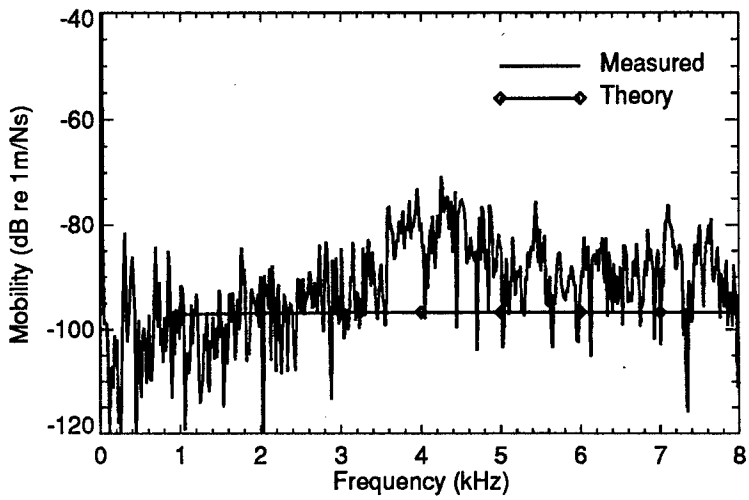

Figure 97: Transfer Mobility, Unsymmetric T-Plate Intersection Input, Plate 27

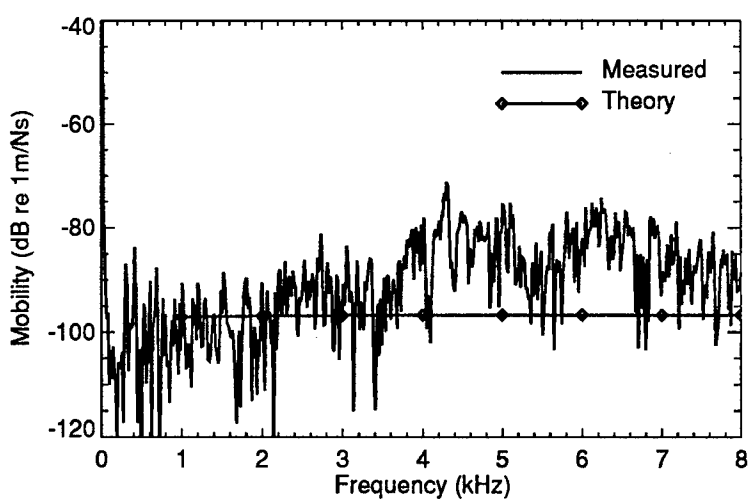

Figure 98: Transfer Mobility, Unsymmetric T-Plate Intersection Input, Plate 28

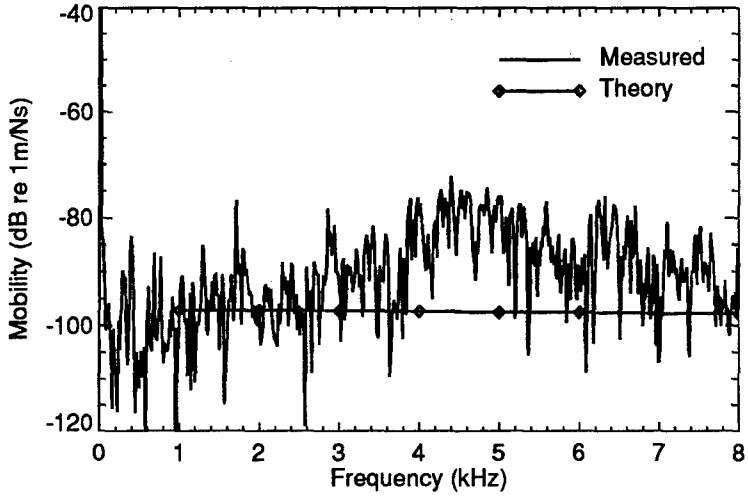

Figure 99: Transfer Mobility, Unsymmetric T-Plate Intersection Input, Plate 29

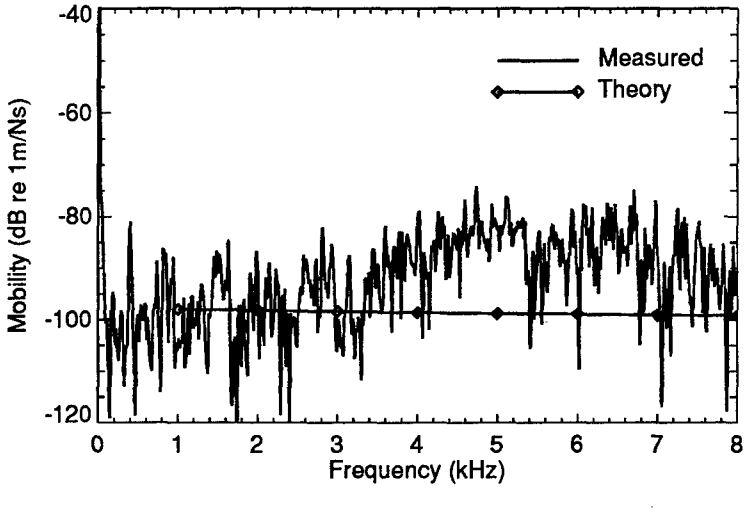

Figure 100: Transfer Mobility, Unsymmetric T-Plate Intersection Input, Plate 30

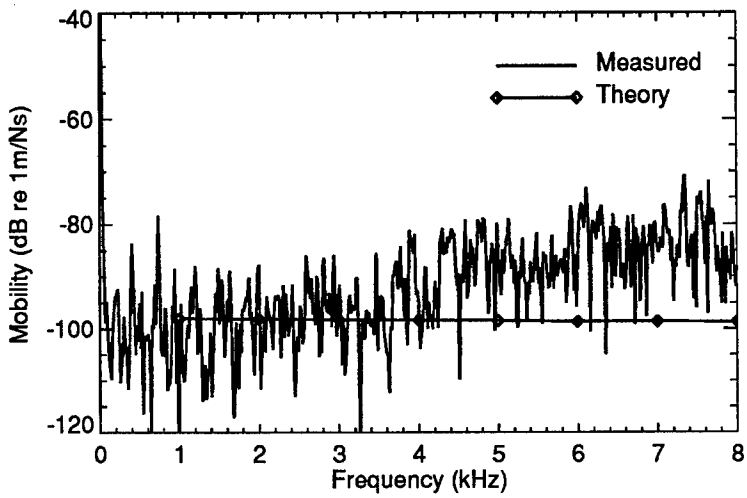

Figure 101: Transfer Mobility, Unsymmetric T-Plate Intersection Input, Plate 31

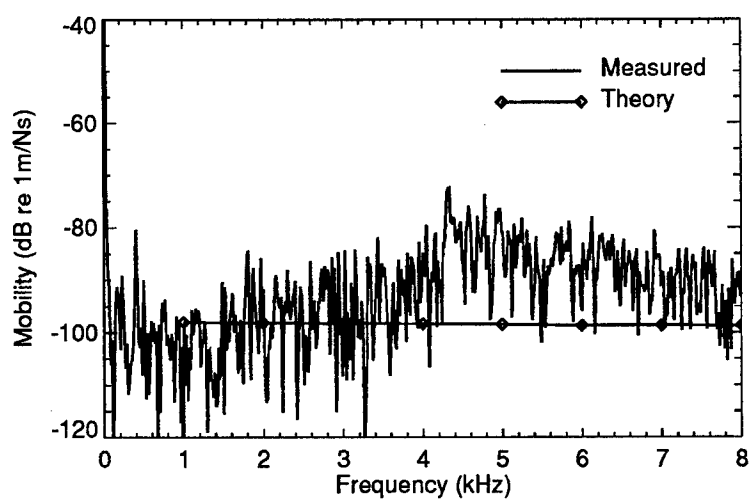

Figure 102: Transfer Mobility, Unsymmetric T-Plate Intersection Input, Plate 32

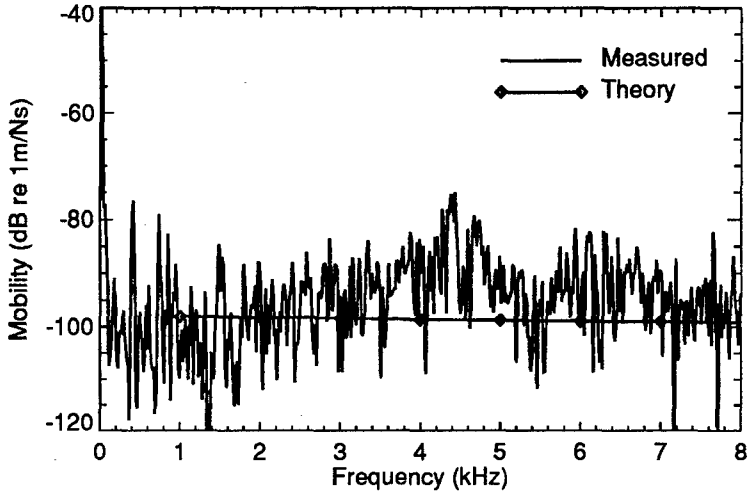

Figure 103: Transfer Mobility, Unsymmetric T-Plate Intersection Input, Plate 33

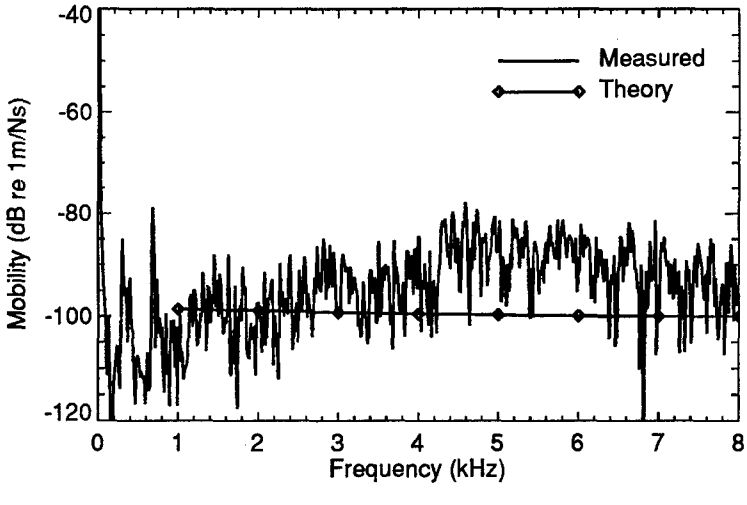

Figure 104: Transfer Mobility, Unsymmetric T-Plate Intersection Input, Plate 34

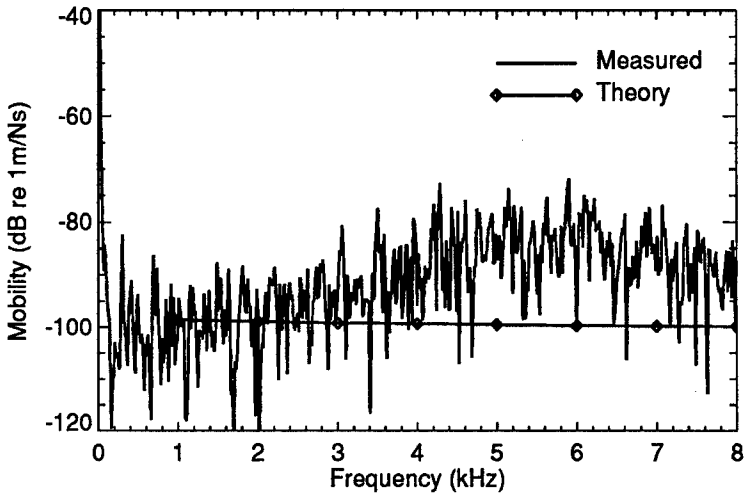

Figure 105: Transfer Mobility, Unsymmetric T-Plate Intersection Input, Plate 35

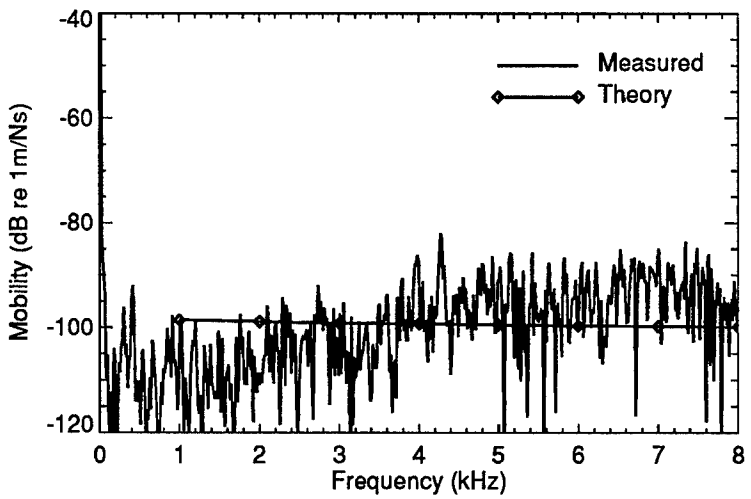

Figure 106: Transfer Mobility, Unsymmetric T-Plate Intersection Input, Plate 36

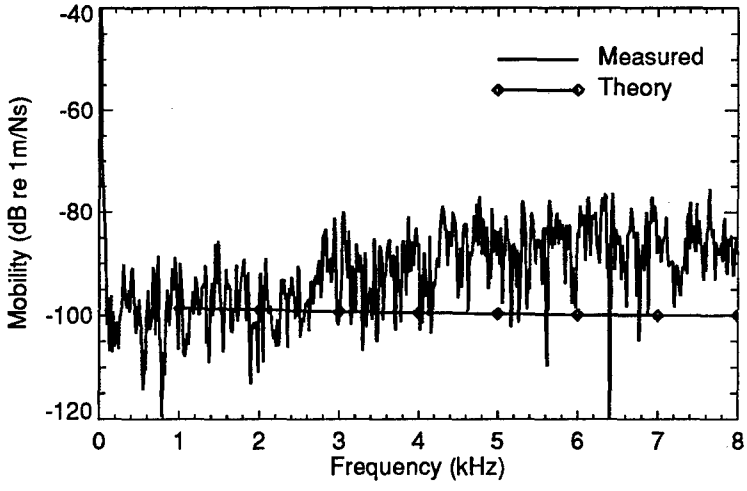

Figure 107: Transfer Mobility, Unsymmetric T-Plate Intersection Input, Plate 37

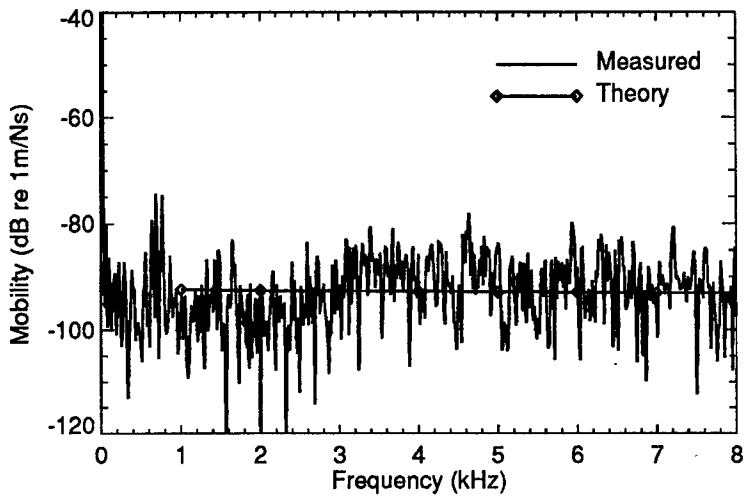

Figure 108: Transfer Mobility, Symmetric T-Plate Intersection Input, Plate 1

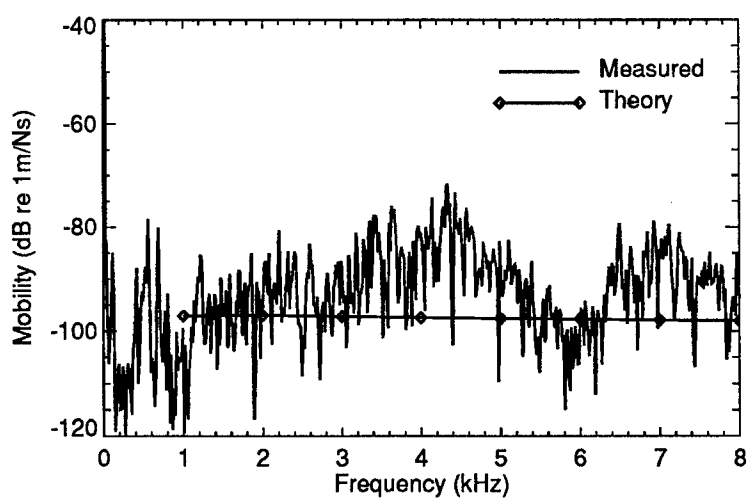

Figure 109: Transfer Mobility, Symmetric T-Plate Intersection Input, Plate 2

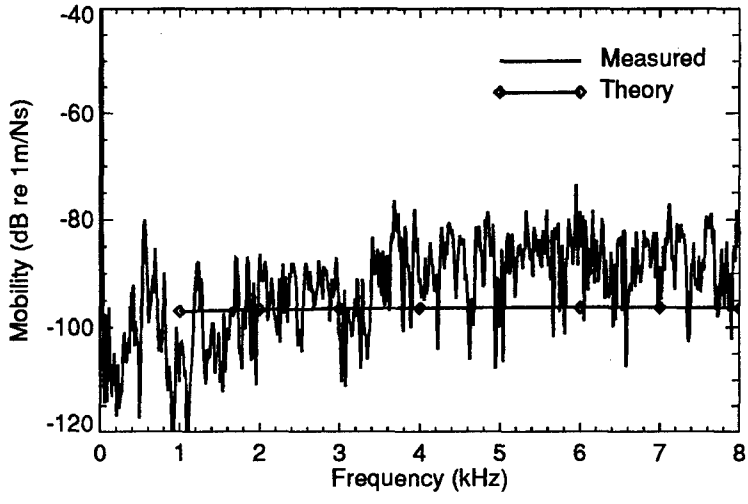

Figure 110: Transfer Mobility, Symmetric T-Plate Intersection Input, Plate 3

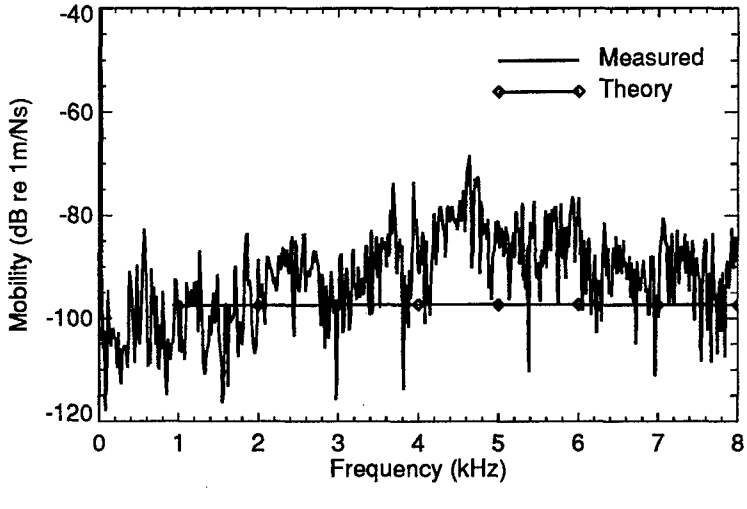

Figure 111: Transfer Mobility, Symmetric T-Plate Intersection Input, Plate 4

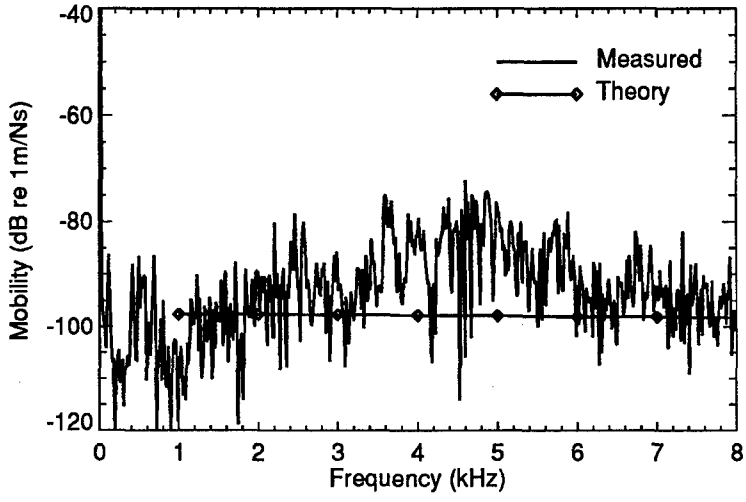

Figure 112: Transfer Mobility, Symmetric T-Plate Intersection Input, Plate 5

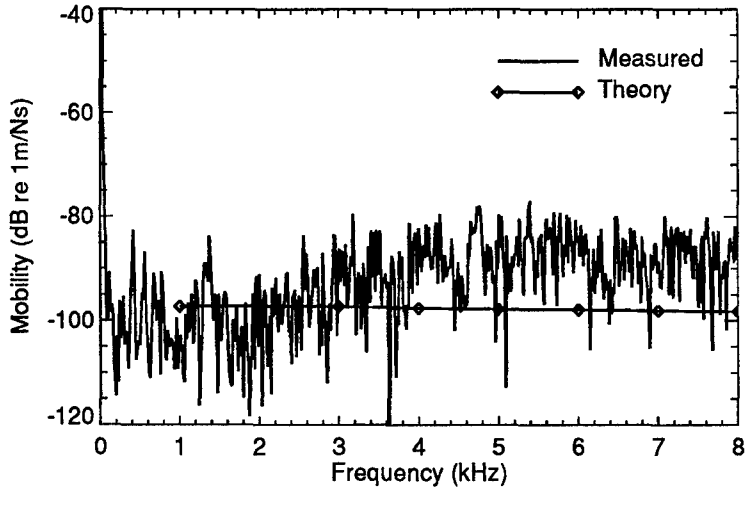

Figure 113: Transfer Mobility, Symmetric T-Plate Intersection Input, Plate 6

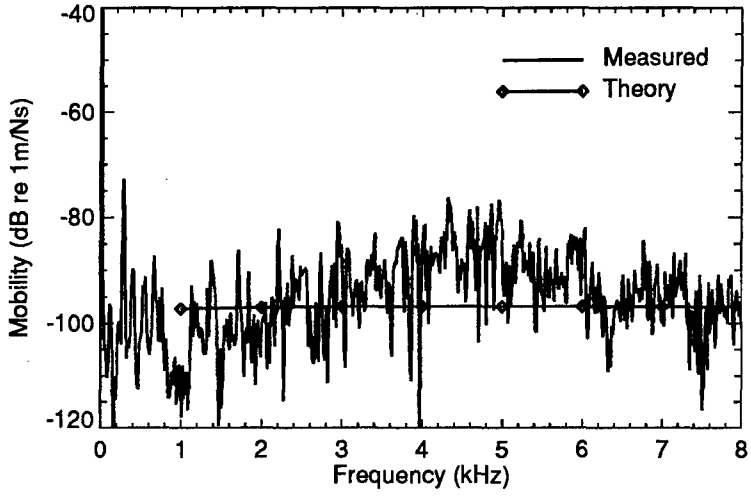

Figure 114: Transfer Mobility, Symmetric T-Plate Intersection Input, Plate 7

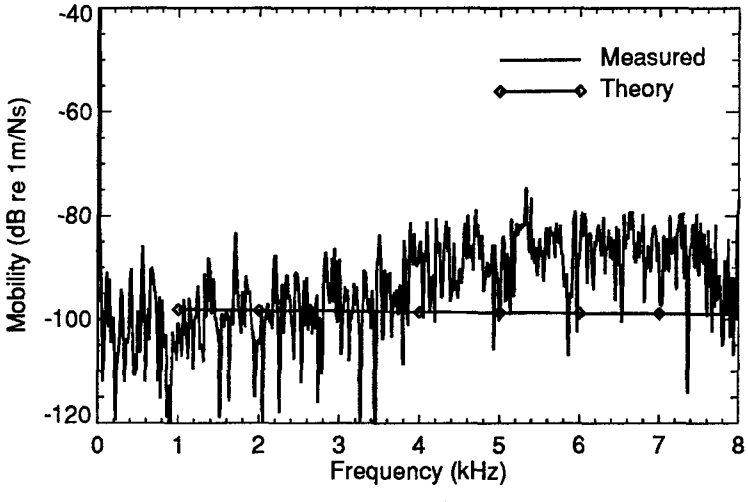

Figure 115: Transfer Mobility, Symmetric T-Plate Intersection Input, Plate 8

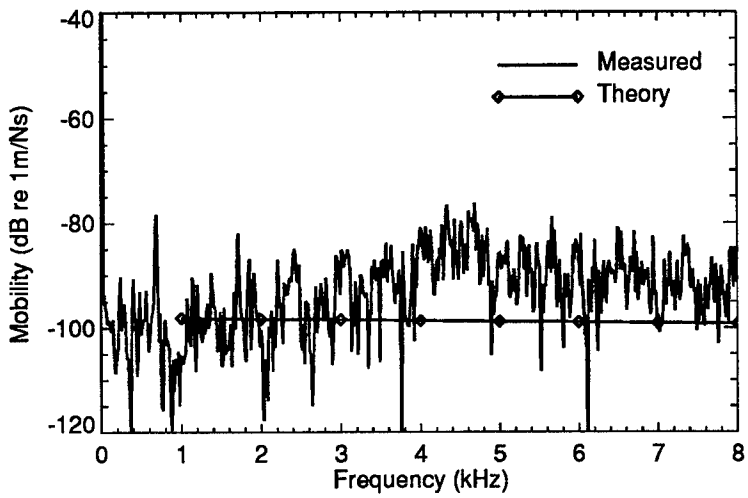

Figure 116: Transfer Mobility, Symmetric T-Plate Intersection Input, Plate 9

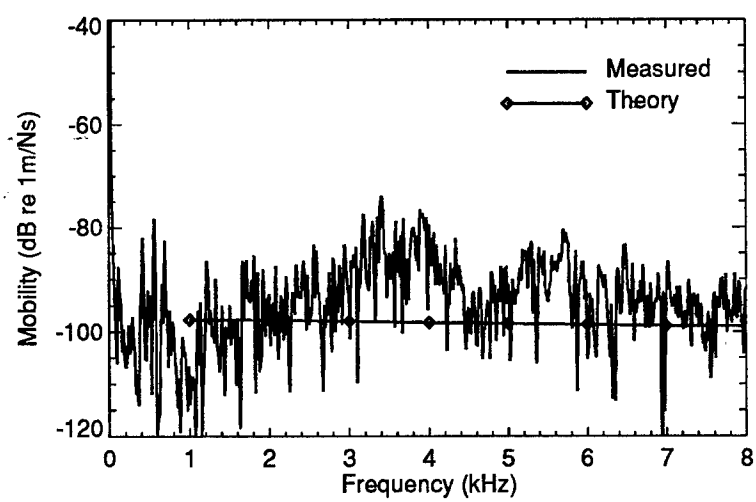

Figure 117: Transfer Mobility, Symmetric T-Plate Intersection Input, Plate 10

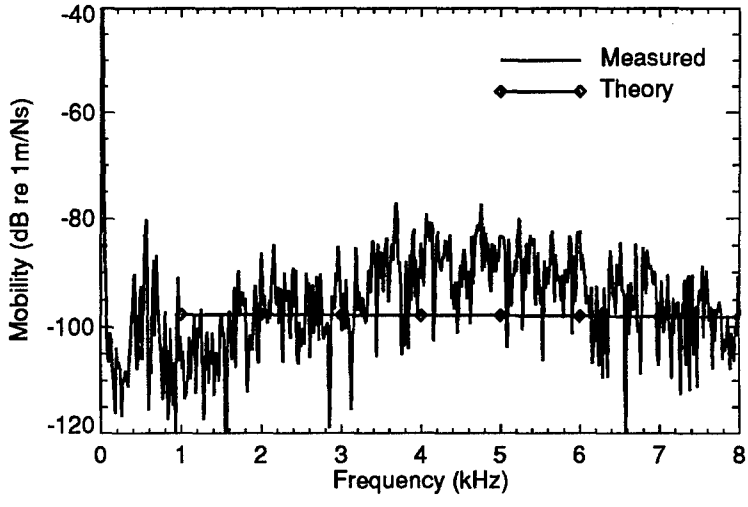

Figure 118: Transfer Mobility, Symmetric T-Plate Intersection Input, Plate 11

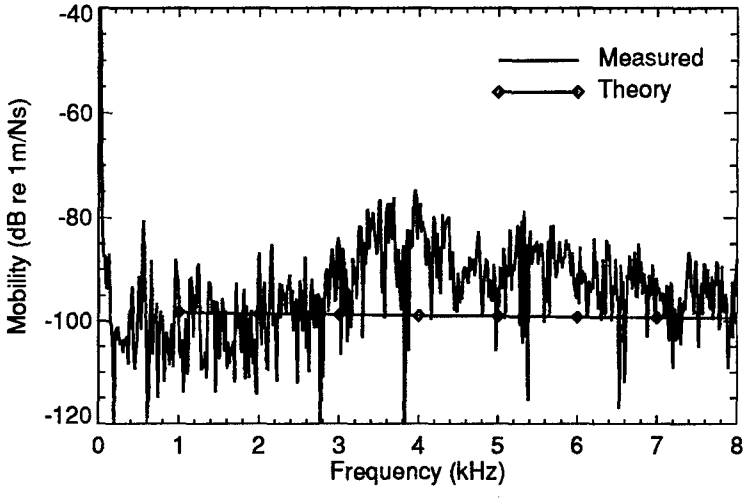

Figure 119: Transfer Mobility, Symmetric T-Plate Intersection Input, Plate 12

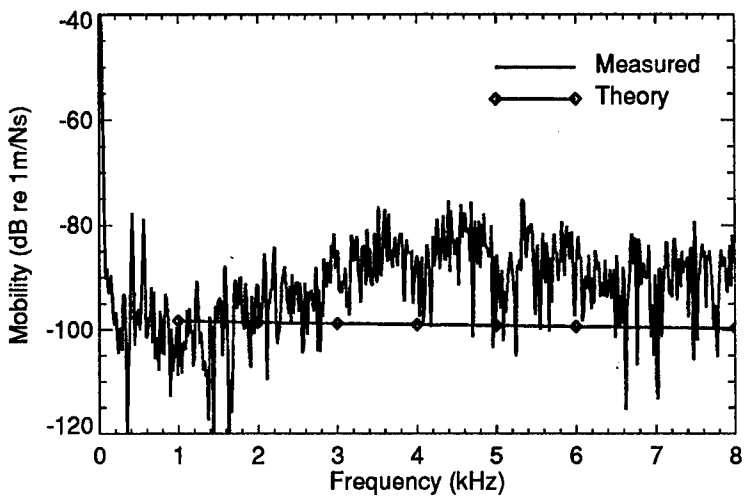

Figure 120: Transfer Mobility, Symmetric T-Plate Intersection Input, Plate 13

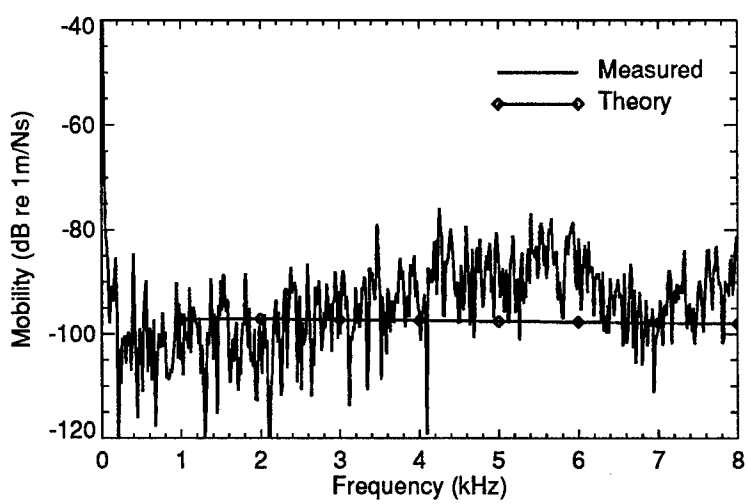

Figure 121: Transfer Mobility, Symmetric T-Plate Intersection Input, Plate 14

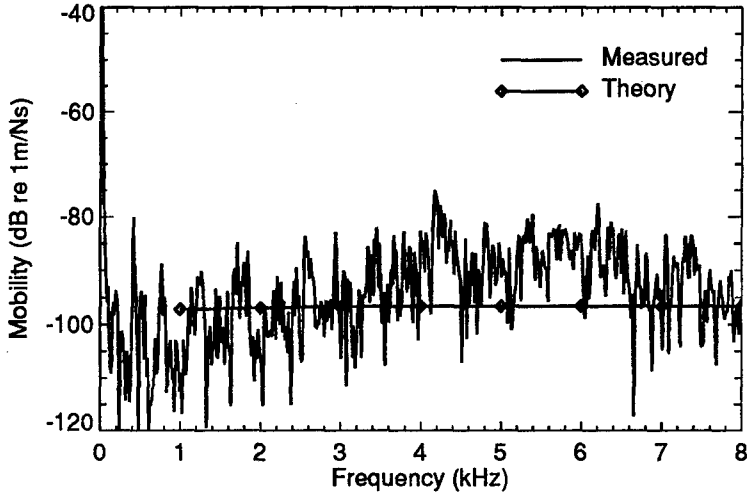

Figure 122: Transfer Mobility, Symmetric T-Plate Intersection Input, Plate 15

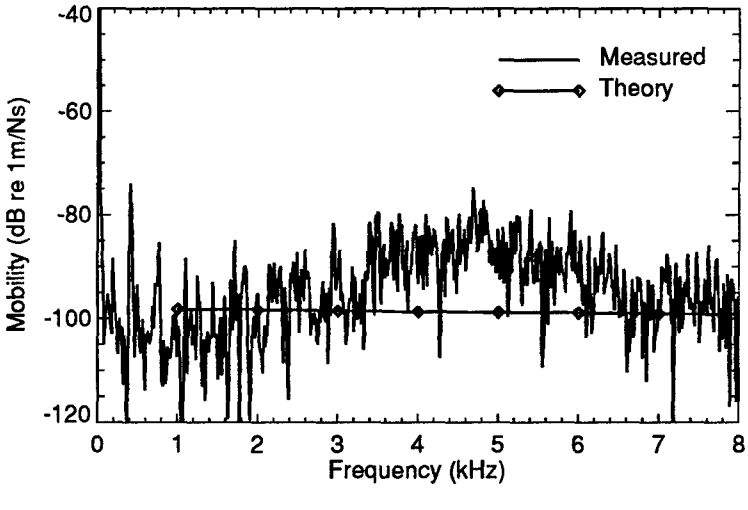

Figure 123: Transfer Mobility, Symmetric T-Plate Intersection Input, Plate 16

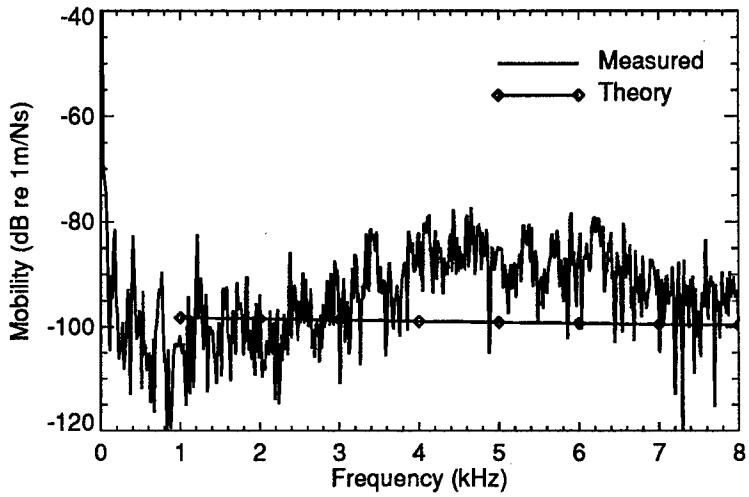

Figure 124: Transfer Mobility, Symmetric T-Plate Intersection Input, Plate 17

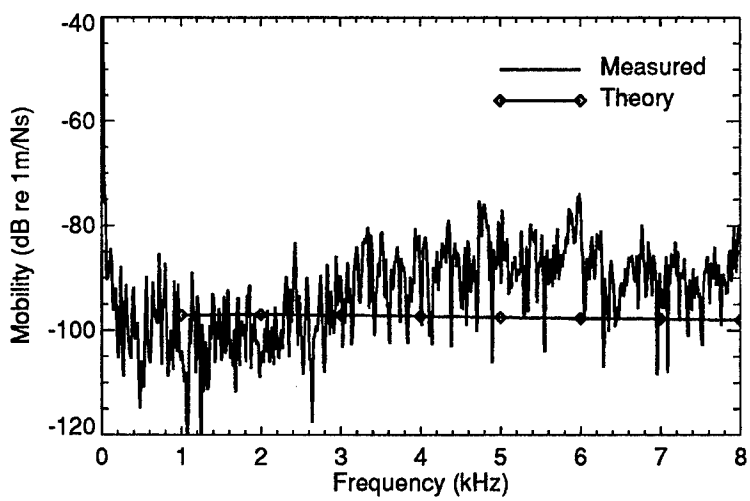

Figure 125: Transfer Mobility, Symmetric T-Plate Intersection Input, Plate 18

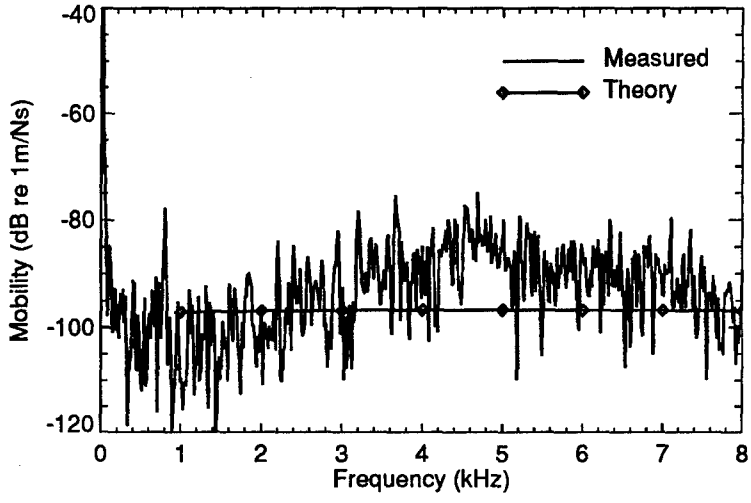

Figure 126: Transfer Mobility, Symmetric T-Plate Intersection Input, Plate 19

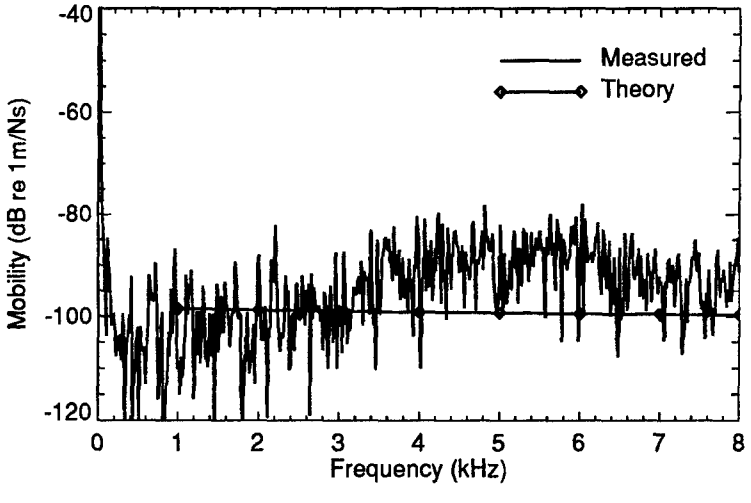

Figure 127: Transfer Mobility, Symmetric T-Plate Intersection Input, Plate 20

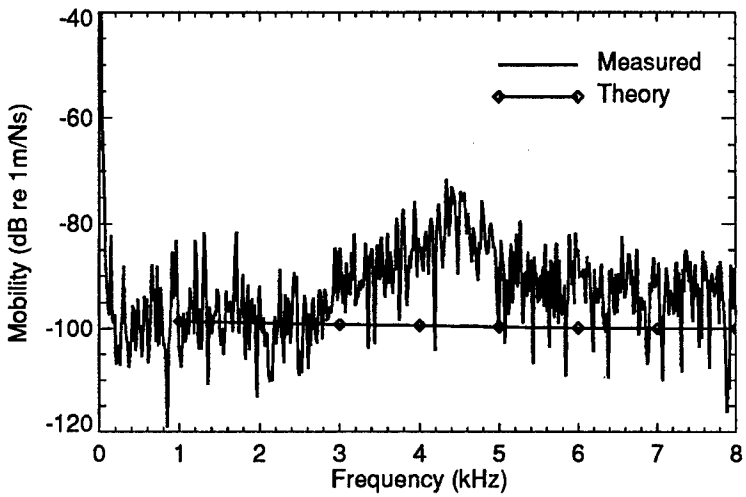

Figure 128: Transfer Mobility, Symmetric T-Plate Intersection Input, Plate 21

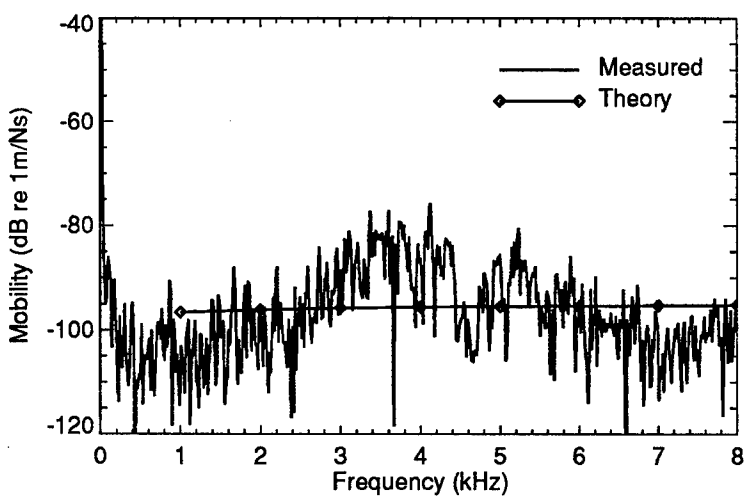

Figure 129: Transfer Mobility, Symmetric T-Plate Intersection Input, Plate 22

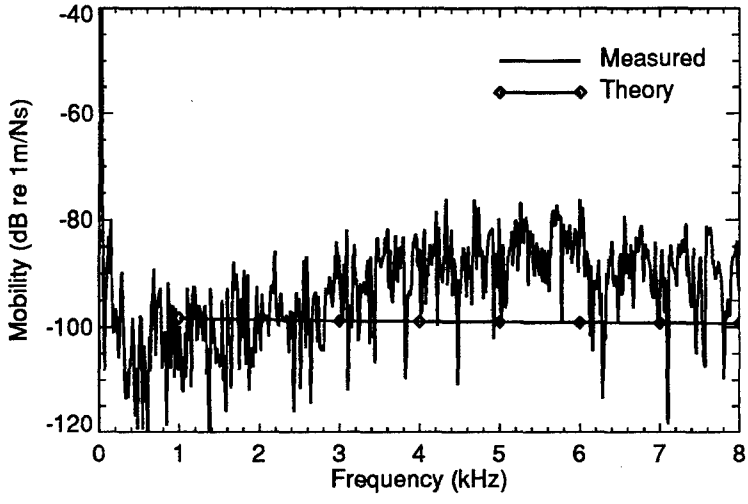

Figure 130: Transfer Mobility, Symmetric T-Plate Intersection Input, Plate 23

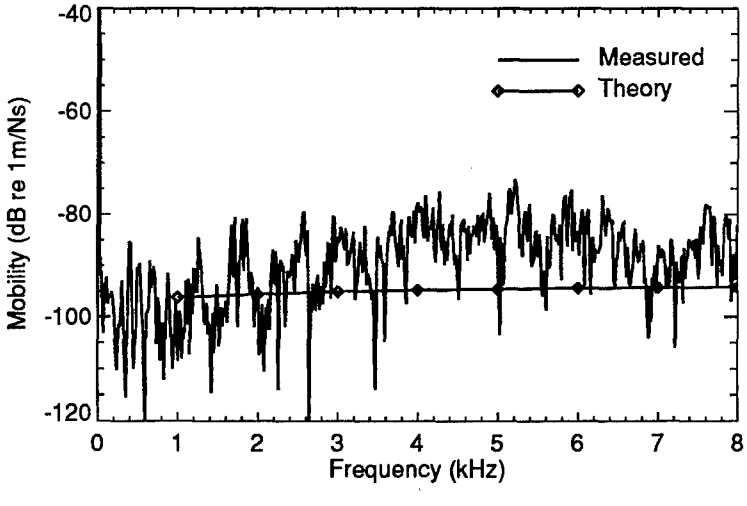

Figure 131: Transfer Mobility, Symmetric T-Plate Intersection Input, Plate 24

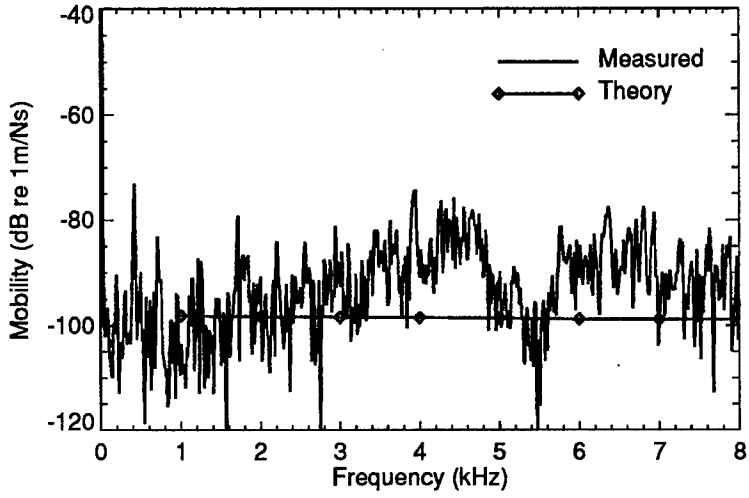

Figure 132: Transfer Mobility, Symmetric T-Plate Intersection Input, Plate 25

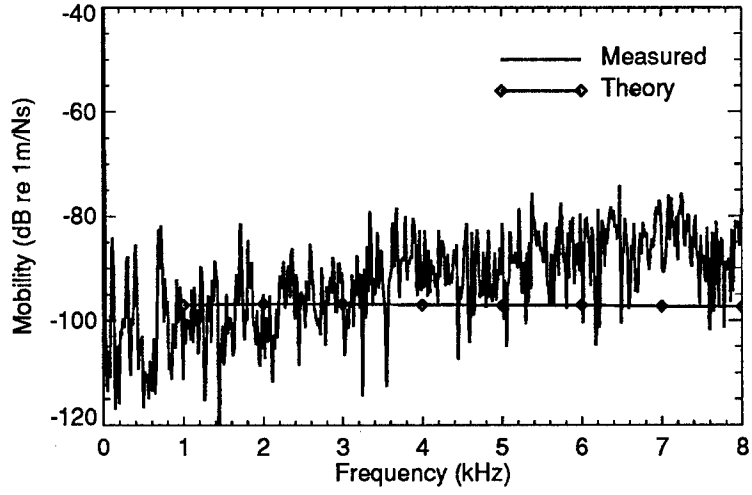

Figure 133: Transfer Mobility, Symmetric T-Plate Intersection Input, Plate 26

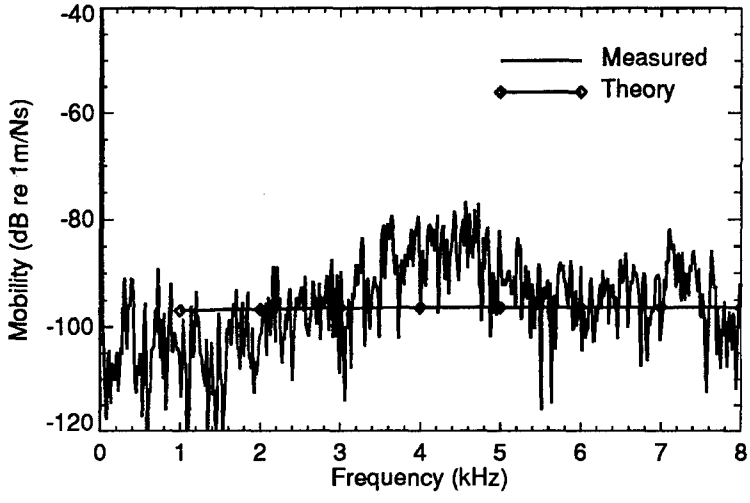

Figure 134: Transfer Mobility, Symmetric T-Plate Intersection Input, Plate 27

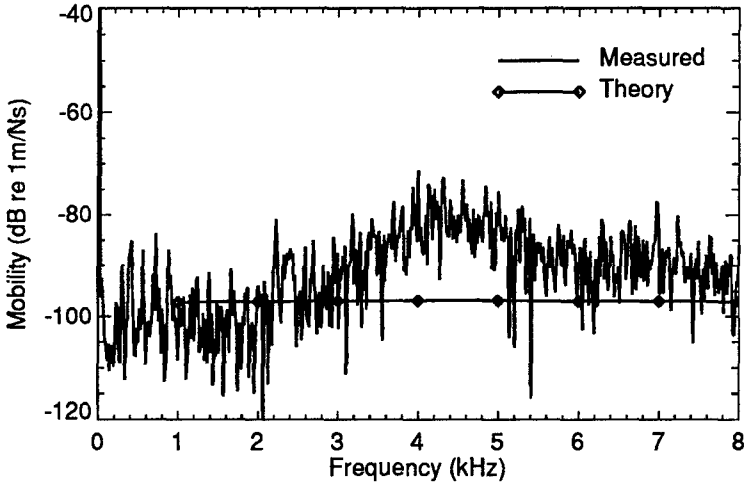

Figure 135: Transfer Mobility, Symmetric T-Plate Intersection Input, Plate 28

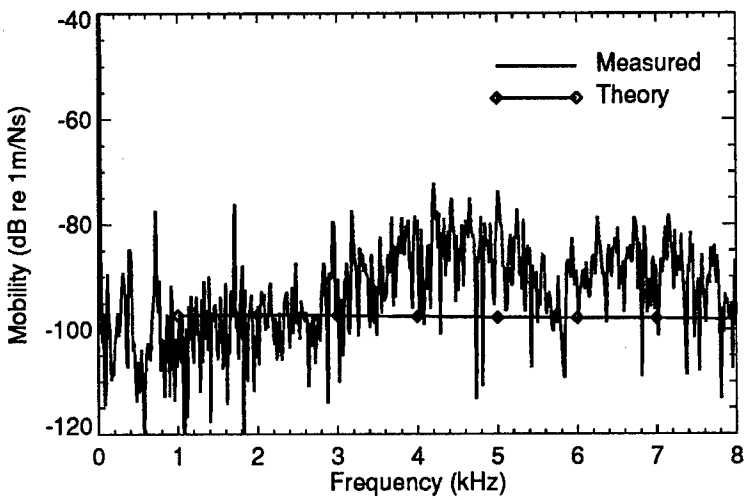

Figure 136: Transfer Mobility, Symmetric T-Plate Intersection Input, Plate 29

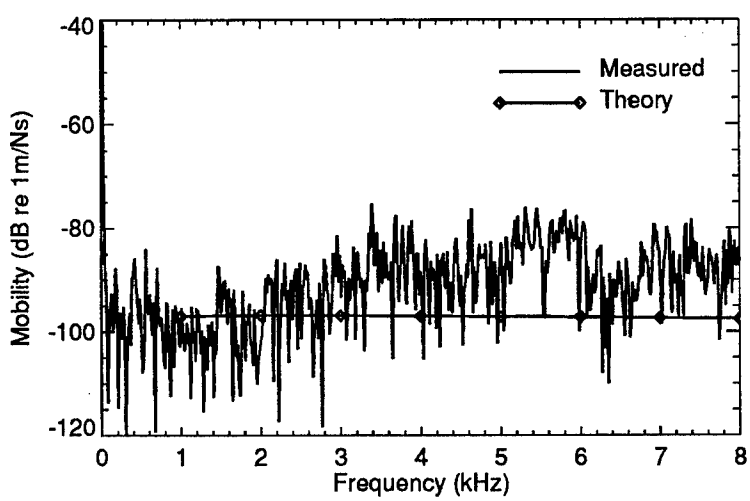

Figure 137: Transfer Mobility, Symmetric T-Plate Intersection Input, Plate 30

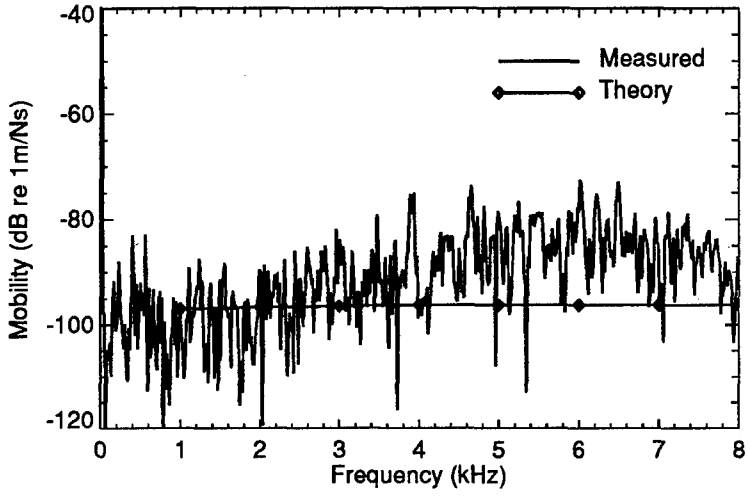

Figure 138: Transfer Mobility, Symmetric T-Plate Intersection Input, Plate 31

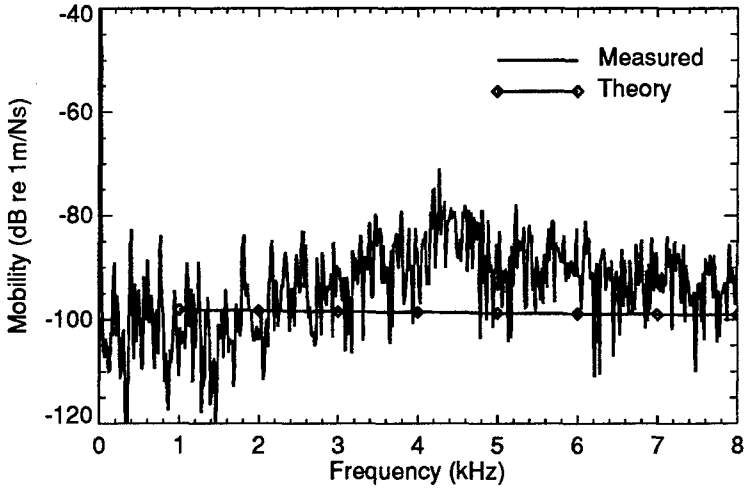

Figure 139: Transfer Mobility, Symmetric T-Plate Intersection Input, Plate 32

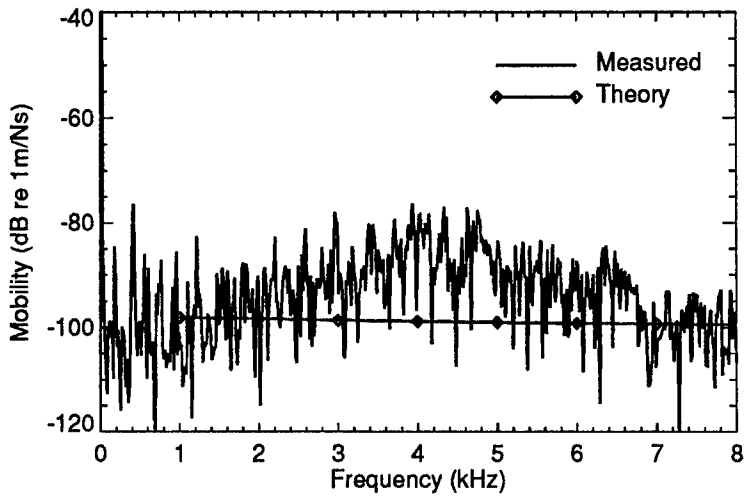

Figure 140: Transfer Mobility, Symmetric T-Plate Intersection Input, Plate 33

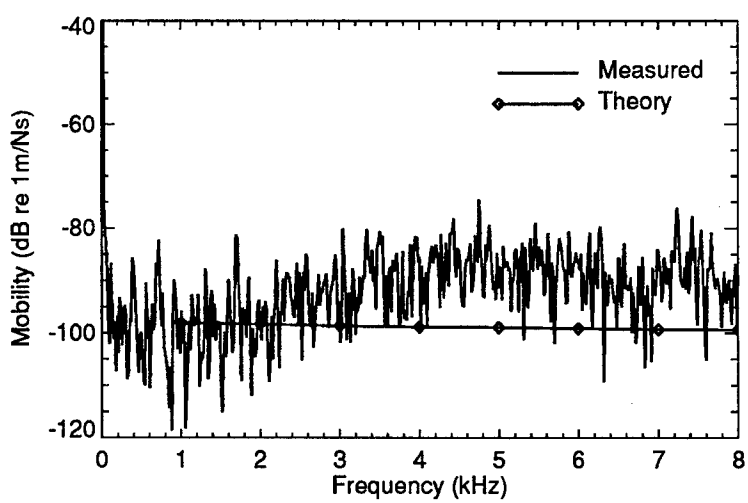

Figure 141: Transfer Mobility, Symmetric T-Plate Intersection Input, Plate 34

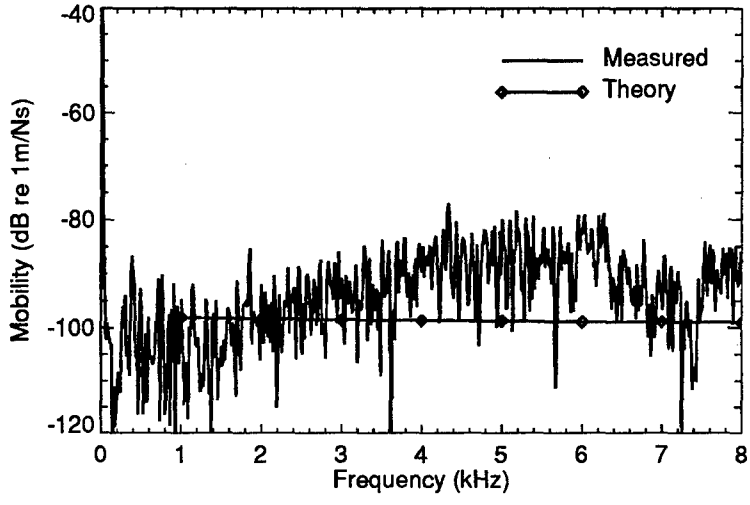

Figure 142: Transfer Mobility, Symmetric T-Plate Intersection Input, Plate 35

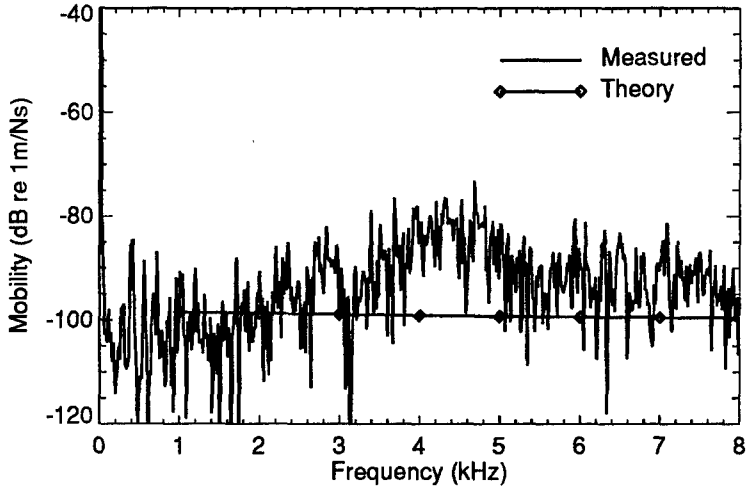

Figure 143: Transfer Mobility, Symmetric T-Plate Intersection Input, Plate 36

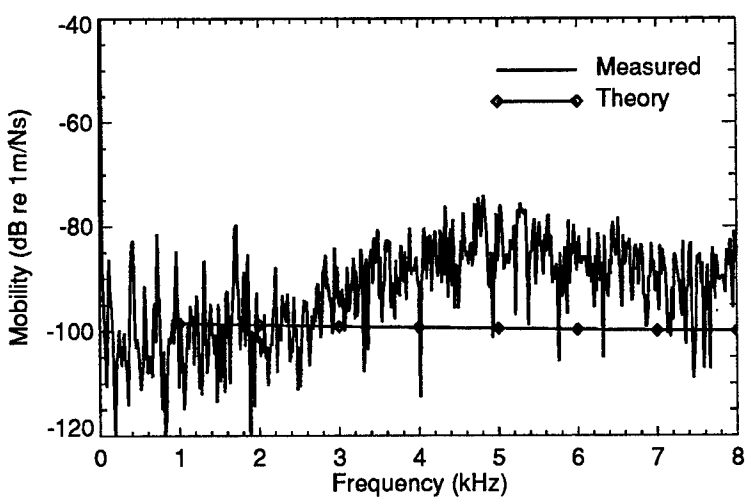

Figure 144: Transfer Mobility, Symmetric T-Plate Intersection Input, Plate 37

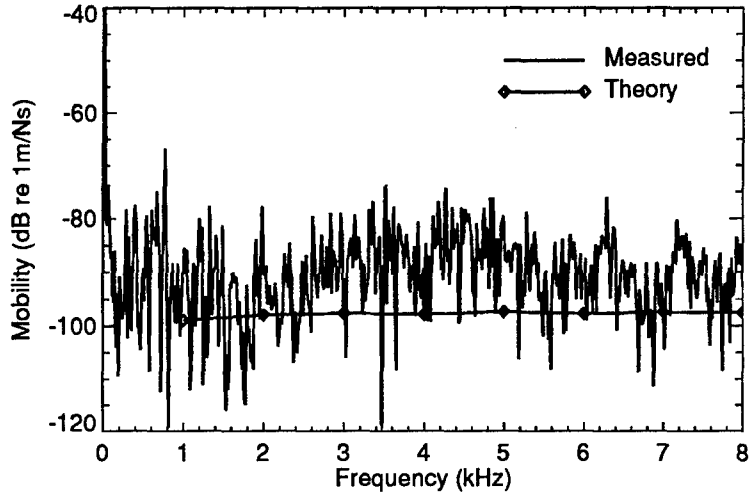

Figure 145: Transfer Mobility, L-Plate Intersection Input, Plate 1

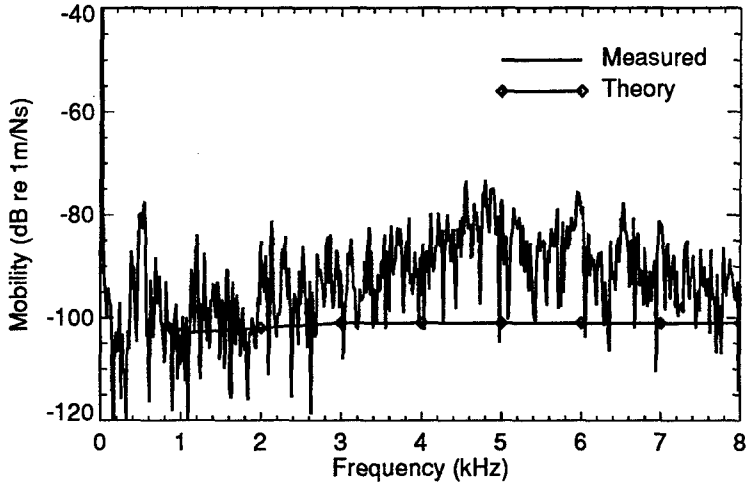

Figure 146: Transfer Mobility, L-Plate Intersection Input, Plate 2

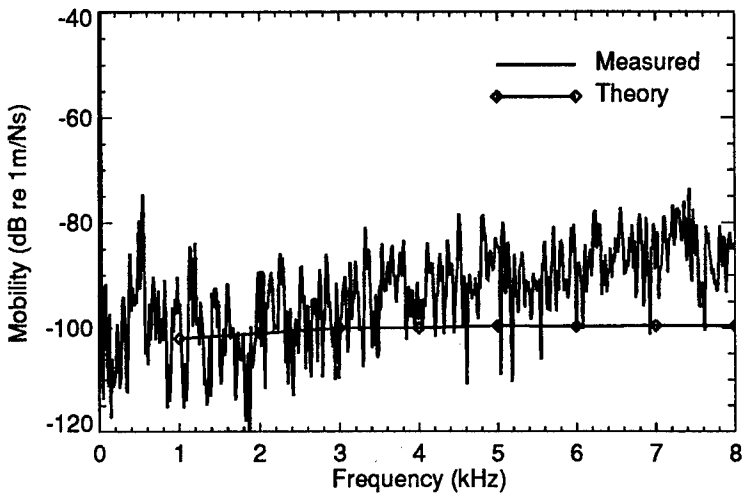

Figure 147: Transfer Mobility, L-Plate Intersection Input, Plate 3

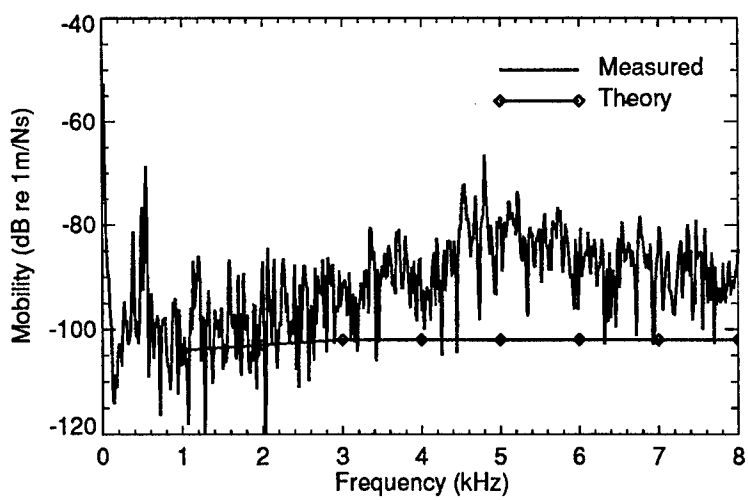

Figure 148: Transfer Mobility, L-Plate Intersection Input, Plate 4

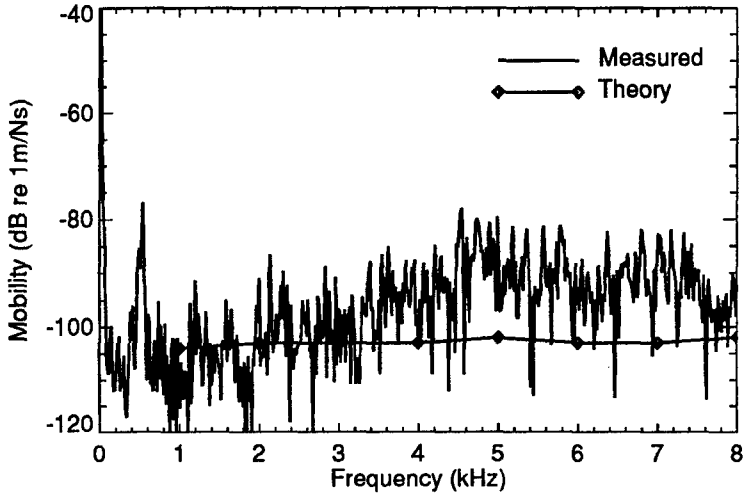

Figure 149: Transfer Mobility, L-Plate Intersection Input, Plate 5

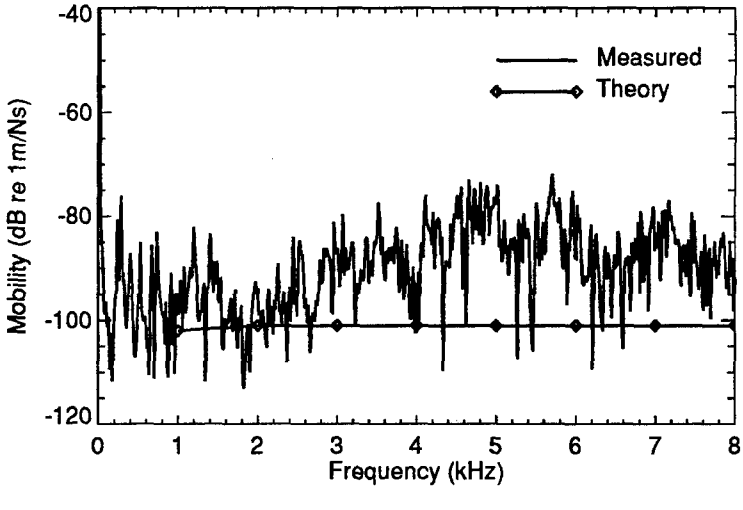

Figure 150: Transfer Mobility, L-Plate Intersection Input, Plate 6

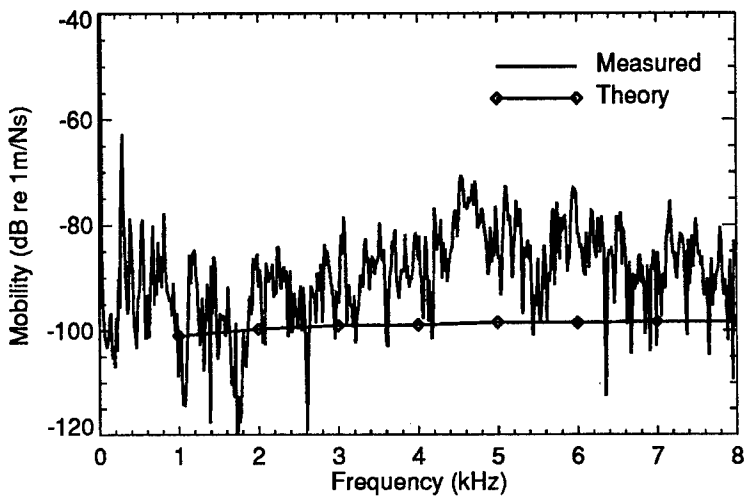

Figure 151: Transfer Mobility, L-Plate Intersection Input, Plate 7

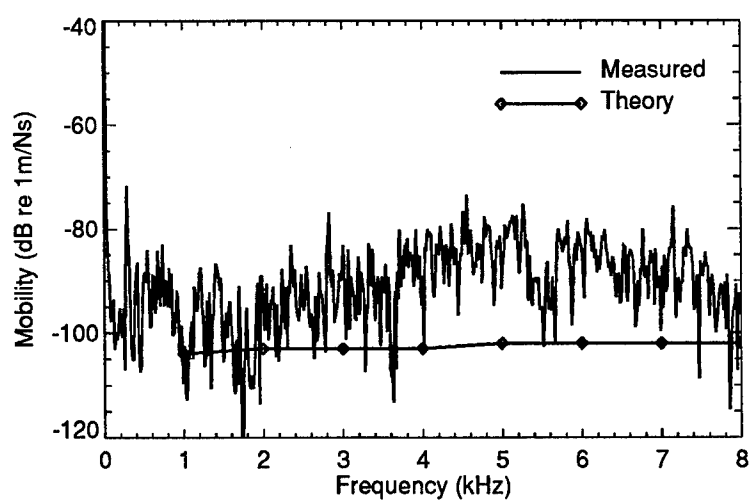

Figure 152: Transfer Mobility, L-Plate Intersection Input, Plate 8

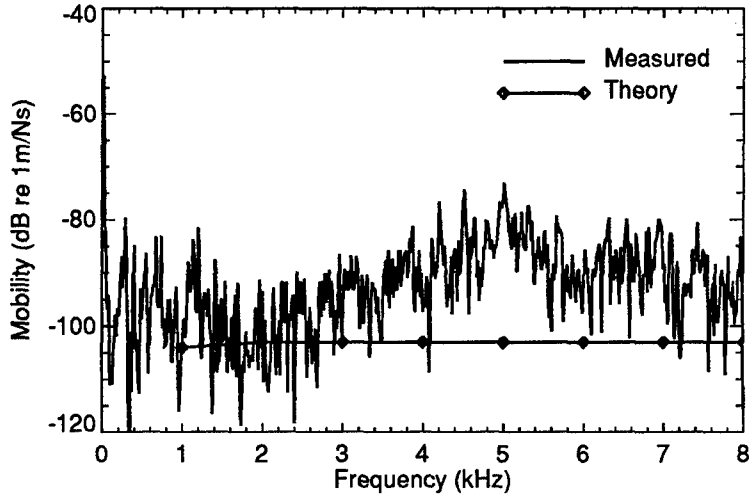

Figure 153: Transfer Mobility, L-Plate Intersection Input, Plate 9

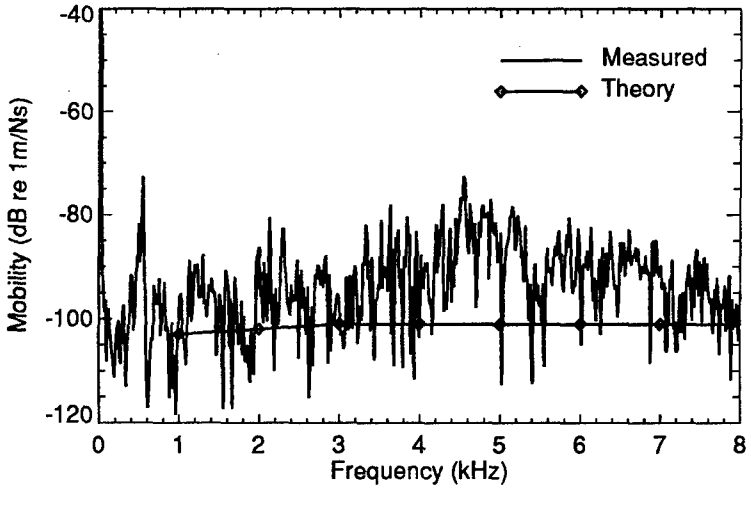

Figure 154: Transfer Mobility, L-Plate Intersection Input, Plate 10

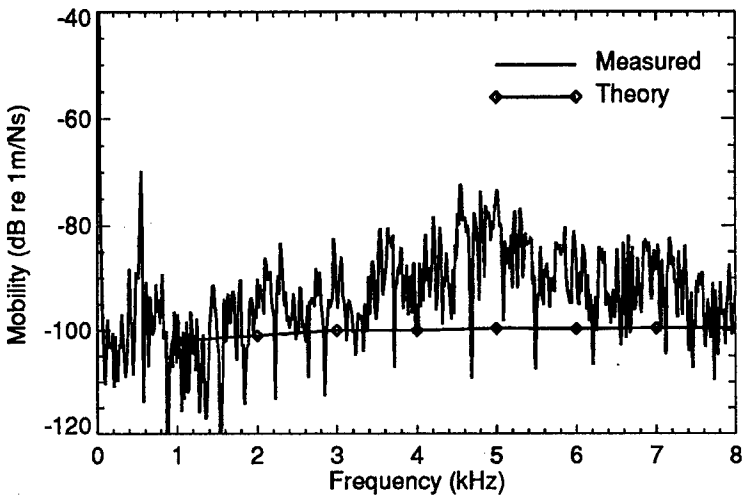

Figure 155: Transfer Mobility, L-Plate Intersection Input, Plate 11

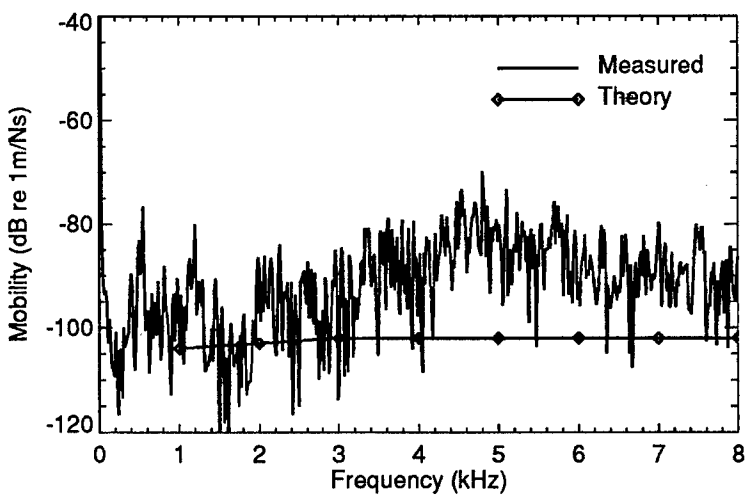

Figure 156: Transfer Mobility, L-Plate Intersection Input, Plate 12

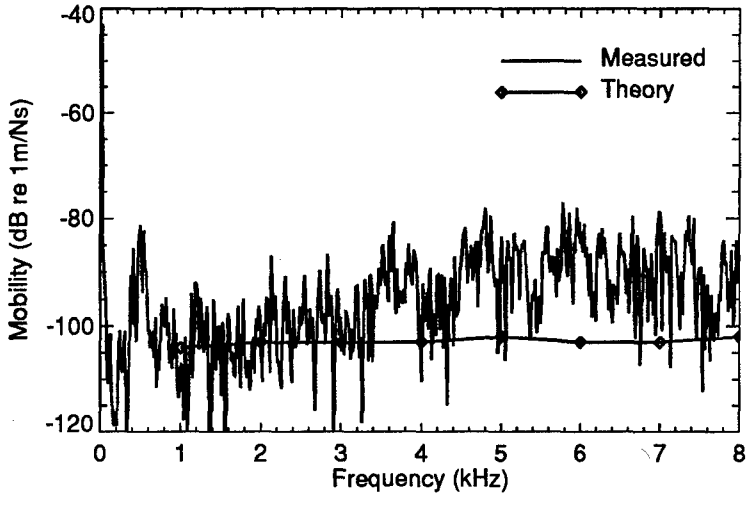

Figure 157: Transfer Mobility, L-Plate Intersection Input, Plate 13

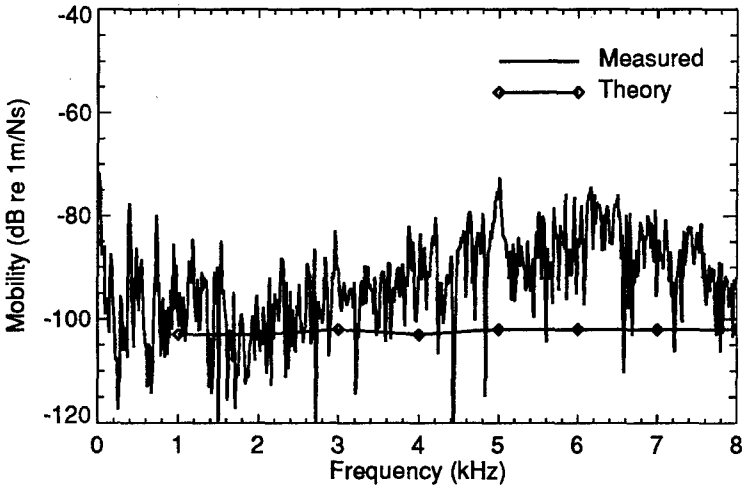

Figure 158: Transfer Mobility, L-Plate Intersection Input, Plate 14

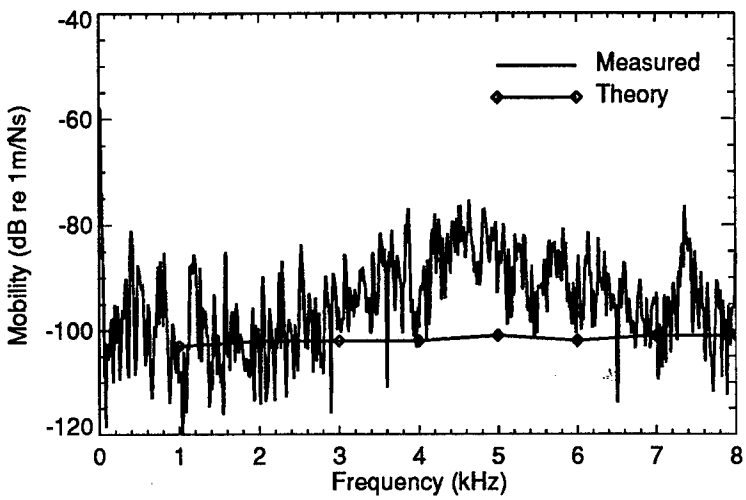

Figure 159: Transfer Mobility, L-Plate Intersection Input, Plate 15

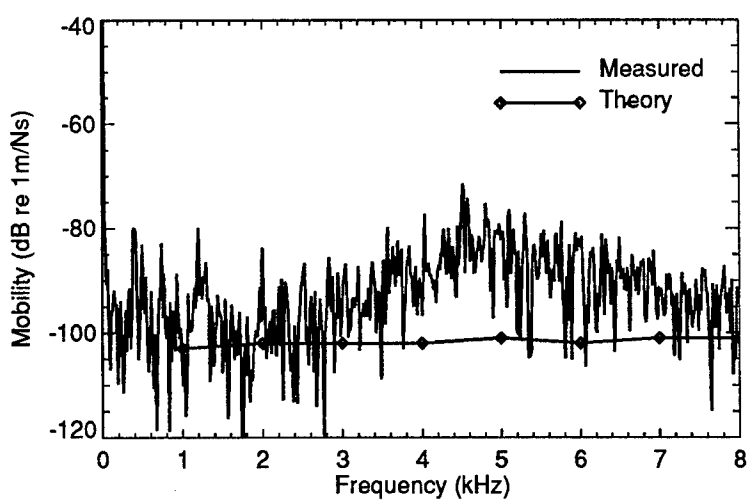

Figure 160: Transfer Mobility, L-Plate Intersection Input, Plate 16

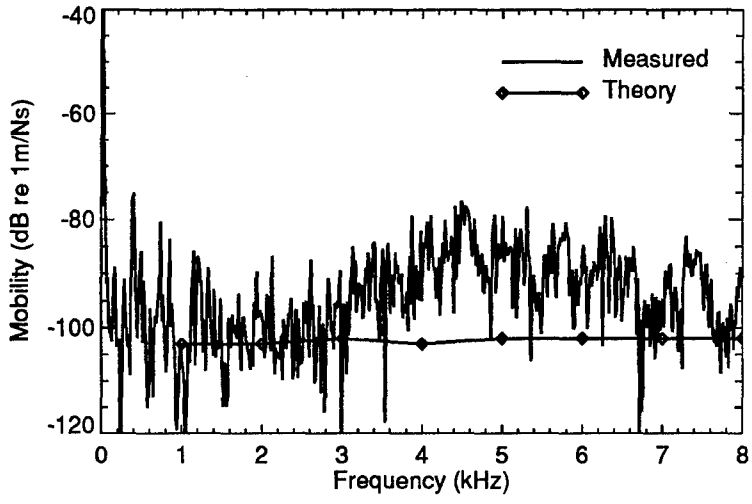

Figure 161: Transfer Mobility, L-Plate Intersection Input, Plate 17

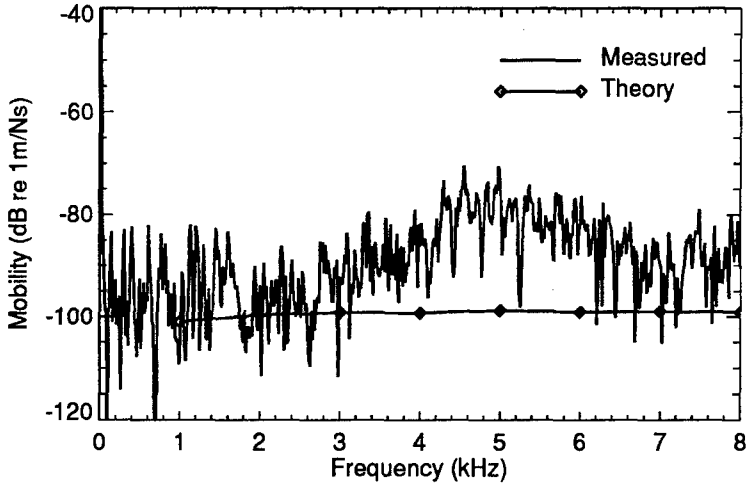

Figure 162: Transfer Mobility, L-Plate Intersection Input, Plate 18

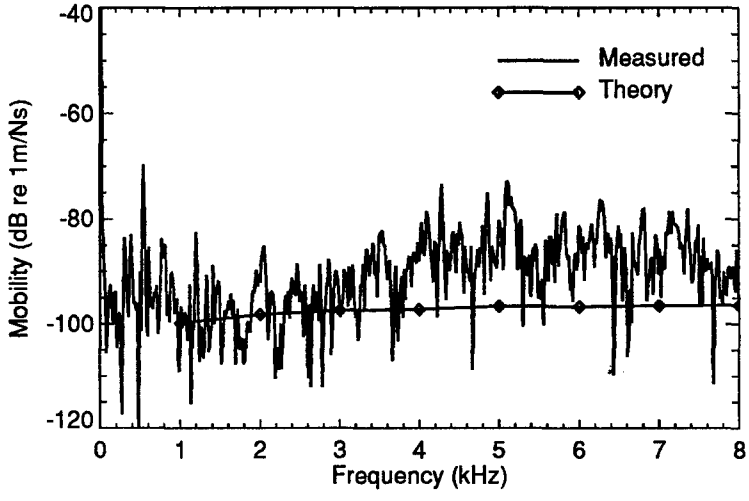

Figure 163: Transfer Mobility, L-Plate Intersection Input, Plate 19

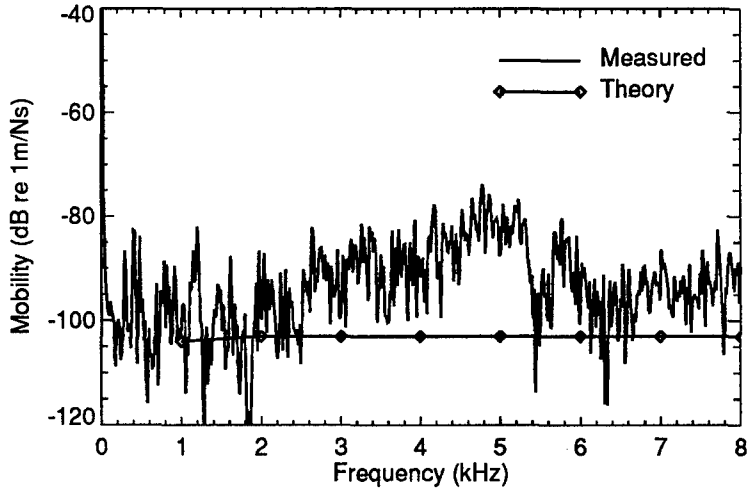

Figure 164: Transfer Mobility, L-Plate Intersection Input, Plate 20

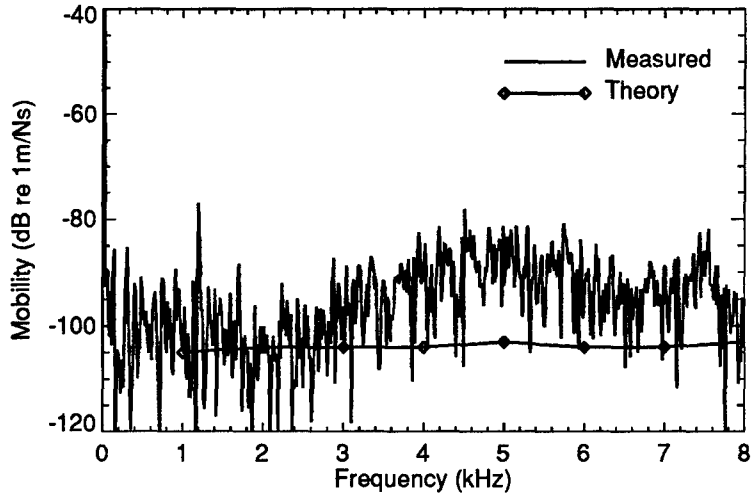

Figure 165: Transfer Mobility, L-Plate Intersection Input, Plate 21

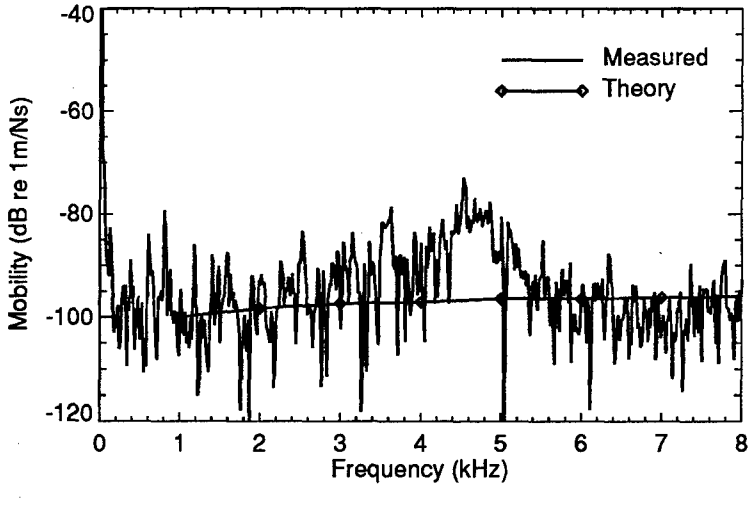

Figure 166: Transfer Mobility, L-Plate Intersection Input, Plate 22

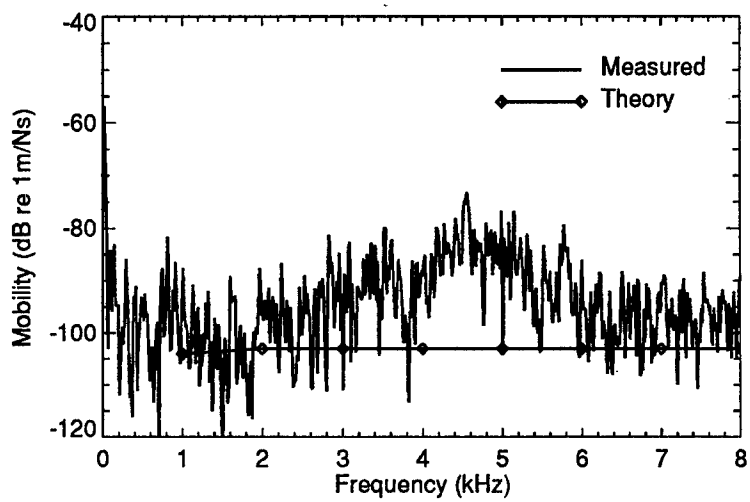

Figure 167: Transfer Mobility, L-Plate Intersection Input, Plate 23

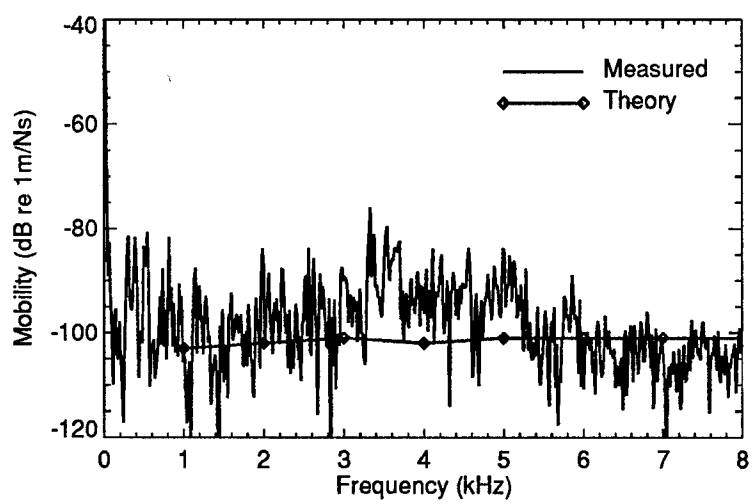

Figure 168: Transfer Mobility, L-Plate Intersection Input, Plate 24

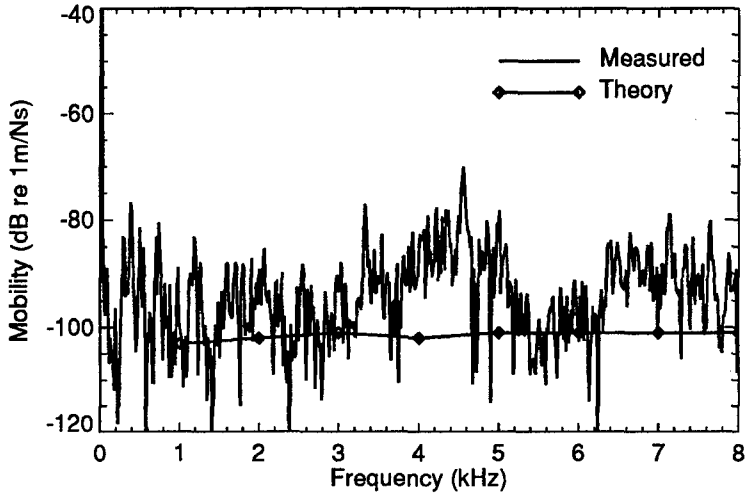

Figure 169: Transfer Mobility, L-Plate Intersection Input, Plate 25

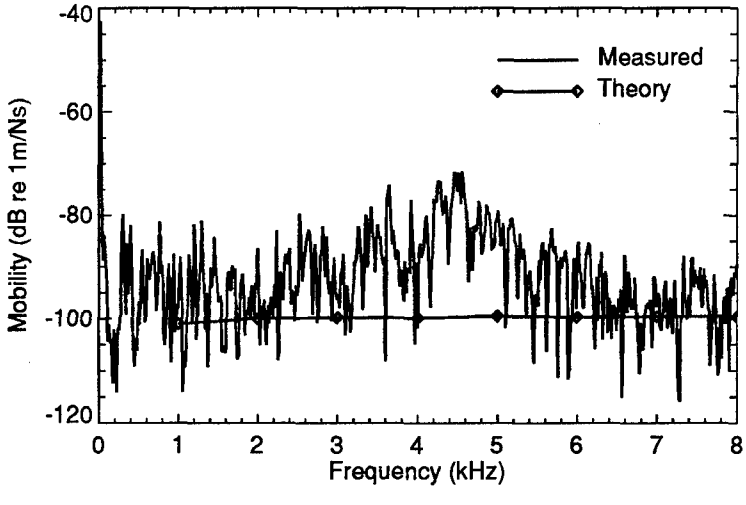

Figure 170: Transfer Mobility, L-Plate Intersection Input, Plate 26

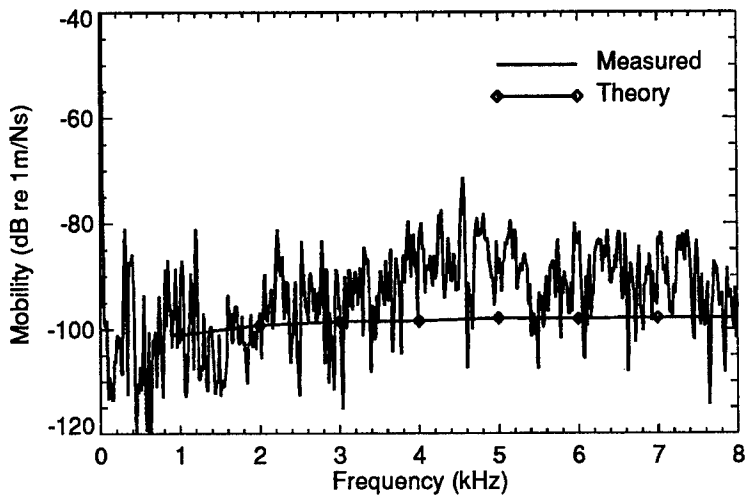

Figure 171: Transfer Mobility, L-Plate Intersection Input, Plate 27

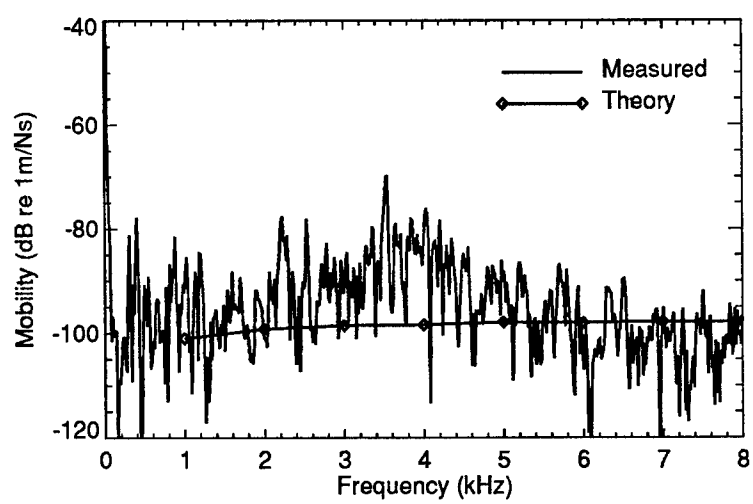

Figure 172: Transfer Mobility, L-Plate Intersection Input, Plate 28

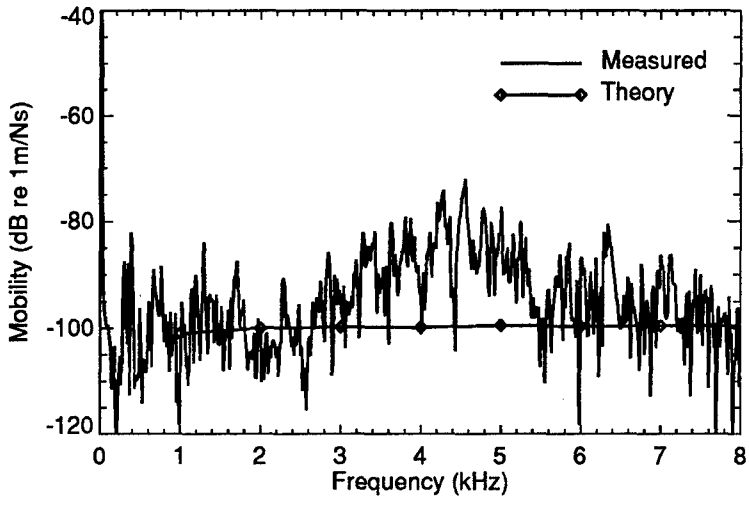

Figure 173: Transfer Mobility, L-Plate Intersection Input, Plate 29

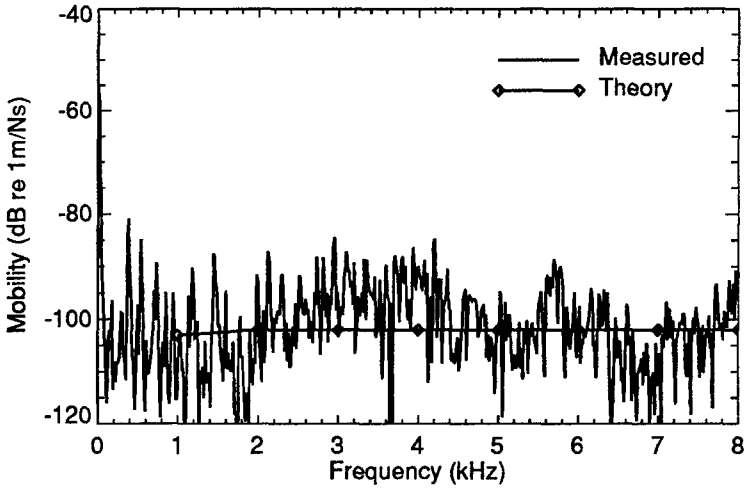

Figure 174: Transfer Mobility, L-Plate Intersection Input, Plate 30

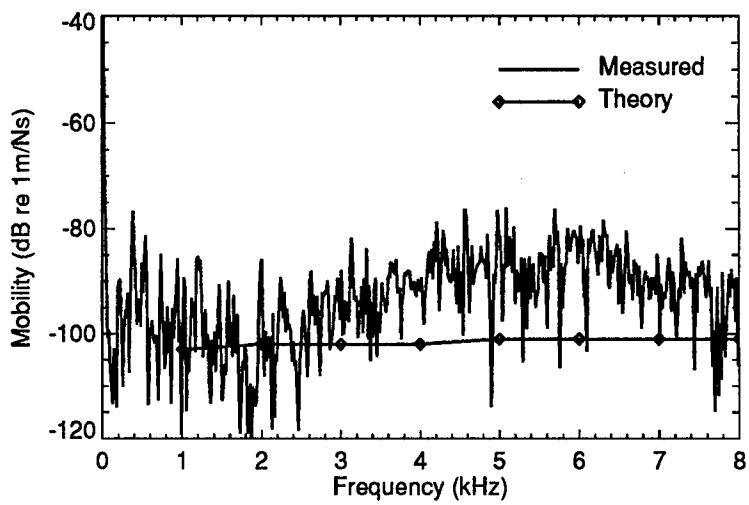

Figure 175: Transfer Mobility, L-Plate Intersection Input, Plate 31

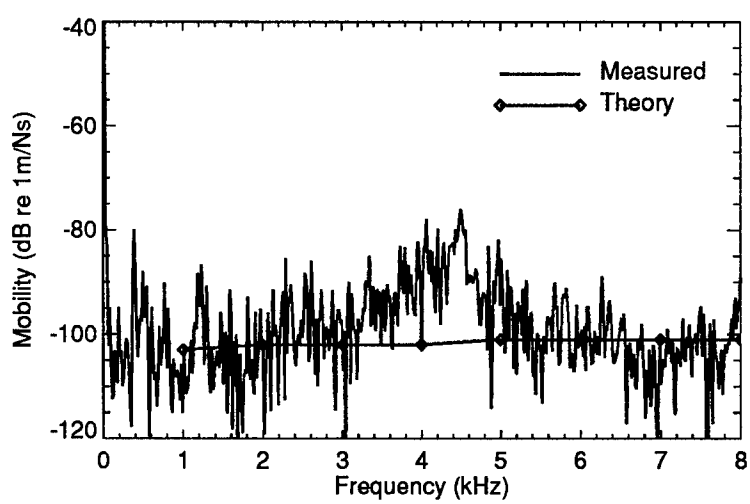

Figure 176: Transfer Mobility, L-Plate Intersection Input, Plate 32

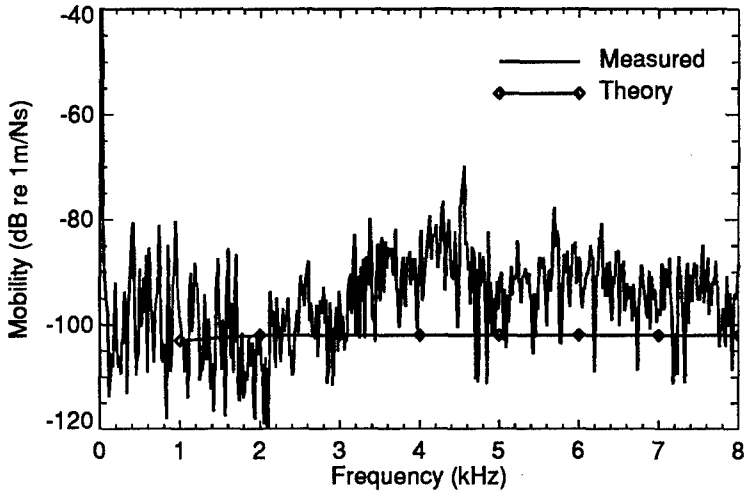

Figure 177: Transfer Mobility, L-Plate Intersection Input, Plate 33

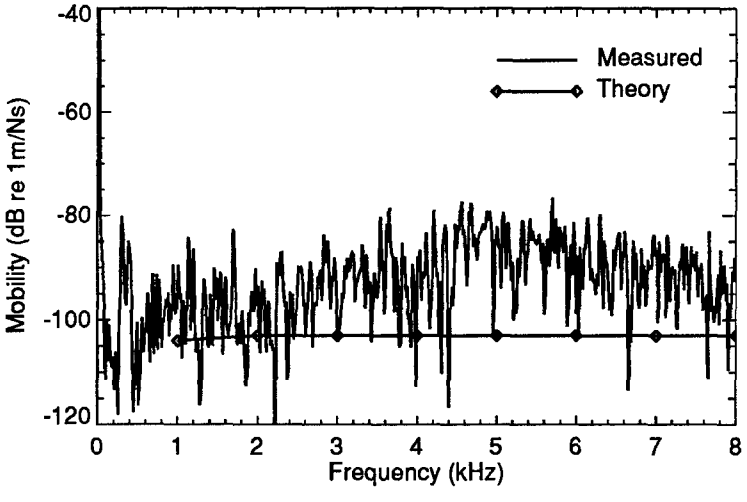

Figure 178: Transfer Mobility, L-Plate Intersection Input, Plate 34

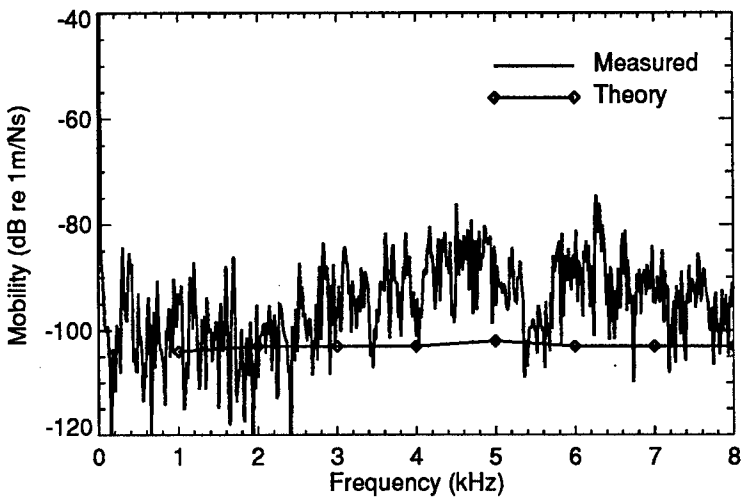

Figure 179: Transfer Mobility, L-Plate Intersection Input, Plate 35

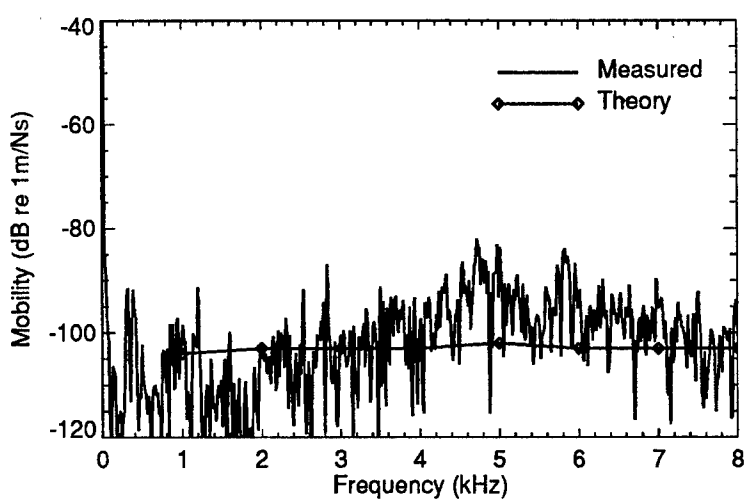

Figure 180: Transfer Mobility, L-Plate Intersection Input, Plate 36

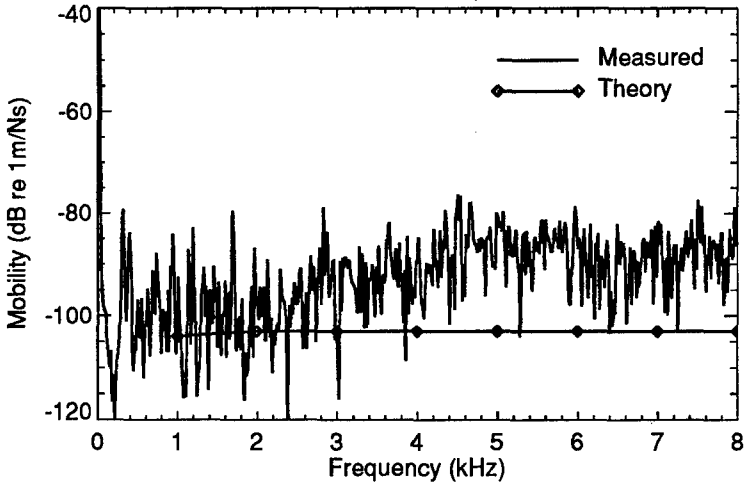

Figure 181: Transfer Mobility, L-Plate Intersection Input, Plate 37

References

[1] Burrell, S.C., Chernuka, M.W., "Extension of Power Flow Finite Element Analysis to Ship Structures - Final Report Part I", Martec Ltd., DREA Contractor Report 91/410, 1990.

[2] Burrell, S.C., Orisamolu, I.R, Chernuka, M.W., "Extension of Power Flow Finite Element Analysis to Ship Structures - Final Report Part II", DREA Contractor Report, CR/93/424, Martec Ltd., 1993.

[3] Burrell, Lieu, Q., S.C., Chernuka, M.W., "Extension of Power Flow Finite Element Analysis to Ship Structures - Final Report Part III", DREA Contractor Report 92/450, 1990.

[4] Smith, M.J., Chernuka, M.W., "Extension of Power Flow Finite Element Analysis to Ship Structures," DREA Contractor Report 96/406, 1996.

[5] Smith, M.J., "Enhancement of Software for PFFEA Modelling and Analysis of Ship Structures," Martec, Ltd., DREA Contractor Report 97/410, 1997.

[6] Smith, M.J., "Advanced Modelling Capabilities for Power Flow Finite Element Analysis (PFFEA)," DREA Contractor Report 97/447, 1997.

[7] Gilroy, L.E., "Mobility Measurements of a Simulated Semi-Infinite Beam Using a Laser Doppler Velocimeter," DREA Technical Memorandum 97/201, 1997.

[8] Gilroy, L.E., "High Frequency Response of a Ring-Stiffened Cylinder," DREA Technical Memorandum 98/221, 1998.

[9] Gilroy, L.E., "Predicting Radiated Sound from a Submerged Ring-Stiffened Cylinder," DREA Technical Memorandum 96/237, 1997.

[10] Gilroy, L.E., "Comparisons of Numerically Predicted and Experimentally Measured Radiated Noise from a Ring-Stiffened Cylinder," DREA Technical Memorandum 96/217, 1996.

[11] McMahon, G.W., "New Floating Laboratory Facilitates Underwater Acoustic Measurements," Canadian Electronics Engineering, February, 1961.

[12] Liu, S.B., Chernuka, M.W., Smith, M.J., "Transient Heat Transfer Capability for the VASTF Software", DREA Contractor Report CR/95/430, 1995.

[13] Skudrzyk, E., "The Mean-Value Method of Predicting the Dynamic Response of Complex Vibrators," JASA, Vol. 67, No. 4, April, 1980.

UNCLASSIFIED
SECURITY CLASSIFICATION OF FORM
(highest classification of Title, Abstract, Keywords)

DOCUMENT CONTROL DATA

(Security classification of title, body of abstract and indexing annotation must be entered when the overall document is classified)

1. ORIGINATOR (the name and address of the organization preparing the document.. Organizations for whom the document was prepared, e.g. Establishment sponsoring a contractor's report, or tasking agency, are entered in section 8.)

Defence Research Establishment Atlantic
PO Box 1012
Dartmouth, Nova Scotia, Canada B2Y 3Z7

2. SECURITY CLASSIFICATION (overall security classification of the document including special warning terms if applicable).

UNCLASSIFIED

3. TITLE (the complete document title as indicated on the title page. Its classification should be indicated by the appropriate abbreviation (S,C,R or U) in parentheses after the title).

High Frequency Response of a Stiffened Box Structure

4. AUTHORS (Last name, first name, middle initial. If military, show rank, e.g. Doe, Maj. John E.)

L.E. Gilroy, M.J. Smith* * Martec Limited

5. DATE OF PUBLICATION (month and year of publication of document)

October 1998

6a. NO .OF PAGES (total containing information Include Annexes, Appendices, etc).

109

6b. NO. OF REFS (total cited in document)

13

7. DESCRIPTIVE NOTES (the category of the document, e.g. technical report, technical note or memorandum. If appropriate, enter the type of report, e.g. interim, progress, summary, annual or final. Give the inclusive dates when a specific reporting period is covered).

TECHNICAL MEMORANDUM

8. SPONSORING ACTIVITY (the name of the department project office or laboratory sponsoring the research and development. Include address).

Defence Research Establishment Atlantic

9a. PROJECT OR GRANT NO. (if appropriate, the applicable research and development project or grant number under which the document was written. Please specify whether project or grant).

Project 1ga14

9b. CONTRACT NO. (if appropriate, the applicable number under which the document was written).

10a ORIGINATOR'S DOCUMENT NUMBER (the official document number by which the document is identified by the originating activity. This number must be unique to this document.)

DREA TM/98/227

10b OTHER DOCUMENT NOs. (Any other numbers which may be assigned this document either by the originator or by the sponsor.)

11. DOCUMENT AVAILABILITY (any limitations on further dissemination of the document, other than those imposed by security classification)

(x) Unlimited distribution
( ) Defence departments and defence contractors; further distribution only as approved
( ) Defence departments and Canadian defence contractors; further distribution only as approved
( ) Government departments and agencies; further distribution only as approved
( ) Defence departments; further distribution only as approved
( ) Other (please specify):

12. DOCUMENT ANNOUNCEMENT (any limitation to the bibliographic announcement of this document. This will normally correspond to the Document Availability (11). However, where further distribution (beyond the audience specified in (11) is possible, a wider announcement audience may be selected).

Full, unlimited

UNCLASSIFIED
SECURITY CLASSIFICATION OF FORM

DCD03 2/06/87-M/ DREA mod. 17 Dec 1997

13. ABSTRACT (a brief and factual summary of the document. It may also appear elsewhere in the body of the document itself. It is highly desirable that the abstract of classified documents be unclassified. Each paragraph of the abstract shall begin with an indication of the security classification of the information in the paragraph (unless the document itself is unclassified) represented as (S), (C), (R), or (U). It is not necessary to include here abstracts in both official languages unless the text is bilingual).

Power Flow Finite Element Analysis (PFFEA) has been under development at Defence Research Establishment Atlantic (DREA) in support of the Ship Noise Project. PFFEA is an analysis method for predicting high frequency structural acoustic and vibration response. The method is based on a vibrational conductivity approach in which the flow of vibrational energy is modelled in a similar fashion to heat conduction with convective losses. This report discusses experiments performed with DREA's ship tank test model to assist in the validation of the PFFEA software for high frequency structural vibrations. The experiments involved excitation of the steel box structure at relatively high frequencies using an electromagnetic shaker driving either the centre plate of the test model or one of three typical plate intersections (a symmetric and unsymmetric T-plate junction and an L-plate junction) making up the structure. Both the input mobility to and the response of the test model were measured under broadband excitation using an accelerometer. The input mobilities predicted by the PFFEA code compared extremely well with the experimental measurements. While the power flow method is unable to accurately predict modal response (in this case frequencies up to about 3~kHz), the model accurately predicted the average behaviour for all four cases. When looking at the response of the ship tank panels, in general, the PFFEA program was able to predict the amplitude of the transfer mobility with some degree of accuracy. However, there were significant variations in amplitude with frequency in the measured data which were not modelled with the PFFEA code. As a result, the PFFEA program should primarily be used when predictions are required over a band of frequencies rather than in support of a harmonic analysis.

14. KEYWORDS, DESCRIPTORS or IDENTIFIERS (technically meaningful terms or short phrases that characterize a document and could be helpful in cataloguing the document. They should be selected so that no security classification is required. Identifiers, such as equipment model designation, trade name, military project code name, geographic location may also be included. If possible keywords should be selected from a published thesaurus. e.g. Thesaurus of Engineering and Scientific Terms (TEST) and that thesaurus-identified. If it not possible to select indexing terms which are Unclassified, the classification of each should be indicated as with the title).

power flow
finite element
acoustic
high frequency
vibration
structure
tank
ship
input mobility
transfer mobility
PFFEA